Sperm cell surface dynamics during activation and fertilization

Arjan Boerke

The research described in this thesis was performed at the Department of Biochemistry and Cell Biology, Faculty of Veterinary Medicine, Utrecht University.

The J.E. Jurriaanse Stichting financially supported the printing of this thesis.

Printed by: Ridderprint BV, Ridderkerk, the Netherlands
Cover design: Nikki Vermeulen, Ridderprint BV, Ridderkerk, the Netherlands
Cover photo:
Lay-out: Nikki Vermeulen, Ridderprint BV, Ridderkerk, the Netherlands

ISBN: 978-90-5335-687-6

Sperm cell surface dynamics during activation and fertilization

Oppervlaktedynamiek van de spermacel tijdens activering en fertilisatie
(met een samenvatting in het Nederlands)

Proefschrift

ter verkrijging van de graad van doctor aan de Universiteit Utrecht
op gezag van de rector magnificus, prof. dr. G.J. van der Zwaan,
ingevolge het besluit van het college voor promoties
in het openbaar te verdedigen op donderdag 27 juni 2013 des ochtends te 10.30 uur

door

Arjan Boerke

geboren op 13 maart 1979 te Zuidelijke IJsselmeerpolders

Promotor:	Prof. dr. J.B. Helms
Co-promotoren:	Dr. B.M. Gadella
	Dr. C.F. van Nostrum

TABLE OF CONTENTS

1

General introduction

Based on:

Capacitation-dependent reorganization of microdomains in the apical sperm head plasma membrane: Functional relationship with zona binding and the zona-induced acrosome reaction; Boerke A, Tsai PS, Garcia-Gil N, Brewis IA, Gadella BM. Theriogenology Volume 70, Issue 8 2008 1188 – 1196

Sperm head membrane reorganisation during capacitation; Gadella BM, Tsai PS, Boerke A, Brewis IA. International Journal of Developmental Biology Volume 52 2008, 473:480

1. INTRODUCTION TO SPERM CAPACITATION

When mammalian sperm cells are ejaculated, they are initially unable to fertilize the oocyte. *In vivo*, sperm are activated and acquire fertilizing potential in the female genital tract especially in the isthmus of the oviduct [1, 2]. This process is termed sperm capacitation and can be mimicked by in vitro fertilization (IVF) media that resemble the ionic and nutritional composition of oviduct: (i) diluted semen is washed through a discontinuous density gradient for almost complete removal of seminal plasma components (decapacitation factors [3]); (ii) the capacitation medium contains high (>15 mM [2, 4]) concentrations of bicarbonate (HCO_3^-) compared to the bicarbonate concentrations in the ejaculate (<5 mM) [5]; (iii) for proper zona-binding and zona-induced acrosome reaction, millimolar levels of extracellular Ca^{2+} ions are required [6] (note that this is prevented in liquid storage media used for porcine artificial insemination (AI) which contains a high concentration of ethylenediaminetetraacetic Acid (EDTA) and thus scavenges all extracellular Ca^{2+}) [7]; and (iv) IVF media contain fatty acid free albumin that specifically extracts free sterols from the surface of capacitating sperm (note that lipoproteins present in the bovine oviduct fluid are supposed to act similarly) [8,9].

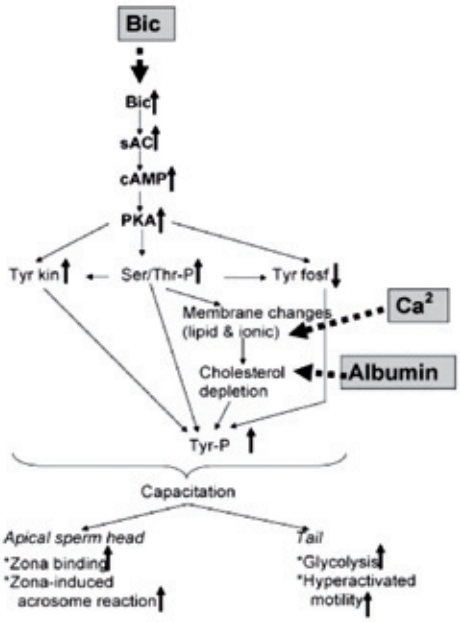

Figure 1. Capacitation-dependent signaling in mammalian sperm cells.

The predominant *in vitro* capacitation factors are indicated in grey textboxes and their role in the capacitation-induced responses is indicated with a broken thick arrow. Abbreviations used: Bic = bicarbonate; sAC = soluble adenylate cyclase; PKA = protein kinase A; Tyr kin = protein tyrosine kinase; Ser/Thr-P = protein serine/threonine phosphorylation; Tyr fosf = protein tyrosine phosphatase; Tyr-P = protein tyrosine phosphorylation. Thin arrows indicate how the capacitation events are linked to each other; up regulation is indicated with an thick upward arrow, whereas inhibition is indicated with a thick downward arrow.

Over the last two decades, various research groups have reported that the sperm cell surface undergoes changes during sperm capacitation (for reviews see Refs. [10,11]). For a summary of the major capacitation factors as well as their effects on sperm cell signaling pathways involved in sperm capacitation see Fig. 1. This general introduction provides an overview of the current knowledge about the organization of the sperm cell plasma membrane. It will deal with the influence of the above mentioned capacitation factors on sperm cell signaling cascades, their effects on the sperm surface organization. The consequences of capacitation in sperm cell physiology will be discussed in terms of i) hyperactivated sperm motility, ii) zona-binding and iii) the zona-induced acrosome reaction. These three different sperm cell transitions need to act in a concerted and coordinated fashion to allow the sperm cell to penetrate the zona pellucida (ZP) and, therefore, enable the sperm cell to fuse with the oolemma and thus fertilize the oocyte.

2. CAPACITATION FACTORS INDUCE HYPERACTIVATED SPERM MOTILITY

Bicarbonate is postulated to enter the sperm cell either by a HCO_3^-/Na^+ co-transporter [12] or by an HCO_3^-/Cl^- anion antiport exchanger [13-15]. Intracellular HCO_3^- subsequently binds to a soluble forskolin-insensitive soluble adenylyl cyclase (sAC) in a stoichiometry of 1:1 [16]. After bicarbonate binding the sAC becomes activated and produces cAMP that in turn activates protein kinase A (PKA) which phosphorylates serine and threonine residues on certain proteins [17,18]. In a Ca^{2+} free medium the bicarbonate effect can be reversed by the depletion of bicarbonate (transient activation of PKA). The bicarbonate-responsive sperm cells require both albumin and Ca^{2+} for the removal of surface cholesterol [8]. The removal of cholesterol will be discussed in the next paragraphs. This removal causes additional and sustained (synergistic) activation of PKA, which is irreversible [18]. As a result of this PKA activation, tyrosine phosphorylation of a number of proteins occurs. Serine phosphorylation of A-kinase anchoring proteins (AKAP-3) is of specific interest as it is a protein that is present in the outer dense fibers of the sperm cell's flagellum [19]. AKAP-3 is suggested to be involved in linking the PKA signaling pathway with the activation of tyrosine kinase that causes extensive tyrosine phosphorylation of proteins in the sperm tail [20]. The altered protein phosphorylation status of tail proteins is believed to be required for obtaining hyperactivated sperm motility and probably coincide with the induction of glycolytic metabolism [21].

Although there is consensus that the cAMP/PKA pathway plays a major role in the increase in protein tyrosine phosphorylation, with the above-described activating role Ca^{2+} and HCO_3^- influx into the sperm cell's interior, other protein kinases have also been found in the sperm cell [22]. For instance, protein kinase C (PKC) isoforms are present in the sperm cell. It has been reported that phorbol esters used to stimulate PKC changed sperm cell motility, the acrosome reaction, and cAMP levels [22]. Other serine/threonine protein kinases identified are *e.g.* the extracellular-signal-regulated kinases 1 or 2 (ERK1/2); glycogen synthase kinase 3 (GSK3); calmodulin-dependent protein kinase IV; casein kinase II or members of the testis-specific serine kinase family [22]. It is also interesting to note

that that cholesterol efflux stimulates protein proline phosphorylation [22]. These results together indicate that multiple pathways are active during sperm capacitation.

3. CAPACITATION FACTORS INDUCE MEMBRANE FLUIDITY CHANGES AT THE SPERM SURFACE

The activation of the sperm cell by bicarbonate/ Ca^{2+}/ albumin also causes sperm cell surface alterations [23]. The sperm cell surface changes elicited by *in vitro* capacitation are often described as a process in which a part of the extracellular coating of the sperm cell (including decapacitation factors) is removed and some sperm activation factors are adsorbed. Albumin mediates the removal of cholesterol, demonstrating that the sperm cell plasma membrane also undergoes changes in lipid composition and consequently alters its membrane fluidity characteristics.

The changes in the sperm head plasma membrane of bicarbonate-responsive cells can be monitored by labeling sperm with specific surface stains such as chlortetracycline [24], merocyanin [25] or filipin [8, 26]. These membrane dyes detect fluidity changes in capacitating sperm [10, 11]. The altered staining patterns correlate with the increased amount of protein tyrosine phosphorylation in the sperm tail and thus to cells with hyperactivated motility [27]: when sperm cells responsive to bicarbonate/ albumin/ Ca^{2+} were measured in a flow cytometer, they all showed extensive protein tyrosine phosphorylation in the sperm tails, whereas non-responsive living cells had no protein tyrosine phosphorylation in the sperm tails. Therefore, both the sperm cell surface responses and hyperactive motility induction occur in the same sperm cell subpopulation and are likely to be mediated by the same signaling events.

The effector enzymes responsible for causing membrane changes have not been identified directly. Two candidates have been suggested: (i) a phospholipid scramblase (human PLSCR2 [27]), since phospholipid scrambling activity has been demonstrated for capacitating sperm [28, 29]; and (ii) a sterol transporter (resembling the scavenger receptor B type 1 [8]) allowing monomeric cholesterol transport to a cholesterol accepting extracellular entity (for *in vitro* fertilization media this is fatty acid free albumin). However, whether or not phospholipid scrambling is a prerequisite for albumin-dependent sterol removal from the surface of activated sperm as proposed in [30] or whether albumin-dependent removal of cholesterol initiates phospholipid scrambling is still a matter of debate. The two scenarios can be summarized as follows: (i) the cholesterol efflux is responsible for the activation of the protein kinase A (PKA) pathway and this induces subsequent phospholipid scrambling (as proposed in [22]) or (ii) PKA pathway activation induces phospholipid scrambling which allows albumin-dependent cholesterol removal at the sperm cell surface [30].

Remarkably, albumin exclusively extracts free sterols (desmosterol and cholesterol) from the sperm cell surface [31]). These rather hydrophobic lipids most likely do not passively diffuse from the sperm surface into the hydrophobic pocket of albumin. Therefore, a model was proposed in which cholesterol transfer from the sperm surface to a hydrophobic pocket of albumin is mediated by an active protein-mediated transport of sterol monomers [31].

4. FUNCTIONAL HETEROGENEITY OF THE SPERM SURFACE

The sperm cell, as a terminally differentiated entity, contains specific morphological features that can be divided into three regions (see Fig. 2): (1) the sperm head which contains a large secretory vesicle called the acrosome and the condensed nucleus containing the male haploid genome; (2) the mid-piece containing the proximal and immobile part of the flagellum and a number of mitochondria responsible for respiration and the generation of aerobic metabolism and energy supply; and (3) the tail with the distal and motile part of the flagellum, additional dense fibers, and elastic fibrous sheath containing cytoskeletal structures surrounding the micro-tubular structures of the flagellum. The specific properties of the flagellum itself and additional structures, as well as the phosphorylation status of proteins within these structures determine the motility patterns of sperm [18, 32].

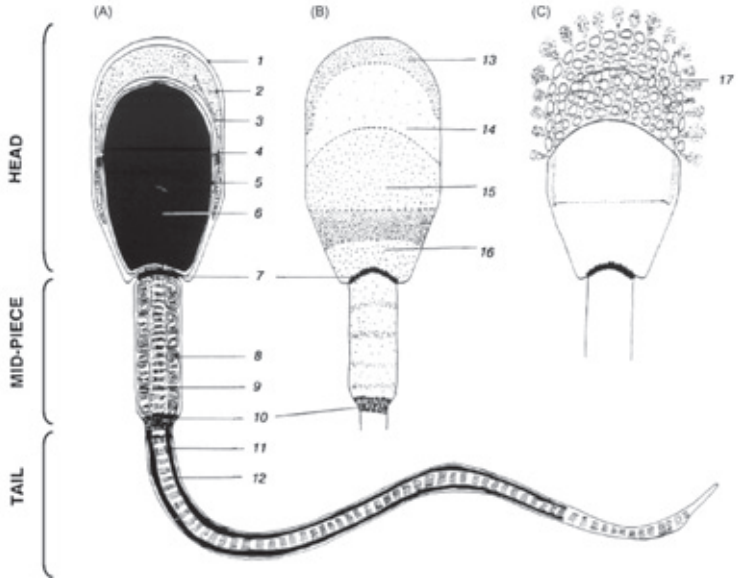

Figure 2. Schematic representation of the boar sperm cell.

(Panel A) A sectional view of the sperm cell. All thin solid lines represent membrane bilayers. 1, plasma membrane; 2, outer acrosomal membrane; 3, acrosomal enzyme matrix; 4, inner acrosomal membrane; 5, nuclear envelope; 6, nucleus; 7, posterior ring and neck; 8, mitochondria; 9, proximal part of the flagellum; 10, annular ring; 11, fibrous sheath; 12, axoneme + outer dense fibers. (Panel B) A surface view of the sperm head and mid-piece with the subdomains. 13, apical ridge; 14, pre-equatorial; 15, equatorial; 16, post-equatorial; (Panel C) The acrosome reaction, (17) represented by formation of mixed vesicles during the acrosome reaction via multiple fusions between the plasma membrane and the outer acrosomal membrane. Note that the equatorial subdomain is not involved in such fusions.

The three sperm cell regions are separated from each other at the sperm surface by two trans-membrane protein ring structures. The posterior and annular rings separate the mid-piece from the

head and tail, respectively (see Fig. 2). Both ring structures are supposed to prevent lateral diffusion of plasma membrane components from the mid-piece to other surface areas and can be considered as a ring-like tight-junction [10].

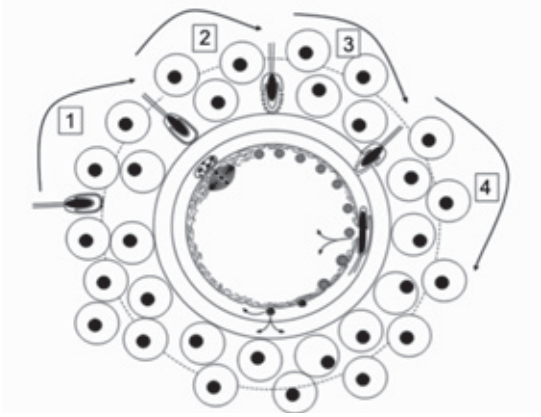

Figure 3. The classical proposed sequence of events around fertilization related to sperm cell–zona interactions. Spermatozoa that have entered the oviduct will shed decapacitation factors that were adhered peripherally to the sperm surface. During this process, the acrosome docks to the sperm cell plasma membrane at the docking area, resulting in the formation of high-affinity zona binding complexes [69-71] (1) It is not clear whether an association between the spermatozoa and the extracellular matrix of the expanded cumulus mass (here represented as a 2-cell layer but, in reality, composed of more cell layers) surrounding the unfertilized oocyte results in the induction of some early steps of acrosomal fusion (as proposed by Jin et al. 2011[72]) or whether acrosome-intact spermatozoa penetrate through the cumulus due to their hyperactive motility in combination with surface proteins [79,80]. Oviductal-secreted proteins have also been reported as important in determining the properties of the cumulus and zona pellucida [73]. (2) Recognition of the zona pellucida (primary zona binding to the zona pellucida (ZP) proteins ZP3/ZP4; [74] and subsequent initiation of the acrosome reaction (or of the acute secretory phase of it; see 1) that is induced by the ZP. (3) The acrosome reaction causes local modifications of zona proteins and the hyperactivated spermatozoa can penetrate this structure due to secondary zona binding (to ZP2). The surface of the penetrating spermatozoa will be further remodeled and this probably enables fertilization fusion [30]). (4) Immediately after fertilization fusion, the cortical reaction results in overall coating of the oolemma, as well as the hardening of ZP, by chemically altering the zona proteins; in particular, cleavage of ZP2 appears to be instrumental for the release of spermatozoa from the ZP and for efficient block of polyspermy (Modified from Tsai and Gadella 2009.) [75].

The sperm head surface possesses lateral surface heterogeneity (see Fig. 2 and for review [10]). In the literature, the boar sperm head surface area is divided into the apical ridge area, the pre-equatorial area, the equatorial area (together the entire acrosome region), and the post-acrosomal area. From a functional perspective, one can appreciate the existence of such sperm head surface domains (see Fig. 3): (1) sperm cell binding to the zona pellucida is initiated to a restricted surface area of the sperm head at the apical ridge; (2) the intracellular membrane fusions involved in the acrosome reaction take place at the acrosomal ridge and pre-equatorial membrane area of the sperm head; and (3) the remaining equatorial plasma membrane is the specific site of the sperm cell that, after zona penetration, becomes involved in oolemma binding and causes fusion at

fertilization. If these three events were organized in different regions of the sperm cell, they would render the sperm cell infertile (incapable of reaching and fusing with the oolemma) [31]. However, when observing freeze–fracture replicas of boar sperm cells, no ultrastructural diffusion barriers were observed in the sperm head [33]. In other words, no ultrastructural barriers that could account for the maintenance of the membrane microdomains were observed. Thus, the functional sperm head membrane heterogeneity remains an enigma for membrane biologists.

5. MEMBRANE MODELS AND SPERM CELL MEMBRANE HETEROGENEITY

In the early 1970s, the Singer–Nicholson model of the fluid-mosaic membrane was proposed to predict the construction of cellular membranes [34]. In this model, the membrane is organized as a bilayer of phospholipids with the hydrophobic moieties (acyl chains) arranged next to each other and the hydrophilic part (the phosphate head groups) either at the cytoplasmic plasma monolayer or at the extracellular monolayer (luminal monolayer for intracellular membranes). Cholesterol also behaves as an amphipathic molecule in the membrane bilayer and the free hydroxyl group in cholesterol can be considered as the hydrophilic part and the steroid backbone as the hydrophobic part. Due to the flat structure of this steroid part, cholesterol stabilizes the membrane bilayer [35].

In the mid-1970s, it was first described that membrane phospholipids were asymmetrically distributed over the membrane lipid bilayer, with the aminophospholipids (phosphatidylserine and phosphatidylethanolamine) enriched in the inner monolayer, whereas choline phospholipids (sphingomyelin and phosphatidylcholine) glycolipids were enriched in the outer mono- layer [36, 37]. Active phospholipid translocases serve to maintain or to scramble the phospholipid asymmetry (for a review see [38]). It was also recognized that a large proportion of the lipids and membrane proteins had lateral mobility [39]. For most cells, their membrane lipids were fluid at physiological conditions and the degree of fluidity depended on the degree of acyl chain length saturation and the amount of cholesterol, as well as on the temperature [40, 41]. Below the phase transition temperature, fluid membrane lipids freeze into a crystalline phase causing lateral phase separation from membrane lipids with still fluid properties (for a more recent review see [42]). The other cause for lipid immobilization is their attachment either cytoskeletal or extracellular matrix components (for models see [18]).

The Singer–Nicholson model predicts that intrinsic membrane proteins also have free lateral diffusion properties whure 5rrols ng enzymesl generated by enzymes isen unbound to the extracellular matrix or the cytoskeleton, albeit with slower diffusion speed due to their larger sizes when compared to the membrane lipids [43]. Therefore, it was surprising in the 1990s that not only sperm membrane proteins [44], but also glycolipids [45, 46] and cholesterol [8] did not randomly diffuse over the sperm head, but emerge in specific domains of the sperm head (see Section 6). Moreover, sperm capacitation led to a redistribution of these proteins [47] and lipids (reviewed in [10]) into other domains of the sperm head in the same living and acrosome-intact sperm cells. For

example, seminolipid moved from the apical ridge towards the equatorial domain of the sperm head [45, 46]. This negatively charged glycolipid is believed to prevent intracellular fusion and a potential explanation for its migration is that it serves to prevent the acrosome reaction in the apical ridge area during ejaculation, while it prevents the equatorial plasma membrane fusion with the outer acrosomal membrane in the equatorial segment formed after the acrosome reaction. This is important because this structure needs to be maintained to bind and fuse with the oolemma. The retrograde movement and concentration of cholesterol [8] into the area where the sperm cell plasma membrane does fuse with the outer acrosomal membrane is also not easily explained in the Singer–Nicholson model.

6. MEMBRANE MICRODOMAINS AND SPERM SURFACE HETEROGENEITY

In the mid-1990s, the fluidity of cellular membranes at physiological temperature was refined by the concept of membrane microdomains containing specific lipids and proteins. In the so-called lipid raft model, small lipid-ordered microdomains were supposed to contain larger proportions of cholesterol, sphingomyelin, gangliosides and phospholipids with saturated long-chain acyl chains, as well as post-transcriptionally lipid-modified proteins such as GPI-anchored proteins and sterol or acyl-modified proteins (for a review see [48]). A questionable [46] but widespread method to isolate these lipid-ordered membrane domains was to subject cells or cell homogenates to a low-ionic detergent at 4 degrees Celsius (see Fig. 4). The non-raft fraction is dissolved by detergent (often Triton X-100), whereas the fraction supposed to resemble the membrane raft remains undissolved. This so-called detergent-resistant membrane (DRM) fraction can be isolated by discontinuous sucrose gradients [49].

DRMs are enriched in membrane-associated proteins that are considered to be raft marker proteins. Two of them, caveolin-1 and flotillin-1 [50, 51], were also shown to be present in sperm [31]. The sperm DRM fraction is also enriched in cholesterol and can be dissolved by cholesterol-disrupting agents, indicating that the DRM of sperm is comparable to that of MDCK cells or other cell lines [52]. Interestingly, caveolin-1 and flotillin-1 were predominantly localized in the area of the sperm cell that is involved in sperm-zona binding and in the zona-induced acrosome reaction [31]. This notion, together with the finding that cholesterol redistribution to this area takes place followed by an albumin-mediated depletion of cholesterol (20-40% of total sperm cholesterol [8]), led to a closer examination of the organization of lipid microdomains in sperm under *in vitro* capacitation/fertilization conditions. Both flotillin-1 and caveolin-1 migrated from the entire acrosome overlying plasma membrane towards the apical ridge area [31]. This process also involved multimerization of caveolin-1, which indicates that sperm rafts aggregate in this membrane area. There are indications that under the changed lateral organization of these lipid microdomains, albumin extracts cholesterol only from the non-DRM membrane area [76]. Perhaps the altered lipid composition of the fluid phase membrane in capacitation-responsive cells allows lipid microdomain aggregation.

It is not yet clear whether this clustering also depends on the altered phospholipid asymmetry and the composition and topographic arrangement of extracellular components attached to the sperm cell surface. Attempts have been made to induce cholesterol depletion from sperm cells by artificial cholesterol acceptors. High levels of methyl-beta-cyclodextrin (a well-known cholesterol depleting agent), was spermicidal to porcine sperm cells [52]. It caused cholesterol depletion from the DRM and the Triton X-100 soluble sperm lipid fraction, as well as disruption of the DRM,,consistent with observations from the group of Jones [53]. The use of 2-hydroxypropyl-cyclodextrin (with lower affinity for free sterols causing a more mild cholesterol depletion) caused some signs of sperm capacitation in animal species with higher cholesterol levels in sperm cells [54]. Both cyclodextrins resulted in low *in vitro* fertilization rates at a very narrow concentration range (in absence of albumin). However, under these conditions the cyclodextrins also induced oocyte deterioration [78]

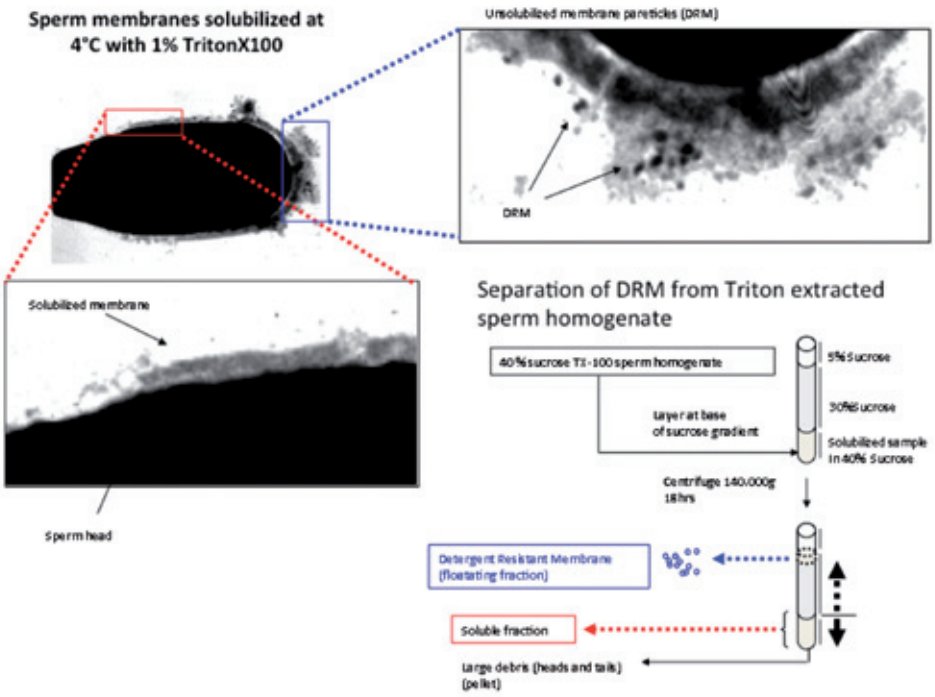

Figure 4. Procedure to isolate the DRM fraction from porcine sperm cells.

The upper left panel shows the sperm cells head imaged by transmission electron microscopy. The boxes in this panel refer to either solubilized membrane lower zoom panel or non-solubilized membrane (upper right panel). Separation of the solubilized or the DRM fraction is achieved by layering the solubilized sperm sample in Triton X-100 in a final concentration of 40% sucrose on top of this a layer of 30% sucrose is added and the last layer consist of 5% sucrose. After centrifugation of 18 hours at 140.000*g* the DRM is present in the interface between 5-30% sucrose.

7. AGGREGATION OF LIPID MICRODOMAINS AND FERTILIZATION

The presence of the capacitation factors albumin, bicarbonate and Ca^{2+} evokes reversible and irreversible cell signaling responses to a subpopulation of sperm cells (the responding cells). Capacitating sperm cells have signs of hyperactivated motility and surface remodeling. Recently advances have been made in the understanding of lipid microdomains in a variety of cell types [49, 50]. These developments demonstrated that one of the surface changes taking place in the capacitating sperm sub-population, the aggregation of lipid microdomains in the apical ridge area of the sperm head, also appears to be required for the generation of hyperactivated motility [30,31]. The aggregated lipid microdomains are highly enriched in proteins that are involved in the primary binding of the zona pellucida and in proteins that are involved in the acrosome docking and reaction [31].

8. SPERM CAPACITATION AND REACTIVE OXYGEN SPECIES.

One of the interesting observations in recent years is the bimodal effects of oxidative stress on sperm cells: not only detrimental effects were observed which should be avoided, but also stimulatory effects were reported on capacitating sperm cells [55, 56]. High levels of reactive oxygen species (ROS), especially H_2O_2, have harmful effects on important sperm functions such as membrane integrity, cell viability, and motility [56]. On the other hand, it has become clear that mild ROS production has a positive effect on the capacitation of sperm and the subsequent acrosome reaction [57]. ROS has been described as one of the regulators that influence protein tyrosine phosphorylation [55] which, as described above, is an indicator of sperm cell capacitation. ROS has also been hypothesized to activate PKA and the ERK pathways, both acting independently on the modulation of protein tyrosine phosphorylation. [55].

Although capacitation leads to the formation of ROS in sperm it is not known how raft dynamics and membrane fluidity is regulated during sperm capacitation and which role ROS plays in this process. The reported increase in membrane fluidity and exact mechanism behind the efflux of cholesterol from the membrane is still unknown. Interestingly, cholesterol is a substrate for enzymatic oxidation with oxysterols as a final product and can be regarded as a reactive oxygen species [58, 59]. The cholesterol molecule can be divided into three regions: i) a lateral chain composed of hydrocarbons, ii) a four hydrocarbon ring structure (termed A, B, C and D) and iii) a hydroxyl group (Fig. 5). The B hydrocarbon ring and its double bond is the most sensitive for auto-oxidation and therefore one of the most common targets for free radical attack. The auto-oxidation of the B hydrocarbon ring leads to different species of oxysterols, 7α and 7β-hydroxycholesterol, 7-ketocholesterol, 5α, 6α epoxycholesterol, 5α, 6β epoxycholesterol and cholestane-3β, 5α, 6β –triol [63]. The formed oxysterols are more polar compounds as compared to cholesterol. Oxysterols are known to cause lateral membrane expansion, reduce the size of the membrane bilayer and thus cause higher membrane permeability (Fig. 6).

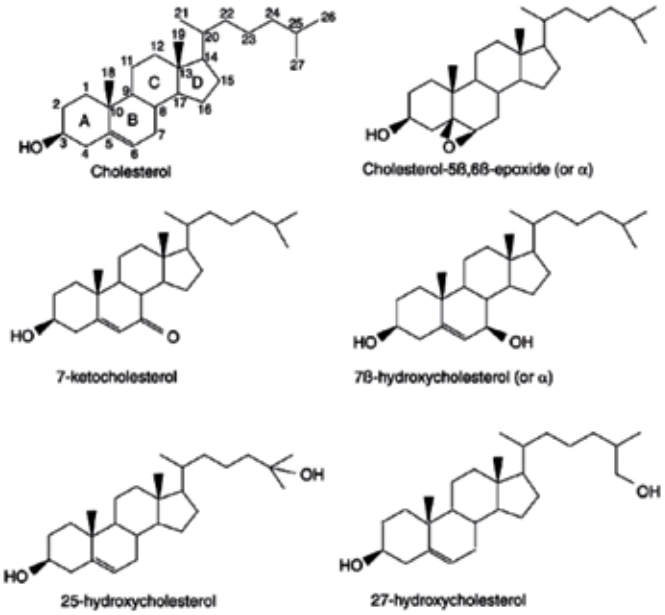

Figure 5. Structure of cholesterol and the major oxysterols resulting from auto-oxidation (7-ketocholesterol; 7α-hydroxycholesterol, and its enantiomer 7β-hydroxycholesterol, cholesterol-5α, 6α-epoxide and its enantiomer cholesterol-5β,6β-epoxide) and enzymatic oxidation of the 25-hydroxycholesterol and 27-hydrocholesterol are also enzymatic products from respectively cholesterol 25-hydroxylase and 27-hydroxylase (CYP27). Adapted from [63]

Table 1. Oxysterol forming enzymes. The distribution and subcellular localization for different enzymes capable of oxidizing cholesterol (CYP- cytochrome P450), adapted from Vejux et al. [63]

	Cellular Distribution	**Subcellular localization**	**Oxysterols**
24-hydroxylase (CYP46A1)	Neurons, neural retina, Hepatocytes	Endoplasmatic Reticulum and Golgi apparatus	24S-hydroxycholesterol
25-hydroxylase	Hepatocytes	Endoplasmatic Reticulum and Golgi apparatus	25-hydroxycholesterol
27-hydroxylase (CYP27)	Hepatocytes Macrophages Endothelial cells	Mitochondria	27-hydroxycholesterol
7α-hydroxylase (CYP7A1)	Hepatocytes Ovary cells	Endoplasmatic Reticulum	7α-hydroxycholesterol
CYP3A4	Hepatocytes	Microsomes	4β-hydroxycholesterol
11β-hydroxysteroid dehydrogenase type-1	Hepatocytes	Microsomes	7-ketocholesterol, 7β-hydroxycholesterol

Due to this the thickness differences cellular membranes they are thought to aid in sorting membrane proteins to their intended place in the membrane [59-62]. Auto-oxidation is not the only process forming oxysterols. There are also enzymes capable of changing cholesterol into oxysterols. Species of oxysterols generated by enzymes are 24S-hydroxycholesterol, 25-hydroxycholesterol 27-hydroxycholesterol and 7α-hydroxycholesterol (see table 1 for matching enzymes) [63]. Oxysterols have been shown to be important in processes related to cholesterol turnover, atherosclerosis and apoptosis among others [62]. The current consensus is that the oxysterols are physiological mediators involved in cholesterol-induced metabolic effects.

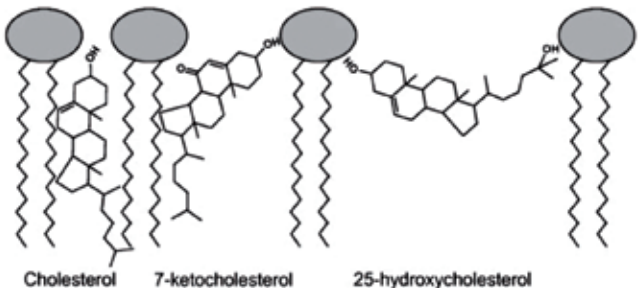

Figure 6. Cholesterol and oxysterol behaviour in model membranes.

The additional added hydroxyl groups cause another topology of the oxysterols in the lipid bilayer (here only drawn for the outer monolayer). Oxysterols are increasingly reoriented more to the polar headgroup side when compared to their native cholesterol molecules. Adapted from [60]

9. SCOPE OF THIS THESIS

It has been described extensively that sperm cell capacitation involves the release of glycocalyx components (decapacitation factors) and cholesterol [77]. During this process the responsive sperm cells also face a complex surface remodeling required for optimal zona binding properties and for preparation of the acrosome reaction [69, 71]. In this thesis the removal of sperm surface components is studied in detail with special emphasis on the relation of this removal with surface remodeling specific for *in vitro* capacitating sperm cells. The mechanism of cholesterol depletion has been investigated in chapters 2 and 3. Subsequently, effects of enzymatic removal of the protein part of GPI-anchored proteins are investigated (Chapter 4). Finally in chapter 5, a new wet mounting atomic force microscopical technique has been employed for detection of ultra structural changes occurring at the sperm cell surface during capacitation and after the induction of the acrosome reaction.

In chapter 2 bovine sperm cells were incubated in several ways to investigate whether these incubations led to the formation of oxysterols. The experimental conditions relate to common commercial bovine sperm processing such as those used for cryopreservation (freeze thawing of

sperm for AI) or as used for *in vitro* embryo production (capacitation). In addition active pro-oxidants were tested for detection of auto-oxidation of cholesterol in sperm cells.

In chapter 3 we studied oxysterol formation more specifically under varying *in vitro* capacitation conditions in porcine and mouse sperm. Detailed information was gathered on the effects of pro-oxidants and hydrophobic anti-oxidants on modulatory effects of sperm capacitation-dependent cholesterol depletion and their relation to oxysterol formation. Moreover, the effect of a specific family of oxysterol binding proteins (OBPs) on sperm capacitation-dependent cholesterol depletion and oxysterol formation was studied. Hypothetically, OBPs might influence (oxy)sterol depletion and/or have a scavenging role by inhibiting the propagation of oxysterol formation.

In chapter 4 a membrane raft enriched group of molecules (beyond the sterols) namely the GPI-anchored proteins was investigated. Sperm cells contain different types of GPI-anchored proteins and some are thought to be involved in the process of fertilization while others are involved in protecting the sperm cell against the foreign immune system [65, 66]. Recently, it has been described that GPI-anchored proteins are removed from the sperm cell surface during capacitation and that this is due to the activation of an endogenous surface enzyme called angiotensin converting enyme (AcE) [67]. In fact, knockout mice for this gene were infertile [67] indicating the importance of GPI-anchored protein removal for fertilization. Another way to cleave GPI-anchored proteins is to add exogenous phosphatidylinositol specific phospholipase C (PI-PLC). In chapter 4 both the autonomous release of GPI anchored proteins during *in vitro* capacitation as well as the PI-PLC induced cleavage of these proteins from the sperm surface have been compared. The effects on sperm membrane raft aggregation, capacitation, acrosome reaction, fertilizing capability and cell integrity were studied.

In chapter 5 we have applied a novel wet mount atomic force microscopical (AFM) technique in order to scan ultrastructural features of the sperm surface with a nanometer sized cantilever tip. Sperm cells were first incubated in media supporting capacitation or inducing the acrosome reaction. The incubated samples were immobilized by chemical fixation and spun down in buffer on a solid glass support. Sperm cells revealed to be a very suitable candidate for wet mount AFM because sperm heads are extremely flat and rigid when compared to other biological cell types [68]. The advantage of this technique, in comparison with transmission or scanning electron microscopical techniques, is that it allows studying the sperm cell surface properties in an environment that resembles the natural environment of sperm (under buffer conditions). Functional activation of the cantilever tip (for instance by covalently linking bioactive groups such as monoclonal antibodies) allows surface interaction mapping of the cantilever tip and the recognized sperm cell surface epitope. Moreover, the wet mount AFM technique reveals superior resolution of specific structural organization at the scanned cell surface compared to the required dehydration procedures involved in electron microscopy and for conventional AFM. We studied with this novel AFM technique the surface remodeling of the equatorial segment during capacitation and after the acrosome reaction. It is likely that the observed sperm cell surface phenomena relate to the preparation of the sperm for fertilization, as this process is unique for the equatorial segment.

Chapter 6 summarizes the results described in this thesis and discusses the possible implications for the fertilization process and the relevance for AI and IVF. Moreover, the obvious experimental next steps that are required to validate, establish and apply the findings of this thesis are discussed.

REFERENCES

1. Rodriguez-Martinez H, Saravia F, Wallgren M, Tienthai P, Johannisson A, Vazquez JM, Martinez E, Roca J, Sanz L, Calvete JJ. Boar spermatozoa in the oviduct. Theriogenology 2005; 63:514-535.

2. Tienthai P, Johannisson A, Rodriguez-Martinez H. Sperm capacitation in the porcine oviduct. Anim Reprod Sci 2004; 80:131-146.

3. Fraser LR, Adeoya-Osiguwa SA, Baxendale RW, Gibbons R. Regulation of mammalian sperm capacitation by endogenous molecules. Front Biosci 2006; 11:1636-1645.

4. Rodriguez-Martinez H, Tienthai P, Suzuki K, Funahashi H, Ekwall H, Johannisson A. Involvement of oviduct in sperm capacitation and oocyte development in pigs. Reprod Suppl 2001; 58:129-145.

5. Rodriguez-Martinez H, Ekstedt E, Einarsson S. Acidification of epididymal fluid in the boar. Int J Androl 1990; 13:238-243.

6. Darszon A, Lopez-Martinez P, Acevedo JJ, Hernandez-Cruz A, Trevino CL. T-type Ca2+ channels in sperm function. Cell Calcium 2006; 40:241-252.

7. Johnson LA, Aalbers JG, Willems CM, Rademaker JH, Rexroad CE,Jr. Use of boar spermatozoa for artificial insemination. III. Fecundity of boar spermatozoa stored in Beltsville liquid and Kiev extenders for three days at 18 C. J Anim Sci 1982; 54:132-136.

8. Flesch FM, Brouwers JF, Nievelstein PF, Verkleij AJ, van Golde LM, Colenbrander B, Gadella BM. Bicarbonate stimulated phospholipid scrambling induces cholesterol redistribution and enables cholesterol depletion in the sperm plasma membrane. J Cell Sci 2001; 114:3543-3555.

9. Ehrenwald E, Foote RH, Parks JE. Bovine oviductal fluid components and their potential role in sperm cholesterol efflux. Mol Reprod Dev 1990; 25:195-204.

10. Flesch FM, Gadella BM. Dynamics of the mammalian sperm plasma membrane in the process of fertilization. Biochim Biophys Acta 2000; 1469:197-235.

11. Harrison RA, Gadella BM. Bicarbonate-induced membrane processing in sperm capacitation. Theriogenology 2005; 63:342-351.

12. Demarco IA, Espinosa F, Edwards J, Sosnik J, De La Vega-Beltran JL, Hockensmith JW, Kopf GS, Darszon A, Visconti PE. Involvement of a Na+/HCO-3 cotransporter in mouse sperm capacitation. J Biol Chem 2003; 278:7001-7009.

13. Jacob P, Rossmann H, Lamprecht G, Kretz A, Neff C, Lin-Wu E, Gregor M, Groneberg DA, Kere J, Seidler U. Down-regulated in adenoma mediates apical Cl-/HCO3- exchange in rabbit, rat, and human duodenum. Gastroenterology 2002; 122:709-724.

14. Mistrik P, Daudet N, Morandell K, Ashmore JF. Mammalian prestin is a weak Cl(-)/HCO(3)(-) electrogenic antiporter. J Physiol 2012; 590:5597-5610.

15. Mogas MT, Alamo MR, Rodriguez-Gil JE. Roles of Na(+)/K(+)-dependent ATPase, Na(+)/H(+) antiporter and GLUT hexose transporters in the cryosurvival of dog spermatozoa: effects on viability, acrosome state and motile sperm subpopulation structure. Theriogenology 2011; 75:1669-1681.

16. Okamura N, Tajima Y, Soejima A, Masuda H, Sugita Y. Sodium bicarbonate in seminal plasma stimulates the motility of mammalian spermatozoa through direct activation of adenylate cyclase. J Biol Chem 1985; 260:9699-9705.

17. Gadella BM, van Gestel RA. Bicarbonate and its role in mammalian sperm function. Anim Reprod Sci 2004; 82-83:307-319.

18. Gadella BM, Visconti PE. Regulation of capacitation. In: C. De Jonge, C. Barrett (ed.), The sperm cell production maturation fertilization regeneration, Cambridge UK: Cambridge University Press; 2006: 134-169.

19. Ficarro S, Chertihin O, Westbrook VA, White F, Jayes F, Kalab P, Marto JA, Shabanowitz J, Herr JC, Hunt DF, Visconti PE. Phosphoproteome analysis of capacitated human sperm. Evidence of tyrosine phosphorylation of a kinase-anchoring protein 3 and valosin-containing protein/p97 during capacitation. J Biol Chem 2003; 278:11579-11589.

20. Leclerc P, de Lamirande E, Gagnon C. Cyclic adenosine 3',5'monophosphate-dependent regulation of protein tyrosine phosphorylation in relation to human sperm capacitation and motility. Biol Reprod 1996; 55:684-692.

21. Miki K. Energy metabolism and sperm function. Soc Reprod Fertil Suppl 2007; 65:309-325.

22. Visconti PE, Krapf D, de la Vega-Beltran JL, Acevedo JJ, Darszon A. Ion channels, phosphorylation and mammalian sperm capacitation. Asian J Androl 2011; 13:395-405.

23. Yanagimachi R. Mammalian fertilization. In: Knobil E and Neill JD (eds.), The physiology of reproduction, 2nd ed. New York, USA: Raven Press; 1994: 189.

24. Mattioli M, Barboni B, Lucidi P, Seren E. Identification of capacitation in boar spermatozoa by chlortetracycline staining. Theriogenology 1996; 45:373-381.

25. Harrison RA, Ashworth PJ, Miller NG. Bicarbonate/CO2, an effector of capacitation, induces a rapid and reversible change in the lipid architecture of boar sperm plasma membranes. Mol Reprod Dev 1996; 45:378-391.

26. Suzuki-Toyota F, Itoh Y, Naito K. Reduction of intramembranous particles in the periacrosomal plasma membrane of boar spermatozoa during in vitro capacitation: a statistical study. Dev Growth Differ 2000; 42:265-273.

27. de Vries KJ, Wiedmer T, Sims PJ, Gadella BM. Caspase-independent exposure of aminophospholipids and tyrosine phosphorylation in bicarbonate responsive human sperm cells. Biol Reprod 2003; 68:2122-2134.

28. Gadella BM, Harrison RA. The capacitating agent bicarbonate induces protein kinase A-dependent changes in phospholipid transbilayer behavior in the sperm plasma membrane. Development 2000; 127:2407-2420.

29. Gadella BM, Harrison RA. Capacitation induces cyclic adenosine 3',5'-monophosphate-dependent, but apoptosis-unrelated, exposure of aminophospholipids at the apical head plasma membrane of boar sperm cells. Biol Reprod 2002; 67:340-350.

30. Tsai PS, Gadella BM. Molecular kinetics of proteins at the surface of porcine sperm before and during fertilization. Soc Reprod Fertil Suppl 2009; 66:23-36.

31. van Gestel RA, Brewis IA, Ashton PR, Helms JB, Brouwers JF, Gadella BM. Capacitation-dependent concentration of lipid rafts in the apical ridge head area of porcine sperm cells. Mol Hum Reprod 2005; 11:583-590.

32. Marin-Briggiler CI, Jha KN, Chertihin O, Buffone MG, Herr JC, Vazquez-Levin MH, Visconti PE. Evidence of the presence of calcium/calmodulin-dependent protein kinase IV in human sperm and its involvement in motility regulation. J Cell Sci 2005; 118:2013-2022.

33. De Leeuw FE, Chen HC, Colenbrander B, Verkleij AJ. Cold-induced ultrastructural changes in bull and boar sperm plasma membranes. Cryobiology 1990; 27:171-183.

34. Singer SJ, Nicolson GL. The fluid mosaic model of the structure of cell membranes. Science 1972; 175:720-731.

35. Chapman D. Fluidity and phase transitions of cell membranes. Biomembranes 1975; 7:1-9.

36. Verkleij AJ, Zwaal RF, Roelofsen B, Comfurius P, Kastelijn D, van Deenen LL. The asymmetric distribution of phospholipids in the human red cell membrane. A combined study using phospholipases and freeze-etch electron microscopy. Biochim Biophys Acta 1973; 323:178-193.

37. Hakomori S, Igarashi Y. Functional role of glycosphingolipids in cell recognition and signaling. J Biochem 1995; 118:1091-1103.

38. Devaux PF, Lopez-Montero I, Bryde S. Proteins involved in lipid translocation in eukaryotic cells. Chem Phys Lipids 2006; 141:119-132.

39. Scandella CJ, Devaux P, McConnell HM. Rapid lateral diffusion of phospholipids in rabbit sarcoplasmic reticulum. Proc Natl Acad Sci U S A 1972; 69:2056-2060.

40. Blok MC, van der Neut-Kok EC, van Deenen LL, de Gier J. The effect of chain length and lipid phase transitions on the selective permeability properties of liposomes. Biochim Biophys Acta 1975; 406:187-196.

41. Cullis PR. Lateral diffusion rates of phosphatidylcholine in vesicle membranes: effects of cholesterol and hydrocarbon phase transitions. FEBS Lett 1976; 70:223-228.

42. Feigenson GW. Phase behavior of lipid mixtures. Nat Chem Biol 2006; 2:560-563.

43. Cherry RJ. Rotational and lateral diffusion of membrane proteins. Biochim Biophys Acta 1979; 559:289-327.

44. Myles DG, Primakoff P, Bellve AR. Surface domains of the guinea pig sperm defined with monoclonal antibodies. Cell 1981; 23:433-439.

45. Gadella BM, Lopes-Cardozo M, van Golde LM, Colenbrander B, Gadella TW,Jr. Glycolipid migration from the apical to the equatorial subdomains of the sperm head plasma membrane precedes the acrosome reaction. Evidence for a primary capacitation event in boar spermatozoa. J Cell Sci 1995; 108 (Pt 3):935-946.

46. Gadella BM, Gadella T, Colenbrander B, van Golde L, Lopes-Cardozo M. Visualization and quantification of glycolipid polarity dynamics in the plasma membrane of the mammalian spermatozoon. J Cell Sci 1994; 107:2151-2163.

47. Myles DG, Primakoff P. Localized surface antigens of guinea pig sperm migrate to new regions prior to fertilization. J Cell Biol 1984; 99:1634-1641.

48. Simons K, Toomre D. Lipid rafts and signal transduction. Nat Rev Mol Cell Biol 2000; 1:31-39.

49. Lingwood D, Simons K. Detergent resistance as a tool in membrane research. Nat Protoc 2007; 2:2159-2165.

50. Smart EJ, Graf GA, McNiven MA, Sessa WC, Engelman JA, Scherer PE, Okamoto T, Lisanti MP. Caveolins, liquid-ordered domains, and signal transduction. Mol Cell Biol 1999; 19:7289-7304.

51. Bickel PE, Scherer PE, Schnitzer JE, Oh P, Lisanti MP, Lodish HF. Flotillin and epidermal surface antigen define a new family of caveolae-associated integral membrane proteins. J Biol Chem 1997; 272:13793-13802.

52. van Gestel R, Helms JB, Brouwers J, Gadella BM. Effects of methyl-β-cyclodextrin-mediated cholesterol depletion in porcine sperm compared to somatic cells. Mol Reprod Dev 2005; 72:386-395.

53. Shadan S, James PS, Howes EA, Jones R. Cholesterol Efflux Alters Lipid Raft Stability and Distribution During Capacitation of Boar Spermatozoa. Biology of Reproduction 2004; 71:253-265.

54. Parinaud J, Vieitez G, Vieu C, Collet X, Perret B. Enhancement of zona binding using 2-hydroxypropyl- beta-cyclodextrin. Hum Reprod 2000; 15:1117-1120.

55. O›Flaherty C, de Lamirande E, Gagnon C. Positive role of reactive oxygen species in mammalian sperm capacitation: triggering and modulation of phosphorylation events. Free Radic Biol Med 2006; 41:528-540.

56. Aitken RJ, Jones KT, Robertson SA. Reactive oxygen species and sperm function--in sickness and in health. J Androl 2012; 33:1096-1106.

57. Griveau JF, Renard P, Le Lannou D. An in vitro promoting role for hydrogen peroxide in human sperm capacitation. Int J Androl 1994; 17:300-307.

58. Travis AJ, Kopf GS. The role of cholesterol efflux in regulating the fertilization potential of mammalian spermatozoa. J Clin Invest 2002; 110:731-736.

59. Olsen BN, Schlesinger PH, Ory DS, Baker NA. Side-chain oxysterols: from cells to membranes to molecules. Biochim Biophys Acta 2012; 1818:330-336.

60. Olkkonen VM, Hynynen R. Interactions of oxysterols with membranes and proteins. Mol Aspects Med 2009; 30:123-133.

61. Bielska AA, Schlesinger P, Covey DF, Ory DS. Oxysterols as non-genomic regulators of cholesterol homeostasis. Trends Endocrinol Metab 2012; 23:99-106.

62. Bjorkhem I, Diczfalusy U. Oxysterols: friends, foes, or just fellow passengers? Arterioscler Thromb Vasc Biol 2002; 22:734-742.

63. Vejux A, Malvitte L, Lizard G. Side effects of oxysterols: cytotoxicity, oxidation, inflammation, and phospholipidosis. Brazilian Journal of Medical and Biological Research 2008; 41:545-556.

64. Hynynen R, Suchanek M, Spandl J, Back N, Thiele C, Olkkonen VM. OSBP-related protein 2 is a sterol receptor on lipid droplets that regulates the metabolism of neutral lipids. J Lipid Res 2009; 50:1305-1315.

65. Watanabe H, Kondoh G. Mouse sperm undergo GPI-anchored protein release associated with lipid raft reorganization and acrosome reaction to acquire fertility. J Cell Sci 2011; 124:2573-2581.

66. Donev RM, Sivasankar B, Mizuno M, Morgan BP. The mouse complement regulator CD59b is significantly expressed only in testis and plays roles in sperm acrosome activation and motility. Mol Immunol 2008; 45:534-542.

67. Kondoh G, Tojo H, Nakatani Y, Komazawa N, Murata C, Yamagata K, Maeda Y, Kinoshita T, Okabe M, Taguchi R, Takeda J. Angiotensin-converting enzyme is a GPI-anchored protein releasing factor crucial for fertilization. Nat Med 2005; 11:160-166.

68. Jones R, James PS, Howes L, Bruckbauer A, Klenerman D. Supramolecular organization of the sperm plasma membrane during maturation and capacitation. Asian J Androl 2007; 9:438-444.

69. Tsai PS, Garcia-Gil N, van Haeften T, Gadella BM. How pig sperm prepares to fertilize: stable acrosome docking to the plasma membrane. PLoS One 2010; 5:e11204.

70. Tsai PS, Brewis IA, van Maaren J, Gadella BM. Involvement of complexin 2 in docking, locking and unlocking of different SNARE complexes during sperm capacitation and induced acrosomal exocytosis. PLoS One 2012; 7:e32603.

71. van Gestel RA, Brewis IA, Ashton PR, Brouwers JF, Gadella BM. Multiple proteins present in purified porcine sperm apical plasma membranes interact with the zona pellucida of the oocyte. Mol Hum Reprod 2007; 13:445-454.

72. Jin M, Fujiwara E, Kakiuchi Y, Okabe M, Satouh Y, Baba SA, Chiba K, Hirohashi N. Most fertilizing mouse spermatozoa begin their acrosome reaction before contact with the zona pellucida during in vitro fertilization. Proc Natl Acad Sci U S A 2011; 108:4892-4896.

73. Aviles M, Gutierrez-Adan A, Coy P. Oviductal secretions: will they be key factors for the future ARTs? Mol Hum Reprod 2010; 16:896-906.

74. Gupta SK, Bhandari B, Shrestha A, Biswal BK, Palaniappan C, Malhotra SS, Gupta N. Mammalian zona pellucida glycoproteins: structure and function during fertilization. Cell Tissue Res 2012; 349:665-678.

75. Gahlay G, Gauthier L, Baibakov B, Epifano O, Dean J. Gamete recognition in mice depends on the cleavage status of an egg›s zona pellucida protein. Science 2010; 329:216-219.

76. van Gestel R.A. Membrane characteristics of sperm cells during capacitation. PhD Thesis Utrecht University ISBN 90-393-3964-3 Ridderprint Press, the Netherlands, Ridderkerk, pp 133

77. Leahy T, Gadella BM. Sperm surface changes and physiological consequences induced by sperm handling and storage. Reproduction 2011; 142:759-778.

78. Nagao Y, Ohta Y, Murakami H, Kato Y. The effects of methyl-beta-cyclodextrin on in vitro fertilization and the subsequent development of bovine oocytes. Zygote 2010; 18:323-330.

79. Gadella BM, Tsai PS, Boerke A, Brewis IA. Sperm head membrane reorganisation during capacitation. Int J Dev Biol 2008; 52:473-480.

80. Florman HM, Jungnickel MK, Sutton KA. Regulating the acrosome reaction. Int J Dev Biol 2008; 52:503-510.

2

Mass spectrometric detection of cholesterol oxidation in bovine sperm

Jos F. Brouwers[1]
Arjan Boerke[1]
Patrıcia F.N. Silva[2,3]
Nuria Garcia-Gil[1,4]
Renske A. van Gestel[1,5]
J. Bernd Helms[1]
Chris H.A. van de Lest[1,3]
Bart M. Gadella[1,2,3]

Departments of Biochemistry and Cell Biology[1], Farm Animal Health[2] and Equine Sciences[3] Faculty of Veterinary Medicine, Utrecht University, Utrecht, The Netherlands

Institute for Food Technology[4], IRTA, Monells, Spain

Department of Biomolecular Mass Spectrometry[5] ,Netherlands Proteomics Centre for Biomolecular Research and Utrecht Institute for Pharmaceutical Sciences, Utrecht University, Utrecht, The Netherlands

Biology of Reproduction July 1, 2011 vol. 85 no. 1 128-136

ABSTRACT

We report on the presence and formation of cholesterol oxidation products (oxysterols) in bovine sperm. Although cholesterol is the most abundant molecule in the membrane of mammalian cells and is easily oxidized, this is the first report on cholesterol oxidation in sperm membranes as investigated by state-of-the-art liquid chromatographic and mass spectrometric methods. First, oxysterols are already present in fresh semen samples, showing that lipid peroxidation is part of normal sperm physiology. After chromatographic separation (by high-performance liquid chromatography), the detected oxysterol species were identified with atmospheric pressure chemical ionization mass spectrometry in multiple-reaction-monitoring mode that enabled detection in a broad and linear concentration range (0.05–100 pmol for each oxysterol species detected). Second, exposure of living sperm cells to oxidative stress does not result in the same level and composition of oxysterol species compared with oxidative stress imposed on reconstituted vesicles from protein-free sperm lipid extracts. This suggests that living sperm cells protect themselves against elevated oxysterol formation. Third, sperm capacitation induces the formation of oxysterols, and these formed oxysterols are almost completely depleted from the sperm surface by albumin. Fourth, and most importantly, capacitation after freezing/thawing of sperm fails to induce both the formation of oxysterols and the subsequent albumin-dependent depletion of oxysterols from the sperm surface. The possible physiological relevance of capacitation- dependent oxysterol formation and depletion at the sperm surface as well as the omission of this after freezing/thawing semen is discussed.

Keywords: cholesterol, cryopreservation, lipid peroxidation, mass spectrometry, oxidative stress, oxysterols, sperm, sperm capacitation

INTRODUCTION

Lipid peroxidation in sperm cells has received much attention during the past years, and beneficial as well as detrimental effects have been attributed to lipid peroxidation, resulting in the idea that pro-oxidant and antioxidant systems need to be carefully balanced for optimal sperm function [1–3]. On the one hand, mild reactive oxygen species (ROS) levels appear to be stimulatory for sperm capacitation [4, 5]. On the other hand, it is evident that extensive peroxidation damages sperm cells, because lipid radicals involved in propagation of the lipid peroxidation chain reaction (see Girotti [6] for an overview of the radical mechanisms involved) are rather indiscriminate toward the biomolecules they target. This extensive peroxidation will ultimately lead to functional impairment of proteins and DNA [7, 8]. One of the conditions that may induce extensive lipid peroxidation is the freeze/thaw process that is routinely performed in livestock breeding industries and human reproductive medicine. We previously confirmed that a freeze/thaw procedure induces peroxidation, and we were able to visualize this process in bovine sperm. In the same study we demonstrated the existence of peroxidized phospholipids [9]. However, the fate of the most abundant lipid molecule in sperm membranes, cholesterol, has remained unresolved.

Handling procedures for sperm storage can cause oxidation damage, as has been observed in food products. From studies on materials delivered from food industries it has been shown that oxidation of lipids is also of great importance and that cholesterol and its oxidation products are important diagnostic parameters for food quality because 1) cholesterol is abundantly present in lipid-rich foods of animal origin; 2) cholesterol is prone to auto-oxidation as well as radical-induced oxidation [10–12], thereby forming an excellent sensor of lipid peroxidation; and 3) several oxysterol species are toxic [13–17]. Although there are more than 30 different oxysterols known, only a few are quantitatively important [11, 18].

Oxysterols can be sensitively analyzed and quantified by liquid chromatography (LC) combined with atmospheric pressure chemical ionization (APCI) mass spectrometry (MS) [13, 19]. Nevertheless, virtually no information is available on the formation of oxysterols in living cells.

The major aim of the present study is to determine the fate of cholesterol in sperm cell membranes. Cholesterol is the most abundant molecule in sperm cell membranes [20], and it stands to reason to apply the analysis of oxysterols to determine the extent of lipid peroxidation in sperm cells. Sterols have a function in sperm membrane stability and play an important role in sperm membrane organization and physiology [20–22]. On the one hand, cholesterol loading of sperm (mediated by cyclodextrins, for instance) improves their cryosurvival [23], whereas depletion of cholesterol may turn sperm unstable and cause premature deterioration after artificial insemination or during incubations of in vitro fertilization [24]. On the other hand, a delicate regulation of cholesterol depletion by albumin has been reported to be instrumental for sperm capacitation in vitro [25, 26]. The present study focuses on the establishment of a mass spectrometric assay to detect the formation of oxysterols formed from cholesterol in sperm cells and the physiological significance of this process. Here, we show that sperm cells do indeed contain oxysterols, even directly after

ejaculation. We report further about the effect of sperm handling procedures on additional oxysterol formation and on the fate of oxysterols during in vitro capacitation.

MATERIALS AND METHODS

Chemicals

All chemicals, including reference lipids, were obtained from Sigma Inc. (St. Louis, MO) and were of the highest purity available unless stated otherwise. Solvents (acetonitrile, chloroform, methanol, and hexane) were of high-performance liquid chromatography grade and were obtained from Labscan (Dublin, Ireland).

Sample Preparation

Bovine ejaculates were collected using an artificial vagina and were immediately processed to generate either fresh sperm samples or frozen/thawed sperm samples at a commercial artificial insemination center of Holland Genetics (Arnhem, The Netherlands). For fresh sperm samples, ejaculates were washed over a discontinuous Percoll gradient as described previously [27]. Pelleted cells were subsequently resuspended in Hepes-buffered Tyrode (HBT; 120 mM NaCl, 21.7 mM lactate, 20 mM Hepes, 5 mM glucose, 3.1 mM KCl, 2.0 mM $CaCl_2$, 1.0 mM pyruvate, 0.4 mM $MgSO_4$, 0.3 mM NaH_2PO_4, and 100 lg/ml kanamycin; 300 mOsm/kg, pH 7.4, supplemented with 0.5 mg/ml polyvinyl alcohol and 0.5 mg/ml polyvinylpyrrolidone), spun down at 750 g to remove any remaining Percoll, and were finally resuspended in HBT at a concentration of approximately 50 million cells per milliliter. These cells are further referred to as "fresh cells." Frozen/thawed sperm samples were generated by resuspension of ejaculated cells in a freezing buffer and freezing in 0.25 ml straws in liquid nitrogen according to the method of van Wagtendonk-de Leeuw et al. [28]. After thawing for 30 sec at 38 °C, cells were washed over a discontinuous Percoll gradient and with HBT as described above, and also resuspended at a concentration of 50 million cells per milliliter. These cells are further referred to as "frozen/thawed cells."

Artificial, protein-free membranes were made from extracted total sperm cell lipids as described previously [29, 30]. In brief, sperm lipids were extracted as described in the next section and were dried under nitrogen in a conical tube to form a lipid film. Lipids were hydrated with 96% (v/v) ethanol and dried again under nitrogen, and HBT was added before extensive vortexing. Finally, small unilamellar vesicles were formed by sonication on ice for 5x5 sec with the probe of a Soniprep 150 (MSE Scientific Instruments, Crawly, U.K.). Artificial protein-free lipid vesicles, fresh sperm, and frozen/thawed sperm were also incubated for 16 h in HBT either in absence of presence of 25 µM tert-butyl hydrogen peroxide to induce stress by radical oxygen species formation [31].

In Vitro Capacitation

Both fresh and frozen/thawed sperm samples were incubated for 4 h in presence of 0.5% (w/v) defatted bovine serum albumin (to replace polyvinyl pyrrolidone/polyvinyl alcohol) in HBT, or in polyvinyl alcohol/polyvinyl pyrrolidone containing HBT without albumin to induce sperm capacitation [20].

Extraction and Isolation of Oxysterols

The total lipid fraction from the sperm suspensions was extracted according to the method of Bligh and Dyer [32]. In addition, the sperm cells were spun down for 10 min at 10 000 x g, and the supernatant was subjected to the same lipid extraction method to discriminate between the extracellular and the total oxysterol pools. Subsequently, cholesterol and oxysterols were separated from phospholipids by solid-phase extraction on 200-mg silica columns (Merck, Darmstadt, Germany). To this end, the lipid extract was dissolved in chloroform and applied to a column preconditioned with acetone, and the cholesterol plus oxysterol fraction was eluted with three volumes of acetone [19, 33]. Acetone was evaporated under a constant stream of nitrogen gas, and cholesterol and oxysterols were stored at -20 °C until use.

High-Performance Liquid Chromatography-MS Analysis

Extracted (oxy)sterols were dissolved in a small volume of acetonitrile:methanol (6:4 [v/v]) and injected on an Aquasil C_{18} (250 x 4.6 mm, particle size of 5 µm) analytical column (Keystone Scientific, Bellefonte, PA) [13]. Elution was performed isocratically with acetonitrile:methanol (6:4 [v/v]) at a flow rate of 1 ml/min, and the column effluent was introduced by an atmospheric pressure chemical ionization (APCI) interface (Sciex, Toronto, ON) into a 4000 QTRAP mass spectrometer. For maximal sensitivity and for linearity of the response, the mass spectrometer was operated in multiple-reaction monitoring (MRM) mode at unit mass resolution. Peaks were identified by comparison of retention time and mass spectrum with authentic standards of the (oxy)sterols described (Merck). Ion transitions monitored were m/z 369.2/161.1 (cholesterol), 401.2/175.1 (7-ketocholesterol), and 367.2/159.1 (other oxysterols and desmosterol). When exploring the existence of other oxysterols (such as desmosterol-derived oxysterols) the mass spectrometer was operated in "enhanced" MS (ion-trapping) mode in the mass range 200–600 amu. Data were analyzed with Analyst software version 1.4.1 (Applied Biosystems, Nieuwerkerk a/d IJssel, The Netherlands).

RESULTS

Detection, Identification, and Quantification of Oxysterols (Oxy)sterols can be ionized readily by APCI (Fig. 1A). In accordance with previous reports [13, 32], (oxy)sterols were not observed as (quasi) molecular ions, but had lost any hydroxyl groups (including that on C-3) as a molecule of water (see Fig. 1A, inset). Product spectra of the $[M+H-H_2O]^+$ ions generated by collisional activation were

complex, and structural information was hard to obtain from these spectra because they consisted of numerous fragment ions that were common to product spectra of many (oxy)sterols (Fig. 1, B–D). The discrimination between (oxy)sterols was therefore based on the different retention times of the oxysterols during reverse-phase chromatography as detected by evaporative light scattering detection (Fig. 2A) or mass spectrometry (Fig. 2B). Calibration curves for quantification purposes were constructed in MS/MRM mode for eight (oxy)sterols that are of physiological importance. All calibration curves were linear up to at least 100 pmol and had correlation coefficients (r^2) between 0.99 and 1.00. The (oxy)sterols were detected with small variations in sensitivity due to differences in their ionization and fragmentation efficiencies, but had limits of detection of around 50 fmol (oxysterols) to 200 fmol (cholesterol and desmosterol; Fig. 3). For assessment of lipid peroxidation, the absolute amounts of cholesterol, desmosterol, and individual oxysterols were calculated using the corresponding calibration curves. Oxysterols were expressed as mole-% of cholesterol.

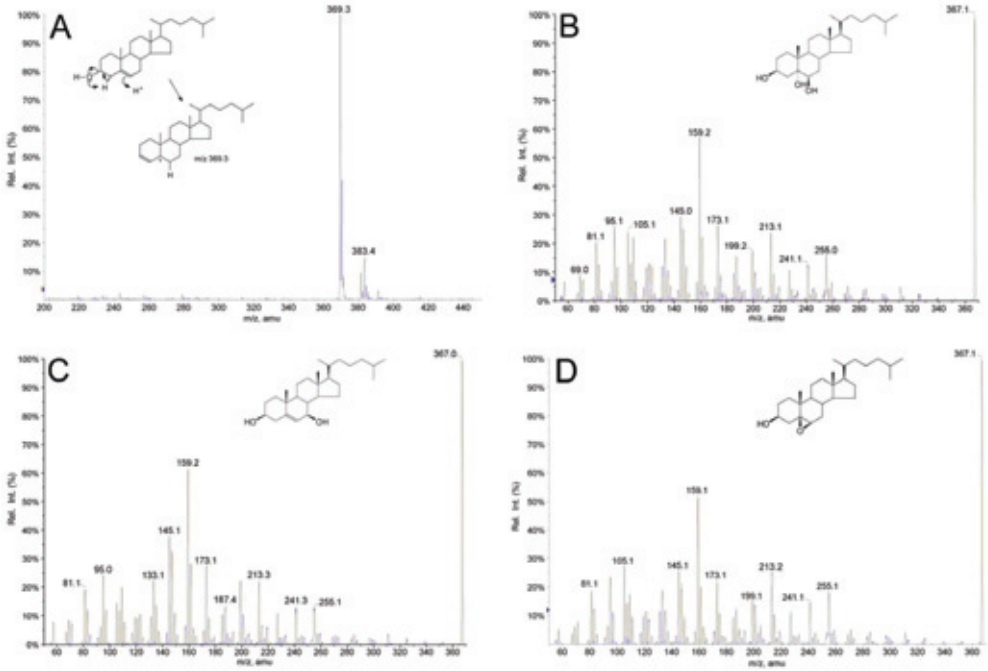

Figure 1. Mass spectrometry of authentic standards of (oxy)sterols.

A) Mass spectrum recorded during the elution of cholesterol. The inset shows a proposed mechanism for the formation of the $[M+H-H_2O]^+$ base peak ion during APCI ionization. **B**–**D**) Indiscriminate and extensive fragmentation of (oxy)sterols. Fragmentation spectra of (oxy)sterols at 35-V collision energy. **B**) Cholestane-3,5,6-triol. **C**) 7β-Hydroxycholesterol. **D**) 5,6β-Epoxycholesterol. Rel. Int., relative intensity.

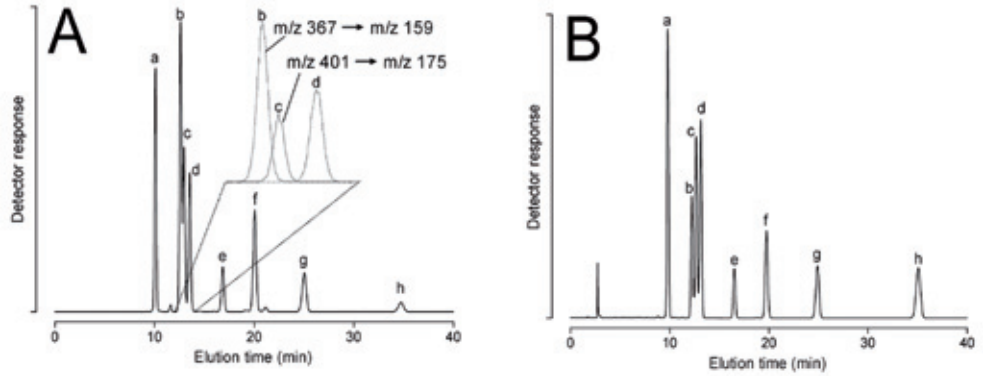

Figure 2. Detection of (oxy)sterol standards by MRM-MS

(**A**) or evaporative light scattering detection (**B**). Standards shown are: cholestane-3,5,6-triol (**a**); 7β-hydroxycholesterol (**b**); 7-ketocholesterol (**c**); 25-hydroxycholesterol (**d**); 5,6β-epoxycholesterol (**e**); 5,6α-epoxycholesterol (**f**); desmosterol (**g**); and cholesterol (**h**). The inset in **A** shows distinction between oxysterols based on different mass spectrometric fragmentations.

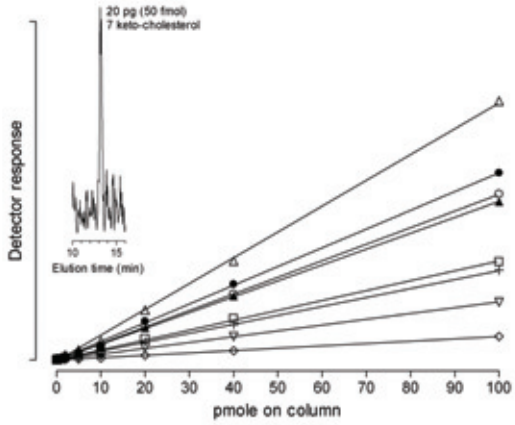

Figure 3. (Oxy)sterols produce linear calibration curves over a broad dynamic range.

Differences in sensitivity result from differences in ionization and fragmentation efficiencies. From top to bottom: 7β-hydroxycholesterol; cholestane-3,5,6-triol; 5,6α-epoxycholesterol; 25-hydroxycholesterol; 7-ketocholesterol; desmosterol; and 5,6β-epoxycholesterol and cholesterol. The inset shows the signal:noise ratio at the lower level of detection of 7-ketocholesterol.

Oxysterols Are Present in Fresh and Frozen/Thawed Sperm Cells

Analysis of Percoll-washed, fresh sperm cells, from which lipids were extracted as soon as feasible after ejaculation, revealed the presence of cholesterol, desmosterol, and oxysterols in these cells (Fig. 4A). All oxysterol levels were highly increased (approximately by a factor of 6) when cells were stressed with tert-butyl hydrogen peroxide, whereas their relative contribution to the total amount

of oxysterol resembled that of unstressed cells (Fig. 4B). However, in protein-free reconstituted vesicles from sperm lipid extracts the production of oxysterols under the same tert-butyl hydrogen peroxide stress doubled (Fig. 4C), which may imply either that the sperm cells possess an antioxidant network preventing cholesterol oxidation or that a higher proportion of cholesterol in sperm cells was not exposed to tert-butyl hydrogen peroxide compared with the reconstituted vesicles.

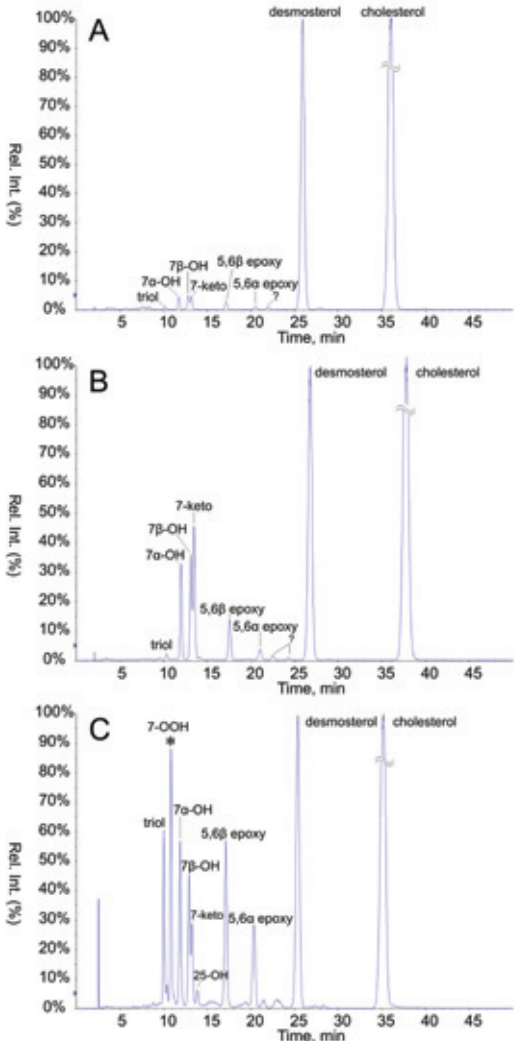

Figure 4. Detection of (oxy)sterols in Percoll-washed sperm cells by MRM-MS. **A**) Bovine sperm cells directly after ejaculation. **B**) Sperm cells incubated in the presence of oxidants. **C**) Small unilamellar vesicles constructed from a sperm cell lipid extract incubated in the same presence of oxidants as in **B**. Figures are normalized to desmosterol for clarity. Compared with the normalized levels of desmosterol, the cholesterol peaks in the chromatograms of **A**, **B**, and **C** were 679%, 622%, and 578%, respectively. Rel. Int., relative intensity.

The peroxidation of protein-free vesicles also led to the formation of different oxysterols, most notably to the reduced abundance of 7-ketocholesterol and the more abundant presence of cholestane- 3,5,6-triol. One additional oxysterol was observed that was not detected in living sperm cells (Fig. 4C, asterisk). Based on its retention time and its fragmentation spectra in positive and negative modes, it was tentatively identified as 7-hydro-peroxycholesterol (data not shown). Note that higher sterol oxidation led to lower cholesterol:desmosterol ratios (Fig. 4).

In addition, based on the identified oxysterol products, indeed apparently cholesterol is predominantly attacked by ROS at three places (illustrated in Fig. 5), of which the attack to the 25 carbon atom of cholesterol is minimal. Reaction products indirectly created after the radical oxygen species collision at the 7 or the 5 and 6 carbon atoms of cholesterol are indicated with arrows in Figure 5.

When sperm cells underwent the freezing protocol (taking a total time of approximately 3 h) and were subsequently thawed, the total amount and composition of oxysterols in these cells remained unaltered compared with fresh cells, showing that the freezing procedure itself did not result in elevated oxysterol levels (P=0.52, n=3; Fig. 6). Subsequent incubation of fresh or frozen/thawed sperm cells for 4 h did not change the oxysterol pattern in frozen/thawed sperm (P=0.12, n=3). In contrast, the amount of oxysterols increased when fresh sperm were incubated in HBT for 16 h (P=0.03, n=3; Fig. 6). The composition of the cholesterol oxidation products was similar for all sperm incubations but differed from the reactive oxygen- stressed protein-free vesicles made from reconstituted sperm lipid extracts (Fig. 6).

Fresh and frozen/thawed sperm cells were incubated for 4 h in HBT without or with 0.5% albumin (in vitro capacitation) to determine whether albumin has an affinity for the oxysterols.

Clearly, as depicted in Table 1, only fresh sperm showed a significant incubation-dependent formation of oxysterols, and the vast majority of these oxysterols were extracted in the presence of albumin. Both responses were found to not be significant in frozen/thawed sperm during the same incubations.

Table 1: Formation, and albumin-dependent extraction of oxysterols in fresh and frozen thawed bull sperm before and after in vitro capacitation.

Incubation	**0 h**	**4 hrs (- albumin)**	**4 hrs (+albumin)**
Fresh semen			
Oxysterol/cholesterol (%)	0.39±0.12	1.43±0.24[a]	1.72±0.25[a]
Oxysterol in sperm (%)	98±2	95±3	14±3[a]
Frozen/thawed semen			
Oxysterol/cholesterol (%)	0.41±0.09	0.56±0.18	0.57±0.27
Oxysterol in sperm (%)	94±3	90±4	83±8

Mean values ± SD are provided, data obtained from 7 bulls, using three individual ejaculates (n=7, r=3). The relative amount of total oxysterol formed from cholesterol (100%) is indicated as well as the distribution of the formed oxysterols (100% in semen), which was recovered in the sperm cell pellet after centrifugation. The supernatant contained the depleted oxysterols. Data indicated with [a] differed significantly from the 0 h condition.

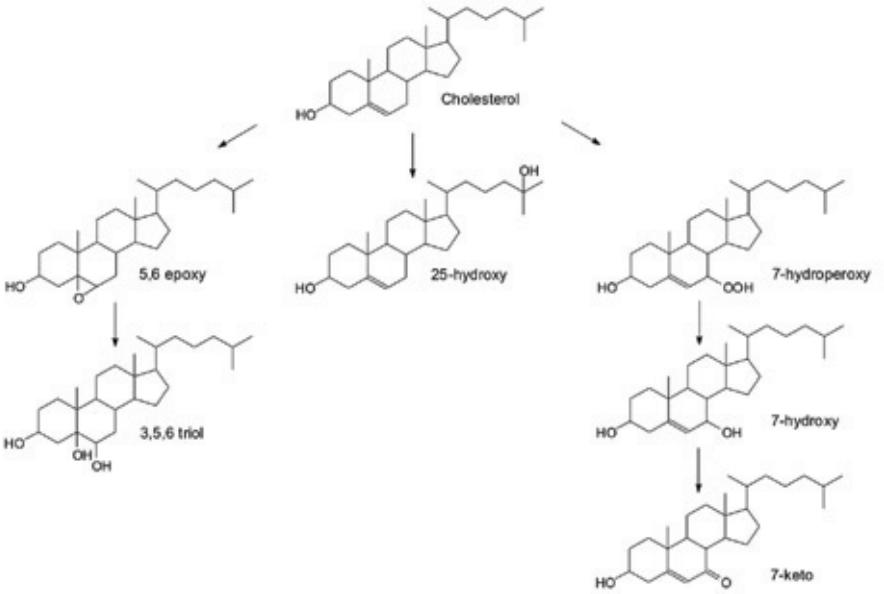

Figure 5. Molecular interpretation of cholesterol oxidation pathways identified in bovine sperm.

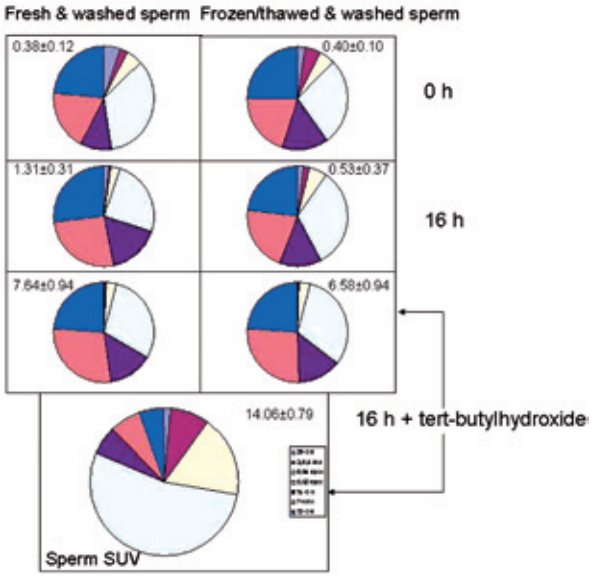

Figure 6. Composition of oxysterols in sperm treated as indicated and in reconstituted small unilamellar vesicles from extracted sperm cell membrane (sperm SUV). Mean ± SD values of total oxysterol formation (in % of total cholesterol) are provided (n = 3). Oxysterol species are presented in following order starting from the north and continuing clockwise: 25-hydroxy (light purple); 3,5,6-triol (dark brown); 5,6α-epoxy (yellow); 5,6β-epoxy (light blue); 7α-hydroxy (dark purple); 7-keto (light brown); and 7β-hydroxy (dark blue). For structures, see Figure 5.

DISCUSSION

Sperm cells contain high amounts of polyunsaturated phospholipids, which makes them particularly vulnerable to lipid peroxidation [33, 34]. Many papers have demonstrated the occurrence of lipid peroxidation during incubation of sperm cells under various conditions [2, 9, 34–36]. However, because these experiments have typically assessed the formation of such lipid peroxidation products as malondialdehyde and 9- hydroxynonenal during incubation, little is known about the amount of other lipid peroxidation products (e.g., oxysterols) in sperm cells directly after ejaculation. Additionally, it is important to realize that in the female genital tract, sperm cells are exposed to an exogenous peroxidative environment, and that this environment is both believed to support sperm activation (under mild radical oxygen species conditions [4, 5]) or may be detrimental to the sperm (for instance, when sperm and leukocytes are in contact and extensive radical oxygen species formation takes place). It is therefore of importance to analyze both the sperm cell's "load" of oxysterols directly after ejaculation and after sperm processing for cryopreservation or during in vitro fertilization treatments. The rationale to set up the oxysterol detection in sperm was 2-fold, namely, 1) cholesterol itself is believed to stabilize sperm, which may attribute to its suitability for successful freeze/thaw procedure survival [23], and 2) on the other hand, sperm capacitation is known to depend on albumin-mediated cholesterol depletion, and an unclear link is reported regarding mild formation of ROS and sperm capacitation as well [4, 5, 37].

Mass Spectrometry

Our observed APCI mass spectra of the individual oxysterols were identical to the spectra shown for processed foods by Razzazi-Fazeli et al. [13]. Many oxysterols are observed at identical mass:charge ratios, particularly after the loss of hydroxyl groups as molecules of water, a typical event during the APCI ionization process. Therefore, it was investigated whether discrimination between oxysterols could be made on basis of their fragmentation spectra. This would allow the oxysterol-specific fragments to be used for mass spectrometric multiple-reaction monitoring during liquid chromatography, which is a sensitive and selective technique for the detection of components. The resulting fragmentation spectra after colli-sional activation of cholesterol and oxysterols showed particular extensive and indiscriminate fragmentation. This clearly implicates that it is not possible to discriminate between (oxy)sterols based solely on their fragmentation spectra, and that chromatography is an indispensable tool to first separate the different types of (oxy)sterols, allowing their mass spectrometric identification. Moreover, many fragment ions showed similar intensities, meaning that there was no fragmentation pathway yielding high amounts of a particular ion to be used in multiple-reaction monitoring. Despite the lack of specific, high-abundance fragment ions, a detection limit of approximately 50 fmol of oxysterol and a linear dynamic range of more than three orders of magnitude were obtained. Approximately 0.1% of cholesterol has been converted into a particular oxysterol (see above). From this number one can calculate that the amount of one oxysterol species can be detected in 50 000 sperm cells. This illustrates that commercial cell

sorters (able to sort cells at typical rates of up to 10 000 cells per second) can easily provide us with sorted sperm subpopulations for investigation of their lipid peroxidation profiles under variable physiological conditions.

Presence of Oxysterols in Fresh Sperm Cells

Oxysterols are still very hydrophobic molecules that are retained in the cellular membranes. Combined with the low level of detection of oxysterols (typically around 50 fmol), this makes analysis of oxysterols the technique par excellence for the assessment of the total oxidative stress cells have encountered. In contrast, peroxidation of phospholipids results in the formation of hydrophilic end products such as malondialdehyde and 9-hydroxynonenal, components that are water soluble and therefore do not remain associated with the sperm cell. Assessment of lipid peroxidation by fluorescent techniques has also successfully been performed in sperm cells, but this only detects oxidative stress from the moment cells have been fluorescently labeled [9, 35], and not (as is the case with oxysterols) the oxidative stress that a cell has encountered so far. Therefore, in our view the detection of oxysterol levels in ejaculated semen samples can be used as a diagnostic tool for screening sperm quality because too high levels of oxysterols reflect too high oxidative stress, which is well known to impair sperm functioning [37].

Analysis of sterols in sperm cells directly after ejaculation revealed the abundant presence of cholesterol and desmosterol, as expected from previous data [38–40]. Small amounts of oxysterols were also clearly present in fresh and in frozen/thawed sperm, demonstrating that sperm cells have been subjected to peroxidation prior to the time they were ejaculated. Based on their retention time and their molecular weights, the observed oxysterols appeared to be derived from cholesterol and not from desmosterol. This is remarkable, considering the fact that around 16% of the sterol in bovine sperm cells is desmosterol, and that the only chemical difference between cholesterol and desmosterol is the double bond between carbons 24 and 25 in desmosterol. Theoretically, desmosterol would be expected to be a better substrate for peroxidation because double carbon atom bonds are preferred sites of oxidation. 25-Hydroxycholesterol is the only oxysterol that could partly be derived from desmosterol, because the double bond between carbon atoms 24 and 25 in desmosterol would have been lost during oxidation. The fact, however, that 25-hydroxycholesterol was only a minor oxidation product in our experiments points toward a different underlying reason for the observed preferred oxidation of cholesterol. One might consider the possibility that the 25 carbon atom of both cholesterol and desmosterol is localized in the membranes in such a way that it is almost hidden for ROS. We are currently performing oxidation assays on sterols in homogeneous solution as well as studies on artificial membranes with various lipid compositions to elucidate this distinct behavior of cholesterol and desmosterol.

Inhibition of Oxysterol Formation by Sperm Cells

To obtain insight into whether or not sperm cells have the capacity to inhibit oxysterol formation, we compared this process under imposed reactive oxygen stress in both sperm cells and artificial vesicles reconstituted from sperm cell lipid extracts. Striking differences in the amount and composition of oxysterols were found between these samples, although the oxidative stress was generated in an identical fashion. This suggests that cholesterol in sperm cells is protected for oxysterol formation (probably by means of an active radical scavenging system). From the apparent differences in specific oxysterol species, one may hypothesize that sperm cells metabolize oxysterols. However, we loaded sperm uniform ^{2}H isotope-labeled oxysterols (prepared from ^{2}H cholesterol; each of the labeled forms of oxysterols as depicted in Fig. 5 were made) and found that bovine sperm did not convert any of these ^{2}H oxysterols at all (data not shown). The best explanation between the different oxysterol species found in the reconstituted vesicles compared with sperm is that cholesterol orientation in the vesicles is different from cholesterol in the parent physiological membranes of the living sperm bilayer from which they were extracted. For instance, lipids are asymmetrically oriented in sperm membranes [41, 42], and cholesterol is also reported to be enriched in the extracellular lipid leaflet and in lipid ordered domains of plasma membranes [43]. In the vesicles probably a more scrambled orientation of all reconstituted sperm lipids has taken place, which could form an explanation for the different composition of oxysterols in oxidation-stressed vesicles compared with sperm.

Effect of the Freeze/Thaw Procedure on Oxysterol Formation

In animal reproduction, freeze/thaw of sperm is common practice to store and distribute sperm before its use in artificial insemination. Freeze/thaw of sperm is also frequently performed in human medicine, for example, when a donor has to undergo chemotherapy, which typically has adverse effects on sperm quality. Analogous to screening the effect of storage in food products for oxysterols [13–17] and the knowledge that the freeze/thaw procedure is known to induce lipid peroxidation in semen [9, 44, 45], we investigated whether the formation of oxysterols was induced in sperm cells that had undergone this treatment. However, frozen/ thawed sperm cells did not show an increase in oxysterol levels upon incubation. This is different from the observations made with the fluorescent peroxidation reporter C11-Bodipy$_{581/591}$ in sperm, where an increased peroxidation was observed under these conditions [9]. Several reasons may cause this difference, such as a different reactivity of cholesterol and the Bodipy probe toward various ROS. Both molecules are oxidized by hydroxyl radicals and peroxyl radicals, as well as by peroxynitrite [6, 46, 47]. However, whereas the reactivity of C11-Bodipy$_{581/591}$ toward ROS is comparable to that of polyunsaturated fatty acids, such as arachidonic acid [48], the reactivity of (monoenoic) cholesterol is considerably lower [6]. Furthermore, it is known that lipid peroxidation is not homogeneously distributed over the sperm cell, but that the mid piece of sperm (the only area of the sperm cell where mitochondria reside) is particularly prone to oxidation [9]. Cholesterol, however, is enriched in the sperm head cell plasma

membrane, where relatively little lipid peroxidation was observed, which offers another explanation for the lower level of peroxidation observed with cholesterol [9, 20].

Oxysterol Formation in and Depletion from Sperm Cells

Interestingly, fresh sperm incubated in capacitation media did give rise to the formation of oxysterols under conditions that are routinely used for in vitro fertilization of mammalian oocytes (i.e., under conditions where sperm function and integrity lead to fertilization [18]). Under in vitro capacitation conditions, in which the medium is enriched in defatty bovine serum albumin, a complete depletion of formed oxysterols into the albumin-enriched medium was noted after 4 h of incubation. The capacitated sperm were virtually devoid of oxysterols, and thus of a fraction of the original cholesterol.

Remarkably, the same treatments to frozen/thawed sperm did not result in the formation of oxysterols or in the albumin-mediated depletion of cholesterol (and oxidized products). Many studies have been performed that suggest that cytotoxicity of oxysterols may result from the induction of apoptosis [15, 49–57]. Sperm cells themselves appear to be well protected for apoptosis because of the absence of cytosol (containing the apoptotic machinery) and the hypercondensation of DNA (preventing fragmentation [58]), but sperm cells loaded with oxysterols could turn out to be poor matches for the egg cell they fertilize. Given the fact that oxysterols are potentially cytotoxic and the fact that sperm capacitation depends on proper sterol extraction, we hypothesize the following: The formation of oxysterols is a part of the ROS-induced initiation of sperm activation and subsequently allows albumin to deplete oxysterols from the sperm surface. It is possible that albumin has a greater affinity for the more hydrophilic oxysterols compared with cholesterol itself, which should be more difficult to extract from the membrane lipid bilayer, but this needs to be further investigated. At any rate, the depletion serves two goals: 1) scavenging of oxysterols from the sperm surface and 2) net depletion of sterols, thus allowing enhanced membrane fluidity, which is thought to be required for sperm capacitation. The fact that endogenous oxysterol formation was not induced by in vitro capacitation treatments of frozen/thawed sperm is interesting. It might show that either some of the ROS signaling pathways involved in sperm capacitation have been lost during the freeze/thaw process or that scavenging of ROS is better functional in fresh and frozen/thawed sperm compared with capacitated sperm. Alternatively, cholesterol ordering in the frozen/thawed sperm cells might be changed, which makes cholesterol less vulnerable for ROS. The lack of formation and removal of oxysterols may form a part of the explanation of why frozen/ thawed sperm have lower fertilization potential compared with fresh sperm.

Future research should focus on the importance of oxysterol formation and subsequent albumin-mediated depletion during sperm capacitation. The relationship between oxysterol formation and sperm motility (signs of sperm capacitation in the tail) as well as sperm-zona interactions and acrosome responsiveness after such binding (signs of sperm capacitation on the sperm head) should be elucidated in such studies. Also, the role of vitamin E (which has been shown to inhibit bovine in

vitro fertilization results [58, 59]) in eventually inhibiting oxysterol and its subsequent removal from the sperm surface formation needs to be addressed. Interestingly, in this light a recent study has shown vitamin E levels to correlate with an inhibition of both oxysterol formation and lipoprotein-mediated uptake of sterols in Caco-2 cells [60]. If a similar scenario is valid for sperm, it may provide us with a more fundamental understanding of how cholesterol is depleted from capacitatingsperm, which for two decades has been known as a classical sperm capacitation response required for sperm to become competent to fertilize.

ACKNOWLEDGEMENTS

This research was supported by the research program Biology of Reproductive Cells of the Graduate School of Animal Sciences from the Faculty of Veterinary Medicine of Utrecht University. Dr Silva is supported by the Portuguese Foundation for Science and Technology, Ministry for Science, Technology and Higher Education, Dr van Gestel was financed by ZON-MW grant number 903-44-156, MSc Boerke A was financed by the High potential program of Utrecht University, and Dr Garcia-Gil by the Spanish Ministry of Education and Science grant number EX 2005-0460.

REFERENCES

1. Aitken J, Fisher H. Reactive oxygen species generation and human spermatozoa: the balance of benefit and risk. Bioessays 1994; 16:259–267.

2. de Lamirande E, Gagnon C. Impact of reactive oxygen species on spermatozoa: a balancing act between beneficial and detrimental effects. Hum Reprod 1995; 10(suppl 1):15-21.

3. Ford WC. Regulation of sperm function by reactive oxygen species. Hum Reprod Update 2004; 10:387–399.

4. de Lamirande E, Lamothe G, Villemure M. Control of superoxide and nitric oxide formation during human sperm capacitation. Free Radic Biol Med 2009; 46:1420–1427.

5. de Lamirande E, Lamothe G. Reactive oxygen-induced reactive oxygen formation during human sperm capacitation. Free Radic Biol Med 2009; 46:502–510.

6. Girotti AW. Lipid hydroperoxide generation, turnover, and effector action in biological systems. J Lipid Res 1998; 39:1529–1542.

7. De Iuliis GN, Thomson LK, Mitchell LA, Finnie JM, Koppers AJ, Hedges A, Nixon B, Aitken RJ. DNA damage in human spermatozoa is highly correlated with the efficiency of chromatin remodeling and the formation of 8-hydroxy-2 0 -deoxyguanosine, a marker of oxidative stress. Biol Reprod 2009; 81:517–524.

8. Koppers AJ, De Iuliis GN, Finnie JM, McLaughlin EA, Aitken RJ. Significance of mitochondrial reactive oxygen species in the generation of oxidative stress in spermatozoa. J Clin Endocrinol Metab 2008; 93:3199–3207.

9. Brouwers JF, Gadella BM. In situ detection and localization of lipid peroxidation in individual bovine sperm cells. Free Radic Biol Med 2003; 35:1382–1391.

10. Girotti AW, Korytowski W. Cholesterol as a singlet oxygen detector in biological systems. Methods Enzymol 2000; 319:85–100.

11. Geiger PG, Korytowski W, Lin F, Girotti AW. Lipid peroxidation in photodynamically stressed mammalian cells: use of cholesterol hydroperoxides as mechanistic reporters. Free Radic Biol Med 1997; 23:57–68.

12. Sevanian A, McLeod LL. Cholesterol autoxidation in phospholipid membrane bilayers. Lipids 1987; 22:627–636.

13. Razzazi-Fazeli E, Kleineisen S, Luf W. Determination of cholesterol oxides in processed food using high-performance liquid chromatography-mass spectrometry with atmospheric pressure chemical ionisation. J Chromatogr A 2000; 896:321–334.

14. Smith LL, Johnson BH. Biological activities of oxysterols. Free Radic Biol Med 1989; 7:285–332.

15. O'Sullivan AJ, O'Callaghan YC, Woods JA, O'Brien NM. Toxicity of cholesterol oxidation products to Caco-2 and HepG2 cells: modulatory effects of alpha- and gamma-tocopherol. J Appl Toxicol 2003; 23:191–197.

16. Sevanian A, Peterson AR. The cytotoxic and mutagenic properties of cholesterol oxidation products. Food Chem Toxicol 1986; 24:1103–1110.

17. Verhagen JC, ter Braake P, Teunissen J, van Ginkel G, Sevanian A. Physical effects of biologically formed cholesterol oxidation products on lipid membranes investigated with fluorescence depolarization spectroscopy and electron spin resonance. J Lipid Res 1996; 37:1488–1502.

18. Guardiola F, Codony R, Addis PB, Rafecas M, Boatella J. Biological effects of oxysterols: current status. Food Chem Toxicol 1996; 34:193- 211.

19. Manini P, Andreoli R, Careri M, Elviri L, Musci M. Atmospheric pressure chemical ionization liquid chromatography/mass spectrometry in cholesterol oxide determination and characterization. Rapid Commun Mass Spectrom 1998; 12:883–889.

20. Flesch FM, Brouwers JF, Nievelstein PF, Verkleij AJ, van Golde LM, Colenbrander B, Gadella BM. Bicarbonate stimulated phospholipid scrambling induces cholesterol redistribution and enables cholesterol depletion in the sperm plasma membrane. J Cell Sci 2001; 114:3543–3555.

21. Osheroff JE, Visconti PE, Valenzuela JP, Travis AJ, Alvarez J, Kopf GS. Regulation of human sperm capacitation by a cholesterol efflux-stimulated signal transduction pathway leading to protein kinase A-mediated up-regulation of protein tyrosine phosphorylation. Mol Hum Reprod 1999; 5:1017–1026.

22. Visconti PE, Galantino-Homer H, Ning X, Moore GD, Valenzuela JP, Jorgez CJ, Alvarez JG, Kopf GS. Cholesterol efflux-mediated signal transduction in mammalian sperm. beta-cyclodextrins initiate transmembrane signaling leading to an increase in protein tyrosine phosphorylation and capacitation. J Biol Chem 1999; 274:3235–3242.

23. Moce E, Blanch E, Tomas C, Graham JK. Use of cholesterol in sperm cryopreservation: present moment and perspectives to future. Reprod Domest Anim 2010; 45(suppl 2):57–66.

24. van Gestel RA, Helms JB, Brouwers JF, Gadella BM. Effects of methyl-beta-cyclodextrin-mediated cholesterol depletion in porcine sperm compared to somatic cells. Mol Reprod Dev 2005; 72:386–395.

25. Cross NL. Effect of methyl-beta-cyclodextrin on the acrosomal responsiveness of human sperm. Mol Reprod Dev 1999; 53:92–98.

26. Travis AJ, Kopf GS. The role of cholesterol efflux in regulating the fertilization potential of mammalian spermatozoa. J Clin Invest 2002; 110:731–736.

27. Flesch FM, Voorhout WF, Colenbrander B, van Golde LM, Gadella BM. Use of lectins to characterize plasma membrane preparations from boar spermatozoa: a novel technique for monitoring membrane purity and quantity. Biol Reprod 1998; 59:1530–1539.

28. van Wagtendonk-de Leeuw AM, Haring RM, Kaal-Lansbergen LM, den Daas JH. Fertility results using bovine semen cryopreserved with extenders based on egg yolk and soy bean extract. Theriogenology 2000; 54:57–67.

29. Gadella BM, Flesch FM, van Golde LM, Colenbrander B. Dynamics in the membrane organization of the mammalian sperm cell and functionality in fertilization. Vet Q 1999; 21:142–146.

30. Gadella BM, Lopes-Cardozo M, van Golde LM, Colenbrander B, Gadella TW. Glycolipid migration from the apical to the equatorial subdomains of the sperm head plasma membrane precedes the acrosome reaction. Evidence for a primary capacitation event in boar spermatozoa. J Cell Sci 1995; 108:935–946.

31. Brouwers JF, Silva PF, Gadella BM. New assays for detection and localization of endogenous lipid peroxidation products in living boar sperm after BTS dilution or after freeze-thawing. Theriogenology 2005; 63:458–469.

32. Bligh EG, Dyer WJ. A rapid method of total lipid extraction and purification. Canad J Biochem Physiol 1959; 37:911–917.

33. Brouwers JF, Gadella BM, van Golde LM, Tielens AG. Quantitative analysis of phosphatidylcholine molecular species using HPLC and light scattering detection. J Lipid Res 1998; 39:344–353.

34. Storey BT. Biochemistry of the induction and prevention of lipoperoxidative damage in human spermatozoa. Mol Hum Reprod 1997; 3:203–213.

35. Ball BA, Vo A. Detection of lipid peroxidation in equine spermatozoa based upon the lipophilic fluorescent dye C1l-BODIPY581/591. J Androl 2002; 23:259–269.

36. Aitken RJ. Free radicals, lipid peroxidation and sperm function. Reprod Fertil Dev 1995; 7:659–668.

37.Aitken RJ, Ryan AL, Baker MA, McLaughlin EA. Redox activity associated with the maturation and capacitation of mammalian spermatozoa. Free Radic Biol Med 2004; 36:994–1010.

38. Lalumiere G, Bleau G, Chapdelaine A, Roberts KD. Cholesteryl sulfate and sterol sulfatase in the human reproductive tract. Steroids 1975; 27:247–260.

39. Nikolopoulou M, Soucek DA, Vary JC. Lipid composition of the membrane released after an in vitro acrosome reaction of epididymal boar sperm. Lipids 1986; 21:566–570.

40.Hinkovska GV, Srivastava PN. Phospholipids of rabbit and bull sperm membranes: structural order parameter and steady-state fluorescence anisotropy of membranes and membrane leaflets. Mol Reprod Dev 1993; 35:209–217.

41. Gadella BM, Miller NG, Colenbrander B, van Golde LM, Harrison RA. Flow cytometric detection of transbilayer movement of fluorescent phospholipid analogues across the boar sperm plasma membrane: elimination of labeling artifacts. Mol Reprod Dev 1999; 53:108–125.

42. Harrison RA, Gadella BM. Bicarbonate-induced membrane processing insperm capacitation. Theriogenology 2005; 63:342–351.

43. Pankov R, Markovska T, Hazarosova R, Antonov P, Ivanova L, Momchilova A. Cholesterol distribution in plasma membranes of beta1 integrin-expressing and beta1 integrin-deficient fibroblasts. Arch Biochem Biophys 2005; 442:160–168.

44. Wang Y, Sharma RK, Agarwal A. Effect of cryopreservation and sperm concentration on lipid peroxidation in human semen. Urology 1997; 50:409–413.

45. Alvarez JG, Storey BT. Evidence for increased lipid peroxidative damage and loss of superoxide dismutase activity as a mode of sublethal cryodamage to human sperm during cryopreservation. J Androl 1992; 13:232–241.

46. Drummen GP, Gadella BM, Post JA, Brouwers JF. Mass spectrometric characterization of the oxidation of the fluorescent lipid peroxidation reporter molecule C11-BODIPY(581/591). Free Radic Biol Med 2004; 36:1635–1644.

47. Pap EH, Drummen GP, Winter VJ, Kooij TW, Rijken P, Wirtz KW, Op den Kamp JA, Hage WJ, Post JA. Ratio-fluorescence microscopy of lipid oxidation in living cells using C11-BODIPY(581/591). FEBS Lett 1999; 453:278–282.

48. Drummen G, van Liebergen L, Op den Kamp JA, Post JA. C11-BODIPY(581/591), an oxidation-sensitive fluorescent lipid peroxidation probe: (micro)spectroscopic characterization and validation of methodology. Free Radic Biol Med 2002; 33:473–490.

49. Gregorio-King CC, Gough T, van der Meer GJ, Hosking JB, Waugh CM, McLeod JL, Collier FM, Kirkland MA. Mechanisms of resistance to the cytotoxic effects of oxysterols in human leukemic cells. J Steroid Biochem Mol Biol 2004; 88:311–320.

50. Ares MP, Porn-Ares MI, Moses S, Thyberg J, Juntti-Berggren L, Berggren P, Hultgardh-Nilsson A, Kallin B, Nilsson J. 7beta-hydroxycholesterol induces Ca(2 þ) oscillations, MAP kinase activation and apoptosis in human aortic smooth muscle cells. Atherosclerosis 2000; 153:23–35.

51. Aupeix K, Weltin D, Mejia JE, Christ M, Marchal J, Freyssinet JM, Bischoff P. Oxysterol-induced apoptosis in human monocytic cell lines. Immunobiology 1995; 194:415–428.

52. Ayala-Torres S, Moller PC, Johnson BH, Thompson EB. Characteristics of 25-hydroxycholesterol-induced apoptosis in the human leukemic cell line CEM. Exp Cell Res 1997; 235:35–47.

53. Christ M, Luu B, Mejia JE, Moosbrugger I, Bischoff P. Apoptosis induced by oxysterols in murine lymphoma cells and in normal thymocytes. Immunology 1993; 78:455–460.

54. Harada K, Ishibashi S, Miyashita T, Osuga J, Yagyu H, Ohashi K, Yazaki Y, Yamada N. Bcl-2 protein inhibits oxysterol-induced apoptosis through suppressing CPP32-mediated pathway. FEBS Lett 1997; 411:63–66.

55. Lizard G, Monier S, Cordelet C, Gesquiere L, Deckert V, Gueldry S, Lagrost L, Gambert P. Characterization and comparison of the mode of cell death, apoptosis versus necrosis, induced by 7beta-hydroxycholesterol and 7-ketocholesterol in the cells of the vascular wall. Arterioscler Thromb Vasc Biol 1999; 19:1190–1200.

56. Lizard G, Lemaire S, Monier S, Gueldry S, Neel D, Gambert P. Induction of apoptosis and of interleukin-1beta secretion by 7beta-hydroxycholesterol and 7-ketocholesterol: partial inhibition by Bcl-2 overexpression. FEBS Lett 1997; 419:276–280.

57. Lizard G, Deckert V, Dubrez L, Moisant M, Gambert P, Lagrost L. Induction of apoptosis in endothelial cells treated with cholesterol oxides. Am J Pathol 1996; 148:1625–1638.

58. Dalvit GC, Cetica PD, Beconi MT. Effect of alpha-tocopherol and ascorbic acid on bovine in vitro fertilization. Theriogenology 1998; 49:619–627.

59. Marques A, Santos P, Antunes G, Chaveiro A, Moreira da Silva F. Effect of alpha-tocopherol on bovine in vitro fertilization. Reprod Domest Anim 2010; 45:81–85.

60. Landrier JF, Gouranton E, Reboul E, Cardinault N, El Yazidi C, Malezet-Desmoulins C, Andre M, Nowicki M, Souidi M, Borel P. Vitamin E decreases endogenous cholesterol synthesis and apo-AI-mediated cholesterol secretion in Caco-2 cells. J Nutr Biochem 2010; 21:1207–1213.

3

Involvement of bicarbonate-induced radical signaling in oxysterol formation and sterol depletion of capacitating mammalian sperm during in vitro fertilization[1]

Arjan Boerke[2]
Jos F. Brouwers[2]
Vesa M. Olkkonen[3]
Chris H.A. van de Lest[2]
Edita Sostaric[4]
Eric J. Schoevers[5]
J. Bernd Helms[3]
Barend M. Gadella[2,5]

[1]This work has been supported by the High Potential Program from Utrecht University.

[2]Department of Biochemistry and Cell Biology, Faculty of Veterinary Medicine, Utrecht University, Utrecht, The Netherlands.

[3]Minerva Foundation Institute for Medical Research, Biomedicum Helsinki 2U, Helsinki, Finland.
[4]Department of Equine Sciences, Faculty of Veterinary Medicine, Utrecht University, Utrecht, The Netherlands.

[5]Department of Farm Animal Health, Faculty of Veterinary Medicine, Utrecht University, Utrecht, The Netherlands

Biology of Reproduction January 1, 2013 vol. 88 no. 1 21

ABSTRACT

This study demonstrates for the first time that porcine and mouse sperm incubated in capacitation media supplemented with bicarbonate produce oxysterols. The production is dependent on a reactive oxygen species (ROS) signaling pathway that is activated by bicarbonate and can be inhibited or blocked by addition of vitamin E or vitamin A or induced in absence of bicarbonate with pro-oxidants. The oxysterol formation was required to initiate albumin dependent depletion of 30% of the total free sterol and -50% of the formed oxysterols. Incubation of bicarbonate treated sperm with oxysterol-binding proteins (ORP-1 or ORP-2) caused a reduction of -70% of the formed oxysterols in the sperm pellet but no free sterol depletion. Interestingly, both ORP and albumin treatments led to similar signs of sperm capacitation: hyperactivated motility, tyrosin phosphorylation, and aggregation of flotillin in the apical ridge area of the sperm head. However, only albumin incubations led to high in vitro fertilization rates of the oocytes, whereas the ORP-1 and ORP-2 incubations did not. A pretreatment of sperm with vitamin E or A caused reduced in vitro fertilization rates with 47% and 100%, respectively. Artificial depletion of sterols mediated by methyl-beta cyclodextrin bypasses the bicarbonate ROS oxysterol signaling pathway but resulted only in low in vitro fertilization rates and oocyte degeneration. Thus, bicarbonate-induced ROS formation causes at the sperm surface oxysterol formation and a simultaneous activation of reverse sterol transport from the sperm surface, which appears to be required for efficient oocyte fertilization.

Keywords: acrosome reaction, in vitro fertilization (IVF), oxidative stress, porcine/pig, sperm capacitation

INTRODUCTION

Before the sperm cell can enter the oocyte, it first needs to be activated. This activation process has been described extensively [1, 2]. One of the hallmarks of this activation process (also termed capacitation) is the increased binding affinity of the sperm cell to the zona pellucida (the extracellular matrix) of the oocyte. The main components thought to be responsible for sperm capacitation are bicarbonate and Ca^{2+} levels. Both ions induce signaling cascades after elevated levels inside the sperm cell [3]. Besides these two ions, albumin acts in synergy by mediating efflux of sterols from the sperm's surface [4, 5]. In boar sperm (one of our model species in this study), albumin is thought to selectively extract free sterols— like cholesterol and desmosterol—from the sperm cells [5–7]. Albumin is rather specific for causing sterol depletion from the sperm surface as phospholipids and glycolipid levels remain unaltered [1, 2]. Cholesterol is preferentially removed from the sperm surface despite of its high hydrophobicity when compared to the other membrane bilayer preferring lipid classes. Normally, albumin is involved in the transport of free fatty acid in the circulation from donor to acceptor tissue [8]. One of the mechanisms that could play a role in sterol depletion is the involvement of an active cholesterol transporter in providing free cholesterol to the hydrophobic pocket of albumin (as hypothesized previously [3]). Another option is that sterols can be oxidized and that their oxidation products (which are more hydrophilic) can be extracted by albumin (observed in bovine sperm [4]) or can facilitate an oxysterol- dependent scavenger-sensitive transport of free sterols to albumin [9]. Inclusion of albumin to in vitro capacitation media as well as the concomitant depletion of sterols by albumin have been shown to be of fundamental importance to achieve in vitro fertilization (IVF) [5].

Sterol Oxidation in Sperm

In bovine sperm, it has recently been demonstrated that sperm capacitation leads to the formation of oxysterols, which are preferentially extracted by albumin [4]. The formation of oxysterols is believed to be initiated by reactive oxygen species (ROS) as it can be induced by tert-butylhydroperoxide [4]. The role of ROS in sperm physiology is ambivalent: On the one hand, mild ROS formation is reported to be relevant for oxidation-mediated sperm signaling events that are involved in sperm capacitation [6, 7]. On the other hand, higher ROS formation rates are reported to be damaging for the sperm cell [10, 11].

Sterols and Lipid-Ordered Microdomain Formation on the Sperm Cell

During in vitro capacitation, a lateral rearrangement of the sperm surface sterols has been shown to be dependent on bicarbonate, and this rearrangement preceded and was required for albumin-mediated sterol depletion [3]. This lateral rearrangement coincides with higher membrane fluidity characteristics of the remaining nonraft membrane area, in which lower sterol levels are detected compared to the apical area of the sperm head, membrane where raft aggregation takes place [2,

10, 12]. When albumin and bicarbonate together are used to capacitate sperm, this causes a partial depletion of sterols (>15% of total sterol and depletion was only from the nonraft membrane area [2]). The treatment also leads to the aggregation of lipid-ordered membrane microdomains at the apical ridge area of the sperm surface in multiple species. Several groups [13] Independently established that the detergent-resistant membrane fraction not only contains raft markers such as caveolin, flotillin, gangliosides, sterols, and sphingolipids (for reviews, see Gadella et al. [14] and Nixon and Aitken [15]) but also is very highly enriched in cumulus- and/or zona-binding proteins [16] and in proteins involved in docking and priming of the sperm plasma membrane with the outer acrosome membrane [17,18]. These surface redistributions are, therefore, considered to be preparative steps for interaction of sperm with the zona pellucida and/or cumulus layer of the oocyte. This binding and induction of the acrosome reaction enables the sperm to reach the oolemma, where eventual fertilization can take place of the oocyte (for review, see Tsai and Gadella [19]).

Sterol Oxidation and Sperm Capacitation

The relationship between capacitation of porcine sperm and oxysterol formation was therefore investigated in the present study with the rationale to see whether this formation could be attributed to the depletion of sterols from the capacitating sperm surface [20]. To this end, we studied whether incubation of sperm with oxysterol-binding proteins could induce in vitro capacitation of porcine sperm and possibly could result in sperm capable of fertilizing oocytes in vitro in albumin-free media. Sperm were, therefore, capacitated in the absence of albumin but in the presence of two recombinant oxysterol- binding protein-related proteins (ORP-1 and ORP-2) [21]. Both ORPs have specific binding pockets for oxysterols and are able to transport bound oxysterols from a donor membrane toward specific acceptor membranes. The ORP-induced effects were compared to methyl b cyclodextrin (MBCD) and to delipidated bovine serum albumin (BSA)-mediated sterol extraction in capacitating sperm. The role of bicarbonate-dependent oxysterol formation and the subsequent (oxy)sterol depletion in the induction of sperm capacitation in vitro, as well as the modulatory role of pro- and antioxidants on these effects, are discussed.

MATERIALS AND METHODS

Animal Experiments

The Institutional Animal Care and Use Committee of Utrecht University approved this study.

Protein Expression of ORP-1 and ORP-2

Plasmid expression vectors for ORP-1 or ORP-2 were used for protein production as previously described [21]. Briefly, glutathione S-transferase fusion proteins of ORP-2 and ORP-1 were produced in E. coli BL21 and purified over glutathione sepharose 4B (GE Healthcare, Amersham, Buckinghamshire, UK) columns as described by the manufacturer's instructions. Protein concentrations of purified

ORP-1 and ORP-2 were determined by the Bradford assay (Coomassie Plus, Pierce, Rockford, IL) according to the manufacturer's instruction. Purity of ORP-1 and ORP-2 protein preparations was analyzed on sodium dodecyl sulfate polyacrylamide gels stained with Coomassie brilliant blue [22].

Sperm Incubations

Ejaculates were collected from boars with proven fertility at Varkens KI Nederland (Deventer, The Netherlands), a commercial enterprise producing insemination doses for pig artificial insemination for sow herds. Freshly ejaculated sperm was filtered through gauze to remove gelatinous material and subsequently diluted and washed in HEPES-buffered saline (HBS; 137 mM NaCl, 2.5 mM KCl, 20 mM HEPES, pH 7.4). Mouse sperm was aspirated from cauda epididymis of wild-type mice (strain B6129SF2/J; stock number 101045 Jackson Laboratories, Bar Harbor, ME). Next, sperm were washed through a discontinuous Percoll (GE Healthcare, Diegem, Belgium) gradient of 70% (v/v) and 35% (v/v) as described [3]. All solutions were made iso-osmotic (290–310 mOsm/kg) with HBS at 238C. Percoll layers were discarded and sperm pellets resuspended at a final concentration of 100 million sperm cells/ml in Hepes- buffered Tyrodes media (120 mM NaCl, 21.7 mM lactate, 20 mM Hepes, 5 mM glucose, 3.1 mM KCl, 2.0 mM $CaCl_2$, 1.0 mM pyruvate, 0.4 mM $MgSO_4$, 0.3 mM NaH_2PO_4; 300 mOsm/kg, pH 7.4; HBT condition hereafter referred to as Bic) or supplemented with 15 mM $NaHCO_3$, equilibrated with 5% CO_2 in humidified atmosphere (hereafter referred to as +Bic). Similarly, sperm were incubated -Bic or +Bic media supplemented with 1) 0.3% w/v BSA (defatted fraction V; Boehringer Mannheim, Almere, The Netherlands) or 2) with 4–16 µg/ml recombinant ORP-1 or ORP-2 or 3) with 0.5–10 mM MBCD. All +Bic conditions were incubated with open vials in 5% CO_2 atmosphere for 2 h at 38.5 °C. All Bic conditions were incubated in airtight vials for 2 h at 38.5 °C in a water bath. In some cases, sperm incubations were carried out in the presence of either 0.5 mM vitamin E (alpha-tocopherol; Sigma-Aldrich, St. Louis, MO) or 0.5 mM vitamin A (retinol; Sigma-Aldrich) or in the presence of a pro-oxidant mix containing 0.2 mM $FeSO_4$ and 1 mM ascorbate or in the presence of 30 µM 3-morpholinosydnonimine hydrochloride (SIN-1; Sigma Aldrich) for the induced formation of peroxynitrite [20, 23].

Lipid Extraction and Mass Spectrometry

After incubation, lipids of 200 million sperm cells were extracted according to the method of Bligh and Dyer (see Brouwers et al. [4]). Lipids were dried under nitrogen and redissolved in chloroform/ methanol (1/9; v/v), and a fraction corresponding to ~1 million cells was subjected to reverse-phase chromatography on a 150-mm x 3-mm Kinetex 2.6-µm column (Phenomenex, Torrance, CA), using isocratic elution (methanol/acetonitrile/2-propanol/ chloroform; 90/90/8.5/1.5; v/v/v/v). The column effluent was introduced into an Atmospheric Pressure Chemical Ionization source of a 4000Qtrap mass spectrometer (AB Sciex, Foster City, CA) operated under multiple reaction monitoring mode. Eluting peaks were identified and quantified based on comparison of retention time and product ion spectra with authentic standard, as described previously [4]. Briefly, a dose-response curve was

made of levels of 50 fmole to 100 pmole of oxysterol standards and of cholesterol and desmosterol that were injected into the same reverse-phase column elution. The integrated detector response (linear to the entire concentration range) was used to calculate the amounts of each individual (oxy) sterol species form sperm extracts that were eluting from the reverse-phase column after injection (for more experimental details, see Brouwers et al. [4]).

Western Blot Immunodetection of Tyrosine Phosphorylation

After incubation, a total of 2 million sperm cells were resuspended in 25 µl of lithium dodecyl sulfate loading buffer (NuPAGE; Invitrogen, Carlsbad, CA) in the presence of 0.1 M dithiothreitol and heated for 10 min at 95 °C. Subsequently, solubilized proteins were loaded and separated on a 12% polyacrylamide gel and run at 40 mA for 45 min. Subsequently, proteins were blotted onto nitrocellulose paper (Protran BA85; Whatman, Dassel, Germany) at 60 V for 1.5 h. In order to prevent aspecific binding of antibodies used later in the blotting procedure, the nitrocellulose paper with blotted proteins was first incubated in blocking buffer (Tris 25 mM, NaCl, pH 7.4, with 0.5% Tween, TBS-Tween 0.5%) for 10 min at room temperature. Subsequently, the nitrocellulose paper with the blotted and blocked proteins was incubated with 1% BSA TBS-Tween 0.05% for 1 h at room temperature. After this step, the nitrocellulose paper, with the blotted proteins, was incubated in 0.1% BSA TBS-Tween 0.05% supplemented with a mouse monoclonal antibody raised against phosphotyrosine residues (PY20; Becton Dickinson Transduction Laboratories, Franklin Lakes, NJ) at a final concentration of 1 µg/ml overnight at 48C. The resulting nitrocellulose paper with blotted proteins was washed six times with 10 min per washing step in TBS. After this washing, the nitrocellulose was placed into TBS-Tween 0.05% containing 0.5 µg/ml monoclonal goat anti-mouse antibody conjugated with horseradish peroxidase (Nordic Immunology, Tilburg, The Netherlands) for 90 min at 4 °C. The resulting nitrocellulose paper with blotted and immunolabeled proteins was washed as described before for removal of unbound PY20 above. Protein bands indirectly immunolabeled with horseradish peroxidase were visualized by chemiluminescence for 5 min (enhanced chemiluminescence detection kit; Supersignal West Pico; Pierce, Rockford, IL) and captured on a Molecular Imager Chemidoc XRS from Bio- Rad Laboratories (Hercules, CA).

Immunofluoresence Detection of Tyrosine Phosphorylation and of Flotillin

After incubation, 200 million sperm cells were subsequently spun down at 600x g and resuspended in 1 ml and fixed in 2% paraformaldehyde in PBS (137 mM NaCl, 2.7 mM KCl, 4.3 mM Na_2HPO_4, 1.47 mM KH_2PO_4, pH 7.4) at room temperature for 10 min. The fixative was removed by three washing steps and centrifugation (600x g) steps, and the final pellet was resuspended with PBS at the original concentration. The washed sperm cells were then smeared on Superfrost (Microm International, Walldorf, Germany) glass slides and dried for 5 min at 37 °C and subsequently placed in a 20 °C methanol bath for 1 min for full permeabilization of membranes to ensure optimal intracellular immunolabeling. The immobilized and permeabilized sperm cells were then incubated in blocking

buffer (PBS containing 1% BSA and 0.05% Tween20) for 1 h in a humid chamber at 37 °C. After this step, cells were incubated in buffer containing 0.1% BSA and 0.05% Tween20 and either supplemented with 5 µg/ml PY20 antibody or 10 µg/ml mouse monoclonal anti-flotillin-1 (Becton Dickinson Transduction Laboratories) for 1 h at 37 °C in a humidified chamber. Unbound antibodies were removed by gently washing the Superfrost glasses with 3 ml of PBS containing 0.1% BSA and 0.05%Tween20. The resulting specimen on Superfrost glass slides was subjected to 2 µg/ml monoclonal rabbit anti-mouse antibody conjugated with Alexa-488 TM (Invitrogen) for labeling PY20 or flotillin-1 for 2 h at 37 °C in a humidified chamber. After immunolabeling, the non-bound antibody conjugates with Alexa-488 TM were removed by three subsequent washing steps with PBS containing 0.1% BSA and 0.05%Tween20 and finally rinsed with PBS and mounted in Fluorsave (Calbiochem, San Diego, CA) and sealed airtight with nail polish. Samples were examined with an Eclipse Ti microscope (Nikon, Tokyo, Japan) equipped with a mercury lamp and appropriate filters at a minimum magnification of 40x.

Motility Assessment of Incubated Sperm

After sperm was incubated in HBT media, sperm motility was measured by the SpermVision computer-assisted sperm analysis (CASA; Minitube, Tiefenbach, Germany) system for 2 h. Sperm motility measurements were performed in this system by using 20-µm-deep Leja-4 chambers (Leja Products, Nieuw Vennep, The Netherlands). Standard instrument settings of SpermVision Version 3.0 were used for analysis of motility, as used by the artificial insemination center (Varkens KI Nederland) [24]. For mouse sperm, the percentage of cells with vigorous lateral head displacement movement was counted.

In Vitro Fertilization

Ovaries were collected from the slaughterhouse material of adult sows (VION, Groenlo, The Netherlands). The 3- to 6-mm follicles from individual ovaries were aspirated to retrieve cumulus-oocyte complexes (COCs). The COCs were individually selected based using criteria previously described [25]. Subsequently, the selected COCs were matured in vitro [25]. COCs were collected in HEPES-buffered M199 (Gibco Laboratories, Grand Island, NY) and washed in pre-equilibrated M199 supplemented with 2.5 mM $NaHCO_3$, 0.1% (w/v) polyvinylpyrrolidone, 100 µM cysteamine, 75 µg/ml potassium penicillin G, and 50 µg/ml streptomycin sulfate (oocyte maturation medium [OMM]). The selected COCs were cultured for 22 h in humidified atmosphere in air with 5% CO_2 at 38 °C in OMM supplemented with 0.05 IU/ml recombinant human follicle-stimulating hormone (rhFSH; Organon, Oss, The Netherlands). Subsequently, the COCs were transferred into OMM without rhFSH for another 22 h. This second step is needed for the oocytes to reach the final meiosis stage II of maturation (the stage they reach in vivo at ovulation). The fully matured oocytes were denuded (removal of cumulus cells) and transferred into an IVF medium (113.1 NaCl, 3 mM KCl, 20 mM Tris, 11.0 mM glucose, 1.0 mM caffeine, 7.5 mM $CaCl_2$, and 5.0 mM Na-pyruvate, supplemented with

either 0.1% [w/v] BSA, 4 µg/ml ORP-1, or 4 µg/ml ORP-2). Oocytes were equilibrated in a humidified atmosphere in air with 5% CO_2 at 38 °C for at least 1 h before adding boar sperm. The sperm was washed through Percoll as described above and diluted to a concentration of 10^5 cells/ml in the same IVF medium as the oocytes. Next, depending on the amount of oocytes (20–30) per group, 20–30 µl of this sperm suspension were added to the IVF media that already contained the oocytes. The resulting IVF media contained a total of 1000 sperm cells per oocyte. Subsequently, the oocytes and sperm cells were incubated in a humidified atmosphere in air with 5% CO_2 at 38 °C for 24 h. Next, the oocytes were washed in PBS with 0.1% BSA and fixed in 4% formaldehyde in PBS for a minimum of 1 h. After fixation, oocytes were labeled with 1 µg/ml Sytox Green (Molecular Probes, Invitrogen, Leiden, The Netherlands) in PBS for 5 min to label the chromatin. Subsequently, the fertilization rate of the oocytes were scored, and for unfertilized oocytes, they were scored for MII maturation phase rate; for the rate of cells that did not develop further, the MI maturation stage or even the germinal vesicle stage were scored as well as the rates of oocytes that were degenerated during this IVF procedure.

IVF in the Presence of MBCD

To determine the fertilization rate of sperm submitted to 0.5–10 mM MBCD, the standard IVF procedure was followed as described above, although all IVF procedures were performed in the absence of BSA. A control IVF experiment was performed on the same collection batch of follicles.

IVF in the Presence of Antioxidants

Washed sperm cells were pretreated for 30 min with 0.5 mM vitamin A or 0.5 mM vitamin E (each with a final ethanol concentration of 0.1 vol%). A control sample was pretreated for 30 min with 0.1 vol% ethanol without antioxidants. The pretreated sperm samples where then diluted 1:10 for further IVF experiments and further processed as described above.

Determination of the Sperm-Zona Interaction at IVF Conditions

After all IVF treatments, individual oocytes were, after extensive washing of each individual oocyte, scored for the amount of sperm cells that had a firm interaction with the surrounding zona pellucida. This was determined by using the Sytox Green immunofluorescence and bright-field view on a Leica TCS SP2 confocal system (Leica Microsystems, Wetzlar, Germany) equipped with a 488-nm laser using the laser power and acquisition settings at a submaximal pixel value.

Measurement of Acrosome Integrity

The acrosome integrity of incubated sperm was measured after 30 and 120 min by flow cytometry. Sperm cells were stained directly from the different incubations conditions diluted and supplemented with 1 µg/ml peanut agglutinin conjugated to fluorescein isothiocyanate (PNA-FITC; EY Laboratory, San Mateo, CA) to distinguish acrosome-reacted cells and with the membrane-

impermeable vital stain propidium iodide (PI; final concentration 25 nM). After gentle homogenizing of the sperm suspension, sperm were analyzed on a FACS Calibur flow cytometer equipped with a 100-mW argon laser (Becton Dickinson, San Jose, CA). At the wavelength of 488 nm, sperm cells were excited, and the FITC and PI emission intensity was detected in the logarithmic mode of FL-1 (530/30-nm band-pass filter) and FL-3 (620-nm long-pass filter). The forward and sideways scatter was detected in the linear mode, and sperm-specific events were gated for further analysis. The resulting two-dimensional dot plots represented 10 000 gated events and were made with FL-1 data expressed on the x-axis and FL-3 data on the y-axis. The amount of cells positively stained with one or both fluorescent dyes was scored using quadrant analysis in Win MDI software (Version 2.8, J. Trotter, freeware). The percentage of sperm that showed high intensities for the FL-1 channel were regarded as acrosome reacted. Sperm samples were also stained for PNA-FITC for microscopic discrimination of acrosome-intact and acrosome-reacted status. Briefly, after fixation in 2% (w/v) paraformaldehyde for 15 min at room temperature, sperm cells were spun down at 600x g and washed in PBS three times. Subsequently, sperm cells were smeared on Superfrost glass slides and dried at 37 °C. Next, sperm cells were incubated with 100 µg/ml PNA-FITC for 30 min at 37 °C in a humid chamber. After this, sperm cells were rinsed with PBS and mounted in Fluorsave (Calbiochem) and sealed airtight with nail polish. Samples were examined with a Nikon Eclipse Ti microscope equipped with a mercury lamp and appropriate filters at a minimum magnification of 40x. Sperm cells with no fluorescence at the acrosome region and with visible apical ridges were considered acrosome intact, whereas sperm cells with PNA-FITC-labeled acrosome regions and no visible apical ridge were considered acrosome reacted.

RESULTS

Bicarbonate Induces an ROS Signaling-Dependent Oxidation of Cholesterol That Can Be Blocked by Vitamin E or Vitamin A

The possible oxidation effects of bicarbonate on free sterols in porcine sperm cells by incubating Percoll-washed sperm in the absence of sterol-depleting agents were examined. Incubation of Percoll-washed sperm cells for 2 h in albumin- free media that were supplemented with bicarbonate induced the formation of oxysterols (Fig. 1). The levels of oxysterols increased ~10-fold, from approximately 0.047 mole % of total sterol (equivalent of 0.062 pmoles oxysterols per million sperm in the absence of bicarbonate; -Bic - BSA) to ~0.49 mole % of total sterol (equaling 0.74 pmoles oxysterols per million sperm in presence of bicarbonate; +Bic BSA). The formation of all types of oxysterols was nearly completely inhibited when 0.5 mM vitamin E or 0.5 mM vitamin A was present during the incubations (Fig. 1). On the other hand, when sperm were incubated in the absence of bicarbonate but with added pro-oxidants ($FeSO_4$ in the presence of ascorbate), similar oxysterol formation was observed when compared to bicarbonate (Fig. 1), while SIN-1 (stimulates peroxynitrite formation) did not cause any oxysterol formation (Fig. 1).

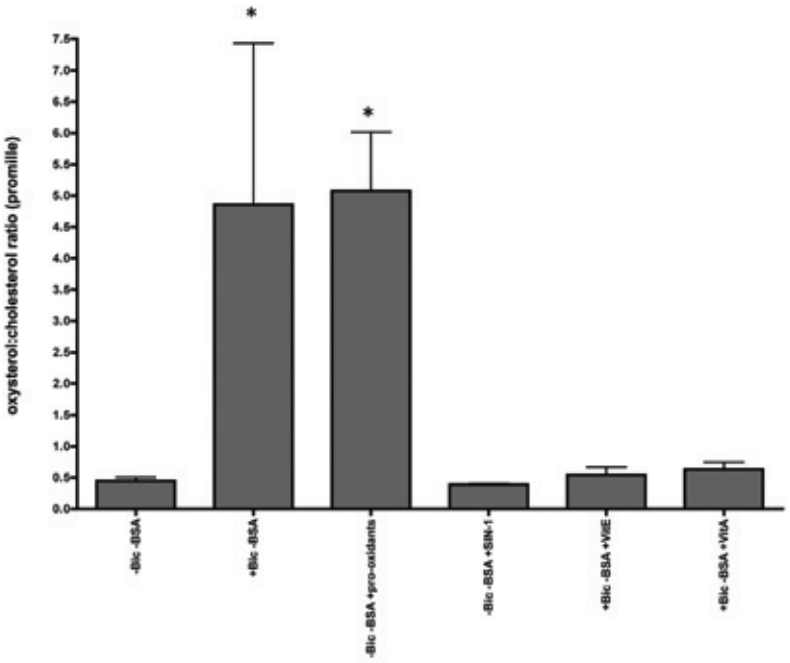

Figure 1. A bicarbonate-activated ROS- dependent pathway induces Oxysterol formation.

Bicarbonate-enriched medium (+Bic) induces radical formation, leads to oxidation of cholesterol, and can be blocked by vitamin E or by vitamin A. Oxysterols were detected by mass spectrometry (see Aitken et al. [20]). The relative amount of oxysterols as percentage of cellular cholesterol is expressed (mean % ± SEM, n=3; ejaculates were obtained from individual boars). * indicates a significant induction of oxysterol formation when compared to -Bic ($P < 0.05$).

The oxysterol species formed after bicarbonate incubation are depicted in the mass spectrometry graphs (Fig. 2), clearly depicting the formation of 7- and 25-hydroxycholesterols, 7- and 22-ketocholesterols, and 5,6a- and b-epoxycholesterols. Note that the intensity of ions detected as depicted in Figure 2 are corrected for (oxy)sterol-specific ion response curves as described previously, and thus the peak height/signal is not necessarily proportional to the amount of oxysterols present [4].

The relative amounts of oxysterol species out of the total amounts of oxysterols recovered from sperm are depicted in Figure 3, and from these data the following findings were derived:

1) In mouse and porcine sperm, the amount of oxysterols formed in sperm incubated with bicarbonate or with pro-oxidants (tested only for porcine sperm; Fig. 1) were similar to the levels depicted in Figure 1 for +Bic BSA and for -Bic -BSA +Pro-oxidants (10-fold when compared to -Bic -BSA; Table 1).

2) In mouse and porcine sperm, the presence of BSA did not change the amount of oxysterols formed compared to the absence of BSA (Fig. 1 and Table 1).

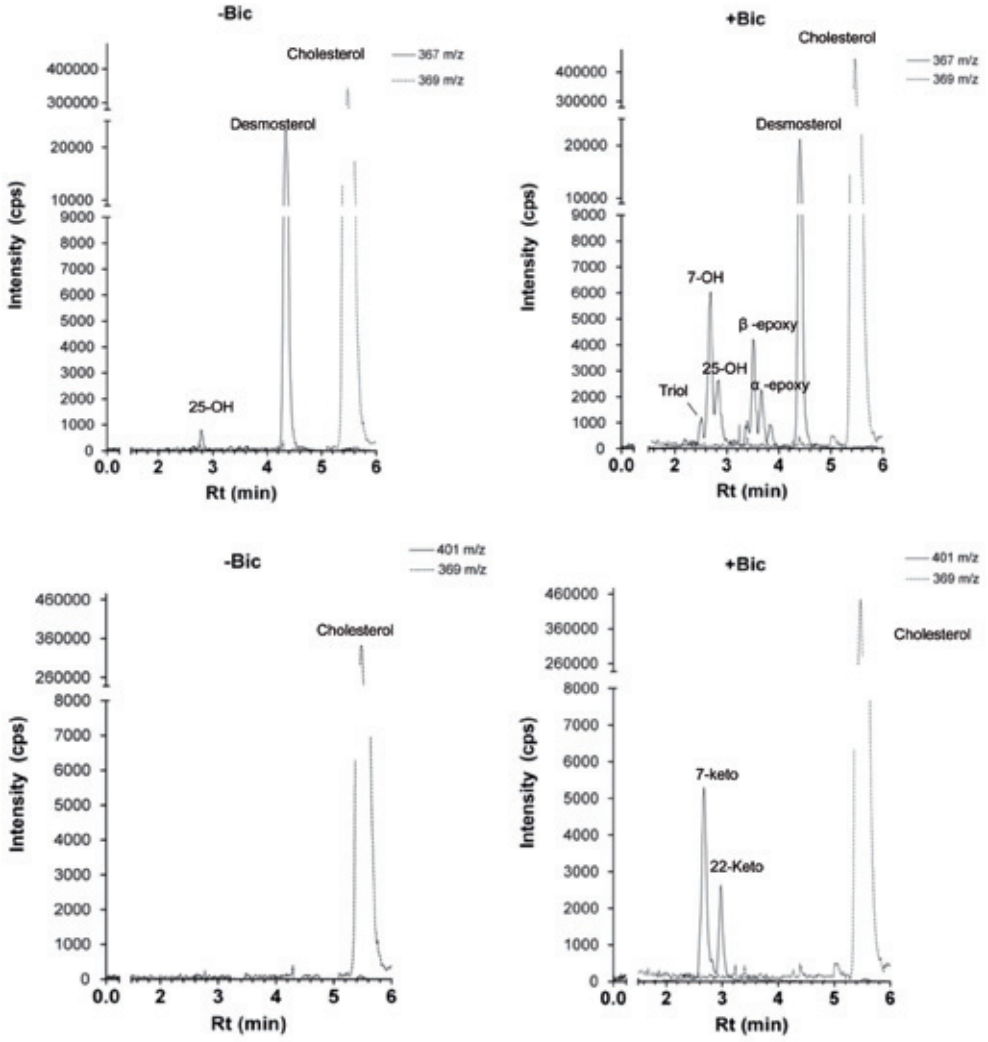

Figure 2. Chromatograms of multiple reaction monitoring during the elution of (oxy-)sterols extracted from sperm cells.

Oxysterols were identified based on retention time and product spectra as annotated: triol, 3,5,6-trihydroxycholesterol; 7-OH, 7-hydroxycholesterol; 7-keto, 7-ketocholesterol; 22-keto,22-ketocholesterol; 25-OH, 25-hydroxycholesterol; b-epoxy, 5,6b-epoxycholesterol; a-epoxy, 5,6a-epoxycholesterol. Each panel represents oxysterols from 1 million sperm cells. The amount of desmosterol and cholesterol (note the discontinuous y-axis to accommodate visualization of the peak height of these much more abundant sterol species) is depicted as well. The elution profile with m/z transitions intensities of 367.2/159.1 was used for oxysterols and desmosterol (indicated as 367), the transition of 369.2/161.1 for cholesterol (indicated as 369), and the transition of 401.2/175.1 for ketosterols (indicated as 401).

Table 1. Formation and albumin-dependent extraction of oxysterols in boar and mouse sperm before and after in vitro capacitation.[a]

		Incubation[c]	
Parameter[b]	0 h	2 h (- albumin)	2 h (+albumin)
Boar semen			
Oxysterol/cholesterol (%)	0.05 ± 0.02	0.82 ± 0.16[d]	0.94 ± 0.20[d]
Oxysterol in supernatant (%)	4 ± 2	8 ± 3	60 ± 18[d]
Mouse semen			
Oxysterol/cholesterol (%)	0.14 ± 0.08	1.03 ± 0.29[d]	1.51 ± 0.60[d]
Oxysterol in supernatant (%)	8 ± 3	11 ± 4	72 ± 12[d]

[a] Data obtained from four boars and four mice, using three individual ejaculates for each boar (n=4, r=3) or aspiration of two mouse epididymis (n=4, r=2).
[b] The relative amount of total oxysterol formed from cholesterol (100%) is indicated, as is the distribution of the formed oxysterols (100% in semen), which was recovered in the supernatant after centrifugation. The remaining proportion of the oxysterols were present in the sperm pellet. For partition of molecular oxysterol species see after capacitation in presence of albumin see Table 2.
[c] Values are mean ±SD.
[d] Data differed significantly from the 0-h condition. Similar data were reported for bovine sperm previously [4].

3) The amount and composition of oxysterols formed in sperm incubated with bicarbonate and vitamin E supplementation did not differ from control cells (Figs. 1 and 3).

4) The relative contribution of 7-ketocholesterol increased and 7-hydroxycholesterols decreased in the presence of bicarbonate or after inclusion of pro-oxidants (Fig. 3).

Table 2. The relative amount of cholesterol, desmosterol, and oxysterol species extracted by albumin from in vitro-capacitating boar and mouse sperm cells.

Relative	**Relative amount in supernatant[a]**	
Component	**Boar Semen**	**Mouse semen**
3,5,6-Trihydroxycholesterol	71 ±11%	74 ±17%
7-Hydroxycholesterol	59 ±14%	75 ±14%
7-Ketocholesterol	62 ±13%	80 ±16%
22-Ketocholesterol	55 ±10%	Not detected
25-Hydroxycholesterol	56 ± 13%	76 ±17%
5,6b-Epoxycholesterol	38 ± 7%	53 ± 13%
5,6a-Epoxycholesterol	35 ±7%	41 ± 9%
Desmosterol	34 ± 5%	38 ±5%
Cholesterol	38 ±5%	37 ±3%

[a] The mean percentage ± SD from the total of each component in semen that is recovered in the supernatant after a 2-h in vitro-capacitating incubation (+Bic, +BSA) is expressed (n=3).

5) Interestingly, in the presence of albumin (+BSA+Bic), a relative low proportion of 5,6a-epoxycholesterol and a much higher proportion of 5,6b- epoxycholesterol and 7-ketocholesterol, as well as a more pronounced decrease in 7-hydroxycholesterols, were detected when compared to +Bic -BSA. This probably relates to the fact the oxysterols formed actively exchange between the sperm membrane and albumin, which may affect molecular interspecies conversions between the sperm surface and the extracellular albumin (detected in both mouse and porcine sperm; Table 2).

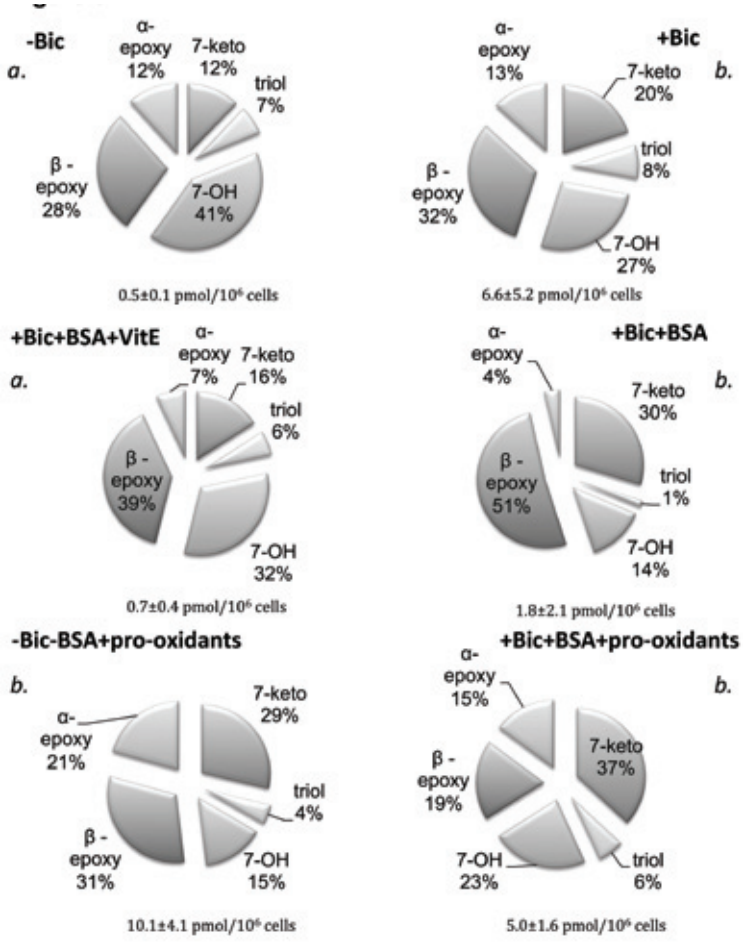

Figure 3. Relative molar contributions of cellular oxysterol species to the total oxysterol content in sperm cells after incubation in media supplemented and centrifugation as indicated. Note the relative decrease of 7-OH and increase of 7-ketocholesterol under conditions with increased oxysterol formation. The top panels refer to -Bic and +Bic, both in the absence of albumin. Conditions are marked "a" where control levels of oxysterol formation were observed and "b" where oxysterol levels were; 10-fold higher than under control conditions (data in Fig. 1). For the definitions of the oxysterol species abbreviations used, see Figure 2 (numbers in graph depict sum of oxysterol species: mean±SD in pmol/10^6 cells; n=3).

Vitamin E and A Inhibit the Induction of Hyperactivated Sperm Motility

Bicarbonate and albumin have been described to synergistically induce hyperactivated sperm motility [26], and we show here that they also induce oxysterol formation, while vitamin E and vitamin A inhibited the formation of oxysterols (Fig. 1 and 3). Thus, we tested whether sperm-hyperactivated sperm motility could be inhibited by vitamin E and vitamin A. About 10% of control (-Bic -BSA; Fig. 4A) sperm showed hyperactivated sperm motility, whereas incubation for 2 h in the presence of bicarbonate (+Bic -BSA) induced signs of hyper- activated sperm motility, as shown with CASA measurements in ~20% of the sperm cells (Fig. 4A). Indeed, a synergistic effect was seen when bicarbonate and albumin (+Bic +BSA) were added. Under these conditions, 45% of the sperm showed hyperactive motility (Fig. 4A). In the presence of vitamin E or vitamin A, hyperactivation of motility by bicarbonate and by the combination of bicarbonate and albumin was completely abolished (Fig. 4A). In the presence of BSA, a higher proportion of sperm cells showed signs of hyperactivated sperm motility (45%; Fig. 4A). When sperm cells were incubated in the presence of vitamin E, the induction of hyperactivated sperm motility, in the presence of bicarbonate alone, was completely inhibited. Likewise, inclusion of vitamin E to the IVF-mimicking medium containing both BSA and bicarbonate also showed a severe but not complete inhibition of hyperactivated sperm motility (Fig. 4A). For the regulation of hyperactivated sperm motility (on tyrosine phosphorylation), similar results were found in mouse sperm, which could be inhibited by vitamin E or with vitamin A (Table 3).

Table 3. Effects of bicarbonate and membrane antioxidants during in vitro capacitation of mouse sperm.[a]

Parameter	-Bic+BSA	+Bic+BSA	+Bic+BSA+VitE	+Bic+BSA+VitA
Hyperactivated motility[b]	4 ±3%	48 ± 14%[d]	14 ± 5%[e]	6 ± 4%[e]
PY20 positive in tail[bc]	3 ± 2%	52 ± 19%[d]	12 ± 8%[e]	7 ± 2%[e]
Membrane intact[b]	93 ± 4%	78 ± 12%	92 ± 5%	89 ±6%

[a] Mean percentage of sperm cells 6 SD with indicated properties after a 2-h incubation (n=3, r=2).
[b] For all samples, the overall amount of motile sperm cells was .75%.
[c] Note that PY20 labeling in some sperm cells was present in the cytoplasmic droplets and/or in the postacrosomal head region. Although the percentage of such aberrant PY20 labeling patterns was ,5%, it was invariable between samples (not induced by bicarbonate or inhibited by hydrophobic antioxidants).
[d] Indicates a significant difference induced by bicarbonate (+Bic+BSA vs. –Bic+BSA).
[e] Indicates a significant inhibition of the bicarbonate-induced effects by inclusion of hydrophobic antioxidants.

Vitamin E and A Reduce Sperm-Zona Binding and IVF

Since both vitamin E and vitamin A inhibited bicarbonate- dependent oxysterol formation and hyperactivated motility response to bicarbonate (in the presence or absence of albumin), we tested whether the sperm-binding properties to the zona pellucida and/or IVF rates were inhibited. We chose to first entrap high levels (0.5 mM) of hydrophobic antioxidants into the plasma membrane of sperm, followed by a 10-fold dilution in antioxidant-free IVF medium, and then perform the IVF experiment for 24 h.

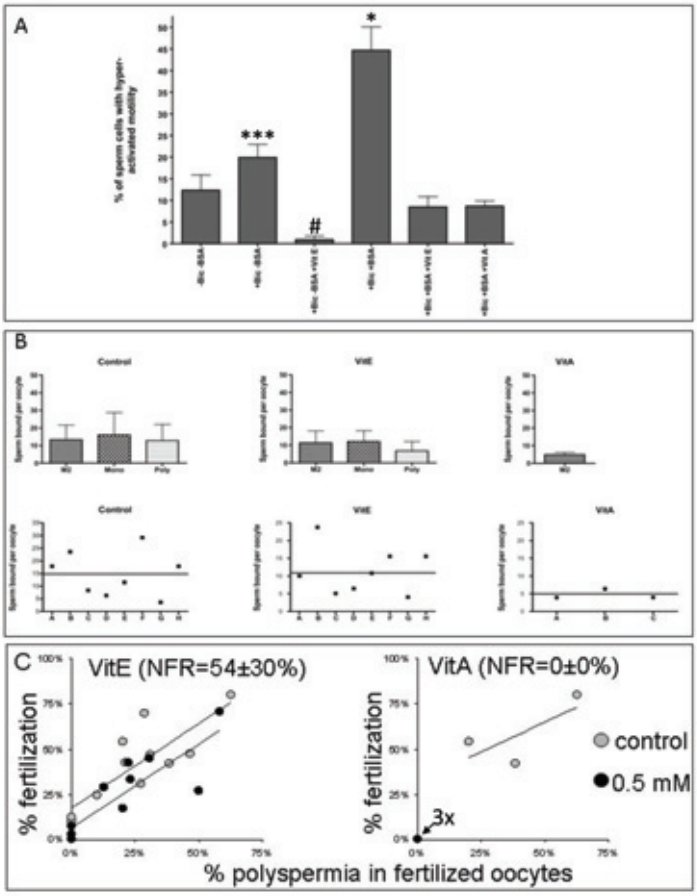

Figure 4. Effects of the bicarbonate/ROS pathway on hyperactivated motility, zona binding, and IVF.

A) Vitamin E and vitamin A inhibit bicarbonate- and albumin-induced hyperactivated sperm motility. Bicarbonate in the absence (+Bic-BSA) and especially in the presence (+Bic+BSA) of albumin induces hyperactivated sperm motility. In the presence of vitamin E or vitamin A, no signs of hyperactivated sperm motility were seen in the absence of albumin (+Bic-BSA+VitE), and in the presence of albumin (+Bic+BSA+VitE; +Bic+BSA+VitA), the levels of hyperactivated sperm motility were comparable to control sperm that were incubated in the absence of icarbonate and albumin (-Bic -BSA). The data represent mean ±SEM, n=3. *indicates a significant increase of effects compared to Bic BSA; *** indicates a significant lower effect compared to Bic+BSA and a significant effect compared to -Bic -BSA; # indicates a significant lower amount of hyperactive motile sperm when compared to Bic -BSA (in all predictions, $P<0.05$). B) Sperm binding to oocytes after a pretreatment of 30 min in the IVF medium containing 0.1% ethanol (control) or in 0.5 mM of vitamin A (VitA) or vitamin E (VitE). The individual black squares indicate the amount of sperm that bound to the zona pellucida for each of the boar ejaculates tested (eight different boars indicated by A-H on the x-axis). The mean amount of sperm bound to unfertilized oocytes (M2), monospermic fertilized oocytes (Mono), and polyspermic fertilized oocytes (Poly) is indicated in the top panels. For control and VitE, eight individual boars were scored for VitA, three boars were scored, and no fertilized oocytes were detected. C) Vitamin A blocked and vitamin E significantly reduced ($P<0.05$) IVF rates. The relative reduction compared to control IVF rates is the expressed normalized fertilization rate (NFR). The fertilization rate (in %, y-axis) and the ratio of polyspermic fertilization/total fertilization (in %, x-axis) are indicated for ejaculate obtained from 11 individual artificially inseminated boars. For each IVF treatment and each individual boar, >30 oocytes were used.

In this way, only sperm and not the oocyte had been in direct contact with high levels of membrane antioxidants. The effective vitamin concentration during the IVF incubation available for the oocytes was <50 µM. Pretreatment of sperm in 0.1% ethanol without antioxidants and 1:10 dilution in IVF medium was used as internal control. In all treatments, the oocytes did not show significant signs of degeneration (in all cases <10%). The pretreatment of sperm for 30 min in 0.1% ethanol (either without antioxidants or with either 0.5 mM vitamin A or 0.5 mM vitamin E) did not affect sperm viability (for mouse, similar findings are presented in Table 3). In fact, sperm that interacted with the zona pellucida remained motile even after 24 h of IVF incubations. As depicted in Figure 4B, a reduction of >60% in sperm binding was noted after a pretreatment of sperm with 0.5 mM vitamin A, and a 35% reduction in sperm binding was detected after a pretreatment with 0.5 mM vitamin E. A considerable variety in amount of sperm bound per oocyte was found for each individual ejaculated producing boar tested (Fig. 4B). Remarkably, the amount of sperm bound to the zona pellucida of unfertilized oocytes (M2), monospermic fertilized oocytes (Mono), and polyspermic fertilized oocytes (Poly) was not different (Fig. 4B). In line with the larger inhibitory effect of vitamin A when compared to vitamin E on sperm-zona binding were their respective effects on inhibition of IVF rates. When sperm were pretreated for 30 min with 0.5 mM vitamin E prior to IVF, a reduction of ~50% in fertilization rates was observed, while pretreatment with 0.5 mM vitamin A completely blocked fertilization (Fig. 4C). Although the vitamin E effect was significant (P >0.05), the inhibitory effect was highly variable between each of the 11 boars tested (Fig. 4C). In line with the absence of sperm and oocyte deterioration was the finding that there was no different correlation between the ratio of monospermic and polyspermic fertilized oocytes after vitamin E treatment. This shows that the diluted vitamin E concentrations (0.05 mM) during the IVF incubation were not affecting the oocyte's receptivity for sperm.

Effects of Oxysterol-Binding Proteins on Sperm Motility

Recombinant oxysterol-binding proteins ORP-1 and ORP-2 were produced and purified as described in Materials and Methods (purity was checked in silver-stained gels; Fig. 5A, lane 4). The effects of varying concentrations (4–16 µg/ml) of ORP-1 and ORP-2 to sperm suspensions were examined. In the presence of bicarbonate but in the absence of albumin (negative control; +Bic–BSA), only 20% of sperm had hyperactivated motility (Fig. 5B), while in the presence of albumin (+Bic+BSA), about 45% of sperm showed hyperactivated motility patterns (Fig. 5B). Both ORP-1 and ORP2 induced very strong hyperactivated motility in response to the sperm with the highest effects in 55% of sperm already at the lowest dose tested of 4 µg/ml (Fig. 5B).

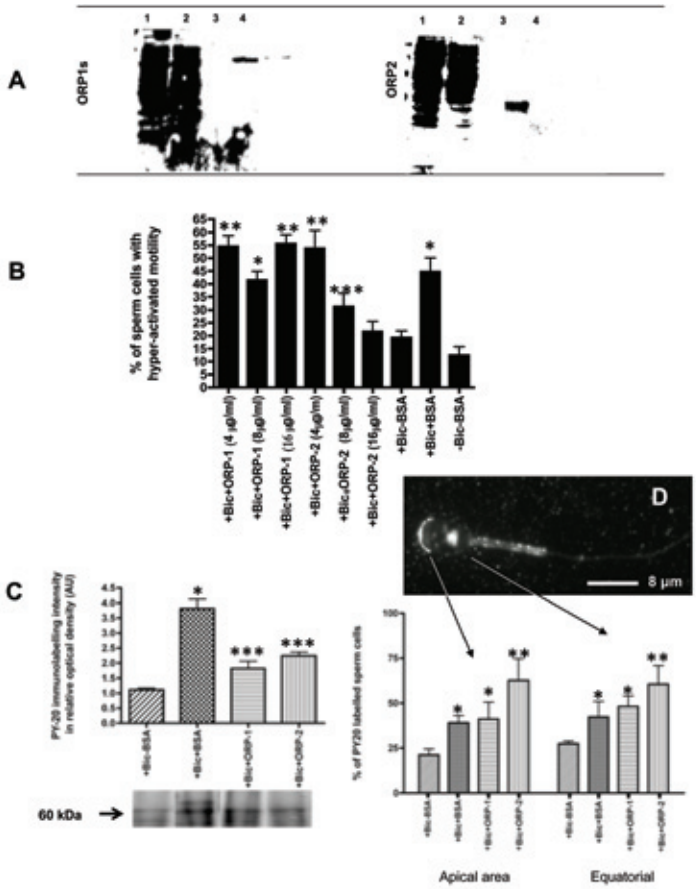

Figure 5. The effects of oxysterol-binding proteins on sperm capacitation.

B) Purification of recombinant oxysterol-binding proteins ORP-1 and ORP-2. A) Silver-stained SDS-PAGE cells loaded with ORP preparations. Lane 1: protein supernatant isolated after ultracentrifugation of transfected E. coli suspensions; lane 2: supernatant after an additional bead treatment with glutathione sepharose; lane 3: the empty wash fraction of glutathione sepharose column; and lane 4: the eluted proteins with 10 mM glutathione, which released the ORP-GSH fusion constructs (see also Suchanek et al. [21]). B) Inclusion of albumin (+Bic+BSA) and 4–16 µg/ml ORP-2 (+Bic+ORP-2) and for lower doses of 4 µg/ml and, to a lesser extent, 8 µg/ml ORP-1 (+Bic+ORP-1) induced hyperactivated sperm motility. The highest dose of 16 µg/ml ORP-1 (+Bic+ORP-1) showed no increase of hyperactivated sperm motility and was comparable to the condition without added sterol-depleting agents (+Bic -BSA). C) Western blot analysis revealed that tyrosine phosphorylation is increased 3.5-fold in the bicarbonate and BSA condition (+Bic+BSA) when compared to the absence of sterol-depleting agents (+Bic-BSA). Inclusion of 4 µg/ml ORP-1 (+Bic+ORP-1) or 4 µg/ml ORP-2 (+Bic+ORP-2) also induced tyrosine phosphorylation albeit to a smaller population of incubated sperm cells. D) Besides tail labeling (causing the hyperactivated motility), PY20 labeling of tyrosine phosphorylated proteins was found on the apical ridge area (left arrow) and at the equatorial area (right arrow) of the sperm head. C) Clearly, the inclusion of albumin (+Bic+BSA), 4 µg/ml ORP-1 (+Bic+ORP-1), or 4 µg/ml ORP-2 (+Bic+ORP-2) to bicarbonate-enriched media induced, in increasing order, more PY20 labeling on both of the sperm head areas when compared to medium without sterol-depleting agents (+Bic -BSA). The data represent mean±SEM, n=3.

* indicates a significant increase of effects compared to -Bic -BSA; ** indicates a significant additional increase of effect when compared to +Bic+BSA; *** indicates a significant lower effect compared to +Bic+BSA and a significant effect compared to -Bic -BSA; (in all predictions, $P < 0.05$).

Effects of Oxysterol-Binding Proteins on Tyrosine Phosphorylation of Sperm Proteins

The hyperactivated motility pattern of capacitated sperm relates to an increase in tyrosine phosphorylation of proteins in the flagellum [27], and we examined whether tyrosine phosphorylation occurred in incubated sperm samples. When sperm were incubated in bicarbonate-enriched media (+Bic -BSA), only a weak protein tyrosine phosphorylation increase as compared to control sperm was recovered (1.1-fold; Fig. 5C). Inclusion of albumin (+Bic+BSA) caused an almost 4-fold increase in protein tyrosine phosphorylation (Fig. 5C). The 4-µg/ml dose of ORP-1 or ORP-2 (eliciting maximal stimulation in hyperactivated sperm motility; Fig. 5B) caused a significant (~2-fold) but less prominent induction of protein tyrosine phosphorylation compared to control sperm (Fig. 5C). Interestingly, when compared to albumin, both ORPs induced tyrosine phosphorylation in the sperm head of a larger subpopulation of sperm cells (Fig. 5D), and this was manifested at the apical ridge area and at the equatorial area of the sperm head (Fig. 5D). Induction of tyrosine phosphorylation was not observed when vitamin E or A was added to bicarbonate-enriched media in hyper the presence or the absence albumin or albumin (data not shown) for mouse sperm (Table 3).

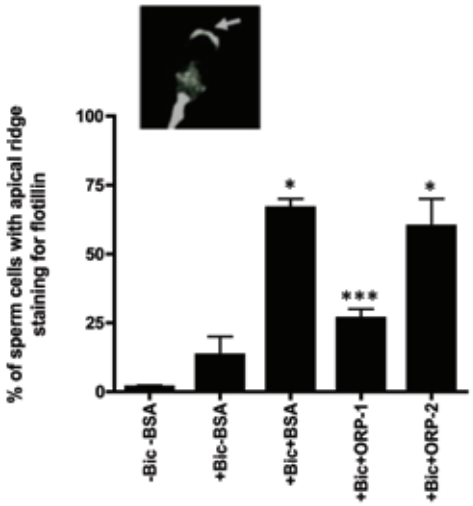

Figure 6. The bicarbonate/oxysterol pathway induces protein tyrosine phosphorylation and aggregation of lipid-ordered domains.

Incubations with specific depletion of oxysterols result in aggregation of flotillin-1 into the apical ridge area of the sperm head. Incubation in the presence of albumin (+Bic+BSA) or 4 µg/ml ORP2 (+Bic+ORP2) induced immunolabeling of flotillin-1 in the apical ridge area of the sperm head when compared to sperm cells incubated in the absence of sterol-depleting agents (+Bic-BSA). Only 4 µg/ml ORP-1 (+Bic+ORP-1) slightly induced the apical ridge of this relocation of flotillin-1. The data represent mean±SEM, n=3. * indicates a significant increase of effects compared to +Bic -BSA; *** indicates a significantly lower effect compared to +Bic+BSA and a significant effect compared to +Bic -BSA (in all comparisons, $P<0.05$).

Effects of Oxysterol-Binding Proteins on the Aggregation of Flotillin into the Apical Ridge Area

In a previous study, the depletion of sterols and the aggregation of lipid raft marker proteins such as flotillin have been demonstrated to result in the capacitation of porcine sperm [2]. We now have extended this observation and studied whether, as compared to sperm treated in bicarbonate-enriched media, the albumin effect on sterol extraction and lipid raft aggregation could be mimicked by incubating sperm in bicarbonate-enriched media supplemented with recombinant ORP-1 or ORP-2. Clearly, as reported previously [2,12], inclusion of BSA to the bicarbonate-enriched medium (+Bic) caused the aggregation of flotillin at the apical ridge area (for topology, see Fig. 6, inset). In the absence of (oxy)sterol- depleting agents, only <20% of the sperm cells had this flotillin distribution, and this proportion increased to 70% in the presence of BSA (Fig. 6). When sperm were incubated in bicarbonate-enriched media with either ORP-1 or ORP-2, this also resulted in a significant increase of aggregation of flotillin in the apical area of the sperm head, although 4 µg/ml ORP-2 was much more efficient (to a similar degree as BSA) when compared to 4 µg/ml ORP-1 (Fig. 6). This phenomenon was not observed when vitamin E or vitamin A was added to bicarbonate-enriched media in either the presence or the absence albumin (data not shown).

Effects of Oxysterol-Binding Proteins and Antioxidants on the Generation of Zona Affinity of Sperm and IVF

In vitro capacitation leads to the generation of hyper- activated sperm motility but also to the generation of affinity for the zona pellucida. In the absence of bicarbonate (-Bic), no sperm bound to the zona pellucida (data not shown). Only a minimal amount of sperm cells showed binding to the zona pellucida (0.8 sperm cells per zona pellucida on average) when incubated in bicarbonate-enriched medium in the absence of (oxy)sterol-interacting proteins (-BSA; Fig. 7A). When incubated in the presence of BSA, an average of eight sperm cells were binding to each zona pellucida (+BSA; Fig. 7A). Incubation of sperm in bicarbonate-enriched media (+Bic) with ORP-1 also induced sperm zona binding (two to three sperm cells per zona pellucida), whereas ORP-2 failed to induce this compared to bicarbonate-enriched medium without (oxy)sterol-interacting proteins (Fig. 7A). The fertilization rates of sperm cells incubated under these four conditions were also followed. IVF in the presence of bicarbonate and albumin (+Bic +BSA) led to a fertilization rate of 60% (Fig. 7B) where omission of (oxy)sterol-binding proteins (BSA) led to fertilization rates of only 2.4%. Despite the positive effects of ORPs on signs of sperm capacitation, they led to only marginal increases of fertilization rates: 3.5% and 4.1% for a 4-µg/ml dose of ORP-1 and ORP-2, respectively. Figure 7C depicts the localization and presence of sperm when interacting with the oocyte-zona complex under IVF conditions. In the absence of (oxy)sterol-interacting proteins, almost no interacting sperm cells were detected. In the presence of ORP-1 or –ORP-2, some sperm cells were present at the zona pellucida and showed some signs of zona penetration, indicating that these cells not only interact with the zona pellucida but also had induced the acrosome reaction, which is a step required for zona penetration (Fig. 7C). However, a deeper penetration as shown for BSA was only rarely found under ORP-1 or ORP-2 incubations.

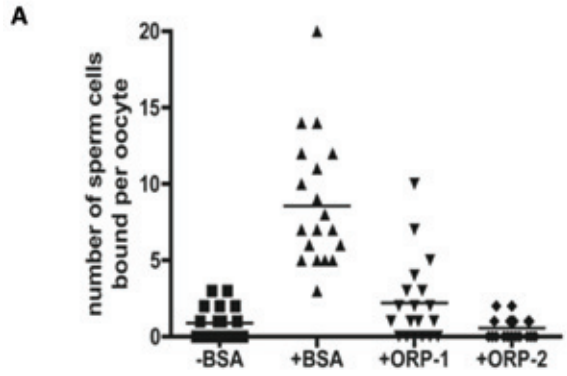

B

	-BSA	+BSA	+ORP-1	+ORP-2
Germinal Vesicle	0.0 ± 0.0	0.0 ± 0.0	1.1 ± 2.0	2.1 ± 1.9
Metaphase I	1.9 ± 2.7	0.0 ± 0.0	3.7 ± 3.6	3.6 ± 4.0
Metaphase II	91.4 ± 1.3	31.0 ± 8.5	86.8 ± 10.2	85.2 ± 12.7
Fertilized	2.4 ± 3.4	60.8 ± 6.2	3.5 ± 3.6	4.1 ± 4.4
Degenerated	4.3 ± 0.6	8.1 ± 6.4	4.9 ± 5.4	4.9 ± 8.5

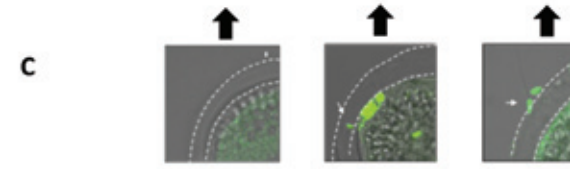

Figure 7. The bicarbonate/oxysterol/BSA pathway generates zona affinity and IVF, but replacement of BSA by ORPs is insufficient.

A) Sperm cells incubated in bicarbonate-enriched medium with albumin (+Bic+BSA) showed affinity for the zona pellucida when compared to bicarbonate-enriched medium without sterol-depleting agents, where essentially no zona binding was observed (+Bic -BSA); 4 µg/ml ORP-1 (+Bic+ORP-1) but not 4 µg/ml ORP-2 (+Bic+ORP-2) caused a smaller but significant increase in zona affinity than +Bic+BSA when compared to +Bic -BSA. B) Only the +Bic+BSA condition gave rise to efficient fertilization rates, while +Bic+ORP-1 or +Bic+ORP-2 did not have positive effects when compared to +Bic -BSA. For each experiment and each incubation type, at least 20 oocytes were used. The data represent mean=SEM, n=3. C) Representative microscopic photographs of sperm-zona interactions under the incubations provided in B. Green fluorescence indicated labeling of DNA and are depicted as merged with the corresponding bright-field images obtained. The dashed lines indicate the border of the zona pellucida. For +Bic-BSA, no sperm interaction with the zona pellucida was noted. In the presence of albumin (+Bic+BSA), full penetration through the zona pellucida was noted, while interaction with the zona pellucida (+BSA+ORP-1) or slight penetration (+Bic+ORP-2) was noted when albumin was replaced with recombinant ORP.

Effects of Oxysterol-Binding Proteins on the Induction of the Acrosome Reaction

The observation that fertilization rates were low in the presence of ORPs in bicarbonate-enriched media (in contrast to BSA) but that sperm incubated with ORPs showed some zona- binding affinity and some zona penetration ability led us to investigate whether ORPs were inducing premature acrosome reactions. Incubation of sperm in bicarbonate-depleted medium or in bicarbonate-

enriched medium (in either the absence or the presence of BSA) did not induce the acrosome reaction (the amount of acrosome-reacted cells that stained positive for fluorescent-conjugated peanut agglutinin; PNA-FITC, positive cells >10%; Fig. 8). Note that BSA had a stabilizing effect on the acrosome integrity, which has been explained in a previous study showing that this condition causes stabilization of docked SNARE complexes [18]. In contrast, ORP-1 and ORP-2 caused premature acrosome reactions in 20%–30% of the sperm cells (Fig. 8, B and C).

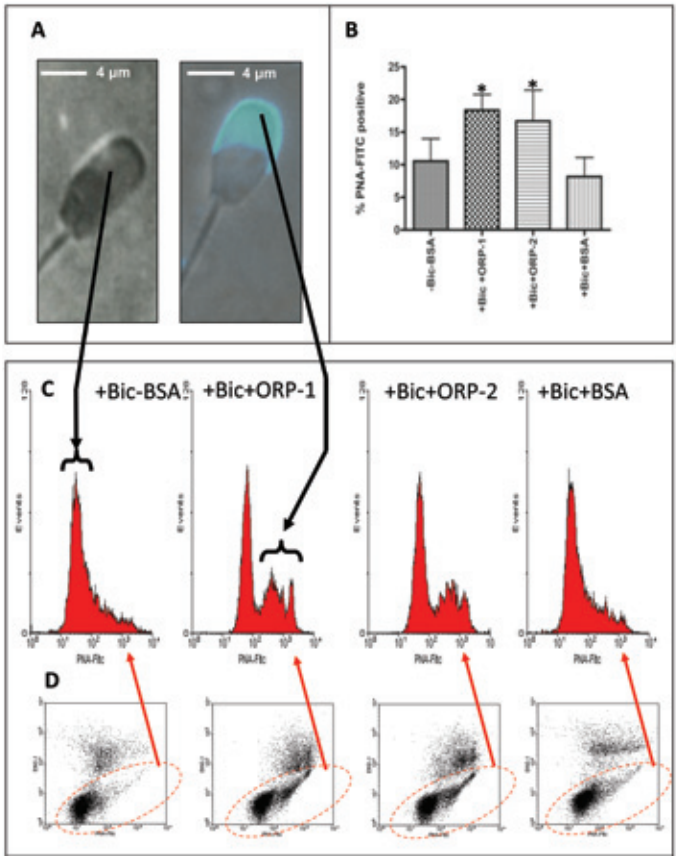

Figure 8. Sperm incubations with ORPs induce the acrosome reaction.

A) Merged phase-contrast image and PNA-FITC labeling of an acrosome-intact sperm (left) and an acrosome-reacted sperm cell (right). B) The relative amount of acrosome-reacted sperm cells in the absence (+ Bic - BSA) and in the presence of sterol-depleting agents (+Bic+ORP-1; B+Bic+ORP-2 or +Bic+BSA, respectively). The doses of ORP were 4 µg/ml. The data represent mean±SEM, n=3. Fluorescence intensity histograms of the PNA-FITC labeling of sperm incubated in the presence of (C) albumin (+Bic+BSA) and in the presence of (D) ORP-1 (+Bic+ORP-1) are included to show the shift in the amount of sperm cells with their acrosome reaction induced by ORP-1 compared to albumin. The left population is acrosome intact, and the right population is acrosome reacted, as depicted with the line connector arrows to A. * indicates a significant increase of effects compared to - Bic - BSA (in all comparisons, $P<0.05$).

Albumin, Oxysterol-Binding Proteins, and Methyl Beta-Cyclodextrin Efficiently Reduce Oxysterol Levels in Bicarbonate Stimulated Sperm

Experiments were designed in which sperm cells were treated with bicarbonate (+Bic) in the absence and in the presence of agents that can reduce sterols and/or oxysterols in sperm. The sterol reducing agents albumin, MBCD, or the recombinant oxysterol-binding proteins ORP1 and ORP2 were tested. All agents caused a reduction of 50% or more of the oxysterols formed when compared to the amount of oxysterols formed under bicarbonate alone (Fig. 9A). Interestingly, both ORPs at 4 µg/ml caused a very reproducible and more pronounced reduction in oxysterols levels than albumin or MBCD (a reduction of 70%; Fig 9A).

Desmosterol and Cholesterol Are Depleted by Albumin but Not by Oxysterol-Binding Proteins in Bicarbonate- Stimulated Sperm

Sperm stimulated with bicarbonate in the presence of albumin (+Bic+BSA) showed a 63% decrease of cholesterol and almost a 34% decrease in desmosterol when compared to the negative control (no bicarbonate; Supplemental Figure S1, available online at www.biolreprod.org), which was recovered in the albumin-containing supernatant after centrifugation (Fig. 8B and Table 2). The depletion of these sterols could be inhibited by vitamin E or vitamin A (Fig. 8B). Independent of bicarbonate inclusion, the MBCD also caused a significant (but lower) depletion of cholesterol (27% and 19%) and desmosterol (27% and 33%) in the absence and the presence of bicarbonate, respectively, in line with previous studies (Fig. 9B and Supplemental Data [2, 3]). Desmosterol is a precursor sterol in the cholesterol biosynthetic pathway present in all samples in a molar ratio of 1.5% relative to cholesterol. Note that the intensity of ions detected as expressed in Figure 2 are detected with varying levels of sensitivity because of the different ionization efficiencies in the APCI process. They were corrected for a response curve made for each individual oxysterol species and sterol species detected as described previously [4]. Interestingly, the addition of pro-oxidants in the presence of albumin and bicarbonate (i.e., under oxysterol- forming conditions; Fig. 1) resulted not only in a modest reduction the level of cholesterol (13%) but also a pronounced reduction of desmosterol (43%) when compared to the -Bic+BSA control (Fig. 9B and Supplemental Figure S1). Moreover, the two oxysterol-binding proteins ORP-1 and ORP-2, although very efficient in reducing oxysterol levels in sperm cells (Fig. 9A), did not cause significant reductions in the levels of cholesterol or desmosterol (Fig. 9B). The incubations with bicarbonate and BSA caused the depletion of oxysterols cholesterol and desmosterol from the sperm surface into the medium (for the partition of each sterol component in in vitro-capacitated mouse and boar sperm, see Tables 1 and 2).

MBCD-Mediated Sterol Depletion Causes Tyrosine Phosphorylation and Hyperactivated Motility in a Different Fashion Than Recombinant ORPs or BSA

In addition to the effects of recombinant ORP-1 and ORP-2 on sperm capacitation, we compared the effects of a much less specific sterol depletor on sperm capacitation (i.e., MBCD). Figure 9 shows that MBCD has the capacity to deplete the bicarbonate-dependent production of oxysterols. However, MBCD is a potent depletor of free sterols in both the absence and the presence of bicarbonate (Fig. 9; [28–30]). In fact, in the dose range of 0.5–10 mM, MBCD caused an increase in tyrosine phosphorylation in both the absence (-Bic) and the presence (+Bic) of bicarbonate (Fig. 10A), with highest stimulation to similar levels as that of BSA (Fig. 4C; note that BSA had this effect only in the presence of bicarbonate). In the absence of bicarbonate, only the specific concentration of 2 mM MBCD led to the induction of hyperactivated sperm motility (Fig. 10B), whereas in the presence of bicarbonate, MBCD did not attenuate the bicarbonate induction of hyper- activated sperm motility and significantly inhibited this response at higher dosages (Fig. 9B).

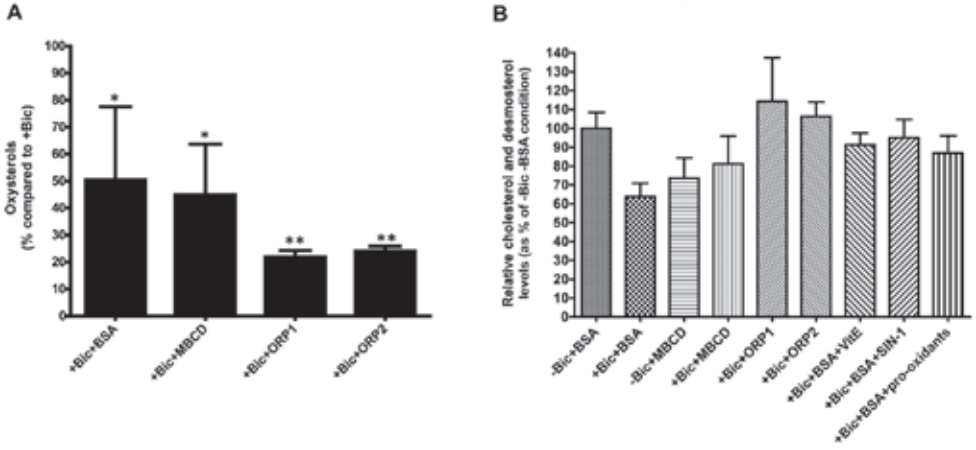

Figure 9. Reduction of cellular cholesterol and desmosterol levels and cellular oxysterol levels after incubation with sterol-interacting proteins.

A) Oxysterol-binding proteins ORP-1 and ORP-2 are more effective in reducing oxysterols from bicarbonate-activated sperm than albumin and MBCD. The total amount of oxysterols indicated is relative to the amount of oxysterols formed in the absence of oxysterol-interacting molecules (-Bic - BSA = 100% conform; Fig. 1). B) The cellular levels of cholesterol and desmosterol (total amount of both sterols indicated here as data for desmosterol and cholesterol separately; Supplemental Figure S1) are reduced by albumin (BSA) in a bicarbonate-specific manner that can be blocked by vitamin E (vitE). MBCD lowers both free sterols to a lesser extent but in a bicarbonate-independent manner. The ORP-1 and ORP-2 treatments did not lower the cellular levels of cholesterol or desmosterol. In all cases, the molar ratio of cholesterol to desmosterol remained approximately 10:1. Nevertheless, a slightly higher proportion of desmosterol was depleted by albumin and MBCD when compared to cholesterol (Supplemental Figure S1). Mean values ± SEM are indicated, n = 3. *indicates a significant effect when compared to +Bic -BSA; **indicates a more pronounced effect when compared to +Bic+BSA (in all comparisons, $P<0.05$). For distribution of molecular oxysterol species, cholesterol and desmosterol in the cell pellet and the supernatant of boar and mouse sperm specimen after treatment see Table 2.

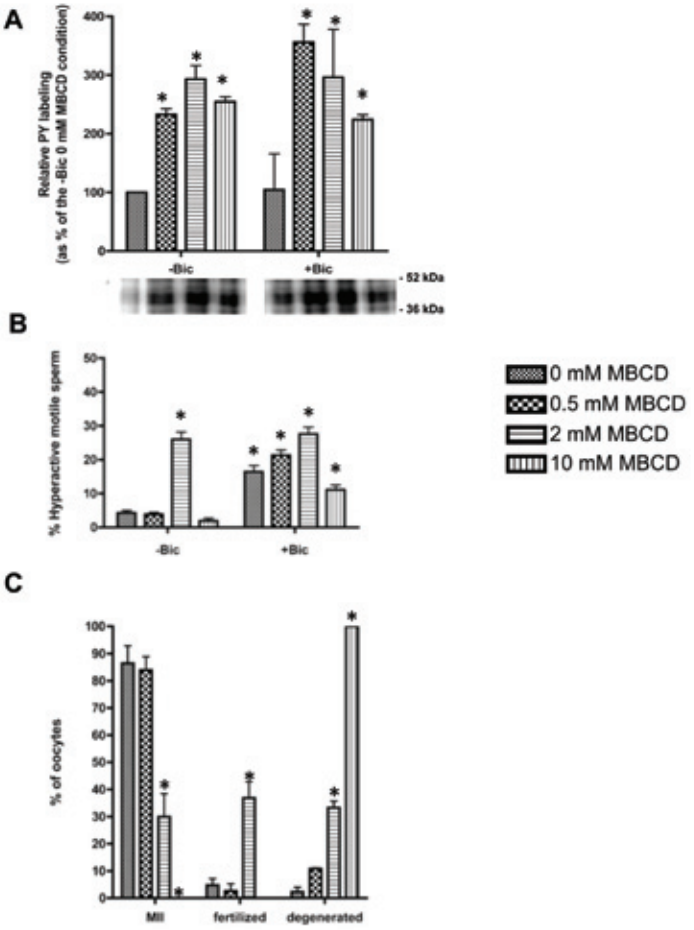

Figure 10. Effects of MBCD-mediated sterol depletion on sperm activation and IVF.

A) In the absence of bicarbonate (-Bic), MBCD induced PY20 labeling in the concentration range of 0.5–10 mM MBCD used and with maximal effect at 2 mM. In the presence of bicarbonate (+Bic), a similar maximal response was seen at 0.5 mM, while the higher doses of MBCD were still but less effective. B) MBCD only induced hyperactivated sperm motility at a 2-mM dose in the absence of bicarbonate (-Bic) but had no effects at lower or higher doses. In the presence of bicarbonate, only a marginal increase of hyperactivated sperm motility was noted at lower doses of MBCD (0.5 or 2 mM), whereas the highest dose of 10 mM MBCD had an adverse effect and inhibited hyperactivated sperm motility. C) MBCD-mediated sterol depletion inhibits IVF and induces oocyte degeneration. Increasing amounts of MBCD in albumin-free bicarbonate-enriched incubation media did not result in high IVF rates. Only at the dose of 2 mM MBCD did ~30 percent of the oocytes become fertilized, which is a relatively poor figure when compared to IVF rates obtained with albumin (Fig. 7). A dose-dependent degeneration of porcine oocytes was noted when IVF was performed in bicarbonate-enriched media with inclusion of MBCD. The data represent mean ± SEM, n=3, per experiment, and for C in each incubation type, at least 20 oocytes were used. * Indicates a significant effect when compared to 0 mM MBCD ($P < 0.05$).

MBCD Treatment Induces Low IVF Rates and Oocyte Degeneration

Analogous to the IVF experiments in bicarbonate-enriched media with BSA or with recombinant ORPs, we tested the effect of MBCD on fertilization rates. The fertilization rates after treatment of sperm with 0.5–10 mM MBCD compared to those of BSA (for BSA >60%, see Fig. 7B) were dramatically reduced (Fig. 10C). However, in contrast to ORP-1 and ORP-2 incubations, the 2-mM-MBCD condition led to much lower fertilization rates (30%). At lower and higher levels of MBCD (0.5 and 10 mM, respectively), even lower fertilization rates were observed when compared to sperm treated with 0mM MBCD (Fig. 10C) or with recombinant ORPs (Fig. 7B). A dose-dependent degeneration of oocytes was observed when IVF was performed in the presence of 0.5–10 mM MBCD. In the presence of BSA, these rates were <10% (Fig. 7B), whereas 2 and 10 mM MBCD caused unacceptably high levels of oocyte degeneration (of 30% and 100%, respectively; Fig. 10C).

DISCUSSION

Induction and Prevention of Oxysterol Formation

In this article, the formation of oxysterols is described in sperm under in vitro-capacitating conditions. Oxysterol formation was dependent on bicarbonate ions that must have induced the formation of radical oxygen species [31] because oxysterol formation was essentially blocked when mouse or porcine sperm cells were treated in bicarbonate-enriched media in the presence of vitamin E or vitamin A. In a previous article, we have shown from bovine sperm that oxysterol formation can be induced by incubating sperm in the presence of pro-oxidants like tert-butylhydroxide [4]. Here we showed that oxysterols can be formed in the absence of bicarbonate under certain pro-oxidant conditions (FeSO4 + ascorbate) but not by the peroxynitrite forming agent SIN-1. Both bicarbonate and the $FeSO_4$ + ascorbate incubations induced especially the production of 7-ketocholesterol and 5,6b-epoxycholesterol.

Oxysterol Formation and Interaction with Oxysterol- Binding Proteins Induces Various Characteristics of Sperm Capacitation

When sperm are capacitated in vitro in the presence of bicarbonate and BSA, they show signs of hyperactivated sperm motility [27], increased levels of tyrosine phosphorylation [27], surface changes (including the already noted removal of sterols [32]), and redistribution and aggregation of lipid microdomains [12], and higher affinity for the zona pellucida [11, 16]. These changes together result in the sperm becoming competent to fertilize the oocyte during IVF incubations [32]. In the present work, in which BSA was replaced for either recombinant ORP-1 or ORP-2, a number of capacitation responses, were detected, including 1) the induction of hyperactivated sperm motility, 2) increased tyrosine phosphorylation, 3) aggregation of lipid- ordered microdomain membrane markers at the apical ridge area of the sperm head, and 4) to some extent higher affinity for the zona pellucida. In fact, ORP treatment led to some limited penetration activity of sperm cells through

the zona pellucida, but this response was limited when compared to BSA. All these responses were present only when sperm were incubated in bicarbonate-rich media (+Bic), and the responses were inhibited in presence of vitamin E or blocked by vitamin A. Thus, an essential part of sperm capacitation is due to the formation of oxysterols and putatively to the interaction of these formed oxysterols with proteins involved in sterol depletion at the sperm surface [8, 19].

Depletion of Oxysterols, Desmosterol, and Cholesterol

Sperm capacitation performed in the presence of the sterol- depleting molecule BSA (routinely done in IVF [11]) resulted in an efficient reduction of the majority of oxysterols (50%) from the sperm surface into the albumin-containing fraction not associated with the sperm surface (recovered in the supernatant after centrifugation). An even more severe reduction of oxysterols were detected when sperm were incubated with recombinant oxysterol-binding proteins (ORP-1 and ORP-2; in both cases, a reduction of >70% of the oxysterols took place), which are known to bind oxysterols [11, 33]. Importantly, ORPs are soluble proteins enhancing exchange of sterols from donor to acceptor membranes over the cytosol in a variety of cells. After isolating these two recombinant proteins from Escherichia coli, we used them as tools for the specific interaction of oxysterols in sperm suspensions under various in vitro capacitation conditions. We must stress here that this extracellular type of action is not mimicking eventually endogenous ORPs under physiological conditions where they (if at all present in sperm) are active intracellularly. The effects of ORPs, similar to BSA, were seen only in bicarbonate- enriched media but not in the absence of bicarbonate. When sperm were incubated with +Bic +ORPs, no depletion of cholesterol or desmosterol was monitored, while +Bic +BSA caused a depletion of >30% cholesterol and desmosterol. Interestingly, ORP treatment caused only a minor depletion (<10%) of the oxysterols in the supernatant after centrifuging sperm. This implies that ORP (in contrast to BSA) does not deplete oxysterols efficiently from sperm but scavenges oxysterols (by binding to the sperm surface?) during the induction of their production at the sperm surface by bicarbonate. It is likely that the bicarbonate-induced capacitation responses are not inhibited (instead, it was even promoted) by ORP treatment, as intracellular ROS formation and ROS signaling is not affected. It seems that the concomitant high levels of oxysterols in sperm treated with bicarbonate alone can be compensated by albumin (depletion) or by ORP (likely surface binding and scavenging). Moreover, pretreating sperm with vitamin A inhibited oxysterol formation; this caused a complete block of IVF, and vitamin E had only a partial inhibiting effect. Both membrane antioxidants also inhibited sperm zona binding but not the integrity of sperm or oocytes. These findings indicate that lowering ROS and ROS- dependent signaling processes at the sperm surface prior to an IVF experiment blocks oxysterol formation and sperm capacitation and reduces sperm-zona-binding and IVF rates. The difference in degree of effect between vitamin A and vitamin E may lie in the intrinsic properties of both hydrophobic antioxidants and the way we pretreated sperm prior to IVF. It is possible that vitamin A either resides better in the sperm surface during the IVF procedure (more hydrophobic) or elicits its antioxidant properties more efficiently

when compared to vitamin E (vitamin A is a stronger antioxidant). Note that the pretreated sperm was diluted 10 times and used for 24 h in the IVF experiment. Under such conditions, back exchange of the antioxidants to albumin may occur. The decrease of IVF rates by vitamin E has been reported for bovine sperm [34, 35]. Moreover, inseminating oocytes with hydrogen peroxide-pretreated sperm has been shown to increase fertilization, cleavage, and blastocyst rates [36]. Taken together, we believe that these data show that depletion of sperm surface lipid peroxides (or, in the absence of bicarbonate, the lack of formation of sperm surface lipid peroxides) causes a reduction in IVF rates. The formation of lipid peroxides under bicarbonate allows reverse transport of (oxy) sterols to BSA and high IVF rates, while excessive lipid peroxidation is detrimental to the sperm cell and thus to fertilization [10].

Oxysterol Reduction Alone Is Insufficient for Obtaining IVF Success

Interestingly, unlike albumin, ORPs were not able to reduce cholesterol or desmosterol, which fits to their higher specific affinity for oxysterols when compared to albumin. This lack of reducing levels of free sterols at the sperm surface likely relates to the fact that incubations of BSA did result in 60% fertilization rates after IVF, whereas ORP incubations largely failed to result in fertilization. Both ORP and BSA incubations induced in vitro sperm capacitation, although ORP also induced preliminary acrosome reactions, while BSA-treated cells remained acrosome intact. Therefore, it is possible that the concentration and length of ORP treatments need to be refined and that the currently used circumstances were simply too rough for the sperm to become fertilization competent. Support for this possibility is that the lowest dose of ORP-1 or ORP-2 caused already maximal stimulation of hyperactivated motility, and higher doses were partly inhibiting this effect. The previously mentioned possibility that ORPs act to inhibit oxysterol formation by scavenging oxysterols may at higher doses become a too efficient process and thus will inhibit ROS- dependent capacitation responses. Presently, we are studying how extracellular added ORPs on the sperm surface cause the cellular responses that in part run parallel to bicarbonate/BSA- induced capacitation. The oxysterol-binding protein family contains >10 proteins, and their role in cell physiology has recently been reviewed [37]. Of course, another possibility for the discrepancies between BSA and ORPs may lie in that BSA has other (oxysterol-independent) effects on sperm [38].

MBCD Causes a Partly Bicarbonate-Independent Sterol Depletion from Sperm

Besides BSA and ORP, another molecule with affinity for sterols, MBCD, has been exploited either to elicit sperm capacitation [30] or to achieve BSA-independent IVF [39]. The latter can be useful in developing methods to treat sperm under fully pathogen-free declared materials. Because only a part of the BSA effects can be obtained by ORP replacement, the effects of MBCD were tested. As reported in the literature, MBCD is indeed capable of inducing hyperactivated sperm motility [40, 41] and tyrosine phosphorylation in the sperm tail [27, 40] and causes a depletion of cholesterol, desmosterol [28], and oxysterols (this study). However, MBCD does work in a different fashion when

compared to BSA and ORP-1 and ORP-2, as it elicits these effects independently from bicarbonate and does not stop extracting sterols in the presence of vitamin E [28, this study]. Moreover, MBCD fails to induce aggregation of flotillin and tyrosin phosphorylation in the sperm head [28] and extracts sterols from both lipid rafts and from the nonraft membranes, whereas BSA extracts sterols only from the nonraft domain [2]. In the presence of bicarbonate, higher levels of MBCD inhibit sperm motility (this study) and also cause sperm membrane deterioration and premature acrosome reactions [29]. Despite all these differences to BSA, 2-mM-MBCD incubation led to IVF rates of 30%. However, already at this concentration, MBCD caused a non-acceptable level of oocyte degeneration (>30%) that was observed for all oocytes at 10 mM MBCD.

In conclusion, the bicarbonate-dependent formation of ROS leads to the production of oxysterols. It is likely that the subsequent interactions of the formed oxysterols with oxy- sterol-binding proteins (ORPs or albumin) and substantial depletion of oxysterols enable sperm capacitation and related specific sperm surface changes [13]. We postulate that that these subtle changes in sperm sterols (only less than 1% of sterols are converted to oxysterols) may activate a sterol transporter protein. In this respect, it is possible that a protein like the CD36 (a multifunctional protein homologous to the class B scavenger receptor SR-B1) acts as a lipid sensor [42] to oxysterols. In fact, a recent report on bull sperm has indicated that CD36 is a biomarker for male fertility [43]. SR-B1 itself (a translation product from the SARB-1 gene) has also been implied in regulating reverse cholesterol transport to high- density lipoproteins in other tissues [44] and could be activated by surface rearrangements typical for capacitating sperm as postulated previously [1]. Other candidates for a reverse sterol transporter potentially active at the sperm surface belong to the ATP cassette transporters; ABCA1, ABCA7, ABCA17, and ABCG1 are all detected in sperm [45, 46], and both ABCA1 and ABG1 have in fact been shown to transport oxysterols out of cells [9].

Our results provide evidence that only with a cholesterol/desmosterol-accepting protein in the sperm incubation buffer do sperm became capable of fertilizing the oocyte. ORP-1 and ORP-2 turned out to be too specific for reducing oxysterol levels but failing to deplete cholesterol/desmosterol, which could render the treated sperm unfertile under IVF conditions. The sperm surface interaction of ORP also induced some premature acrosome reactions. Under bicarbonate conditions, BSA was capable of extracting cholesterol desmosterol and oxysterols, thus allowing the depletion of a large amount of total free sterols, an effect apparently required for fertilization. Blocking oxysterol formation in the sperm membrane with hydrophobic antioxidants reduced sperm motility tail tyrosine phosphorylation and IVF rates and, to a lesser extent, inhibited sperm-zona binding. This may indicate that ROS formation and peroxidation of sterols (and possibly other lipids) in the sperm membrane are required for proper zona penetration rather than the recognition of this structure. The bicarbonate- and ROS- independent sterol depletion by MBCD also induces some aspects of sperm capacitation but fails to generate good IVF results because of the adverse effects on oocyte physiology. It is likely that more subtle treatments with ORPs or MBCD could result in better IVF results. The balance between the rate of oxysterol formation and of oxysterol

depletion are probably determining how the sperm are going through the time window of sperm capacitation b to reach the state of deterioration (see the model in Fig. 11; see also Aitken [31]). Thus, this study has shed new light on the mechanisms of how oxysterols are formed in the sperm and that this process precedes free sterol depletion from the sperm surface during IVF. Apparently, a bicarbonate-induced ROS-dependent membrane process is required to activate reverse (oxy) sterol transport from the capacitating sperm surface. From this study it is not clear whether the formation of oxysterols itself is involved in the activation of a reverse sterol transporter or whether they are just molecular signs of ROS emerging in the sperm surface and indirectly linked to the depletion of (oxy) sterols by albumin. Future research should focus on the exact conditions that can be used to optimize IVF with sterol-depleting agents. More important, experiments should be planned to unravel the mechanism of reverse sterol transport from capacitating sperm as well as determining the involvement of oxysterols in this sterol transport, which is crucial for IVF.

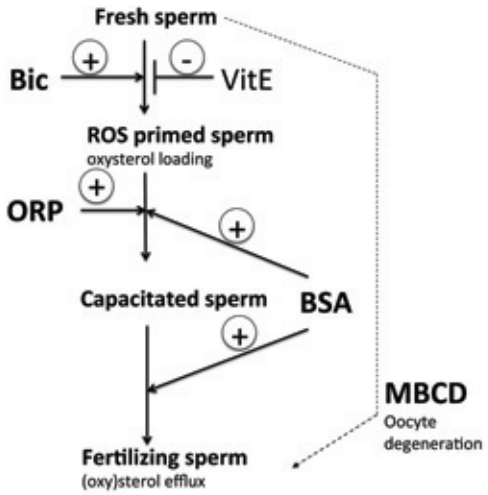

Figure 11. Schematic presentation of bicarbonate-induced ROS-dependent oxysterol loading and removal of excessive oxysterols.

These two processes induce signs of sperm capacitation, which does not depend on removal of cholesterol and desmosterol, as has been shown by the use of ORPs. However, the formation of oxysterols allows a downstream depletion of cholesterol and desmosterol by BSA, which is required for IVF. Indicated as a dashed line is the action of MBCD causing a completely bicarbonate, ROS, oxysterol-independent cholesterol, and desmosterol removal from sperm. Although only a small concentration range of MBCD gave moderately low IVF rates, it also led to very substantial oocyte degeneration.

ACKNOWLEDGMENT

Dr. R.L. Serrano has helped with the transfection experiments and purification of recombinant ORP-1 and ORP-2 proteins. Dr. P.S. Tsai has helped with IVF and sperm incubation experiments.

SUPPLEMENTARY

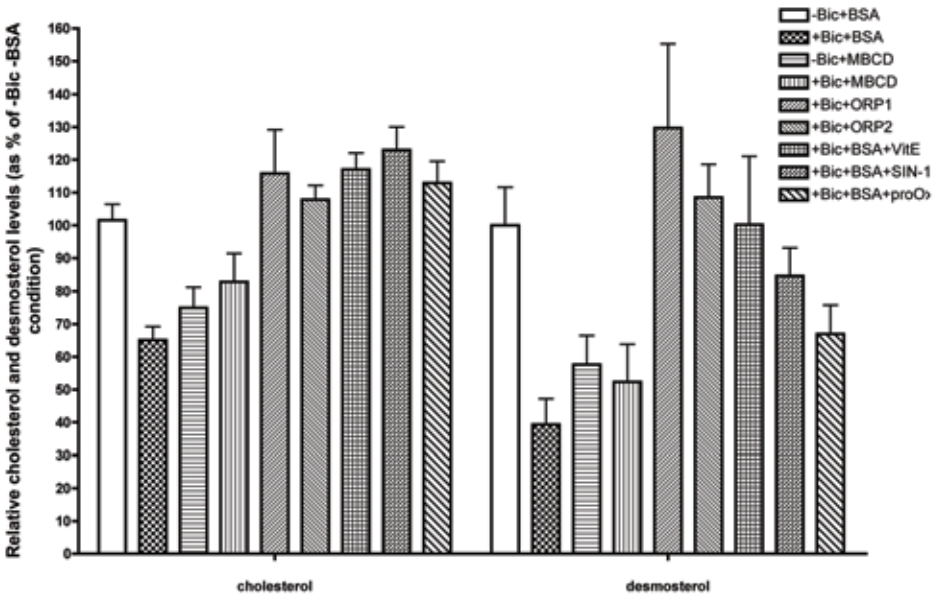

Supplemental Figure S1. Supplementary data for the individual free sterol species that are cumulatively expressed in figure 9B (for further information see legends to Figure 9B).

REFERENCES

1. Flesch FM, Gadella BM. Dynamics of the mammalian sperm plasma membrane in the process of fertilization. Biochim Biophys Acta 2000;1469:197–235.

2. van Gestel RA, Brewis IA, Ashton PR, Helms JB, Brouwers JF, Gadella BM. Capacitation-dependent concentration of lipid rafts in the apical ridge head area of porcine sperm cells. Mol Hum Reprod 2005; 11:583–590.

3. Flesch FM, Brouwers JF, Nievelstein PF, Verkleij AJ, van Golde LM, Colenbrander B, Gadella BM. Bicarbonate stimulated phospholipid scrambling induces cholesterol redistribution and enables cholesterol depletion in the sperm plasma membrane. J Cell Sci 2001; 114:3543–3555.

4. Brouwers JF, Boerke A, Silva PF, Garcia-Gil N, van Gestel RA, Helms JB, van de Lest CH, Gadella BM. Mass spectrometric detection of cholesterol oxidation in bovine sperm. Biol Reprod 2011; 85:128–136.

5. Boerke A, Tsai PS, Garcia-Gil N, Brewis IA, Gadella BM. Capacitation- dependent reorganization of microdomains in the apical sperm head plasma membrane: functional relationship with zona binding and the zona- induced acrosome reaction. Theriogenology 2008; 70:1188–1196.

6. de Lamirande E, Lamothe G, Villemure M. Control of superoxide and nitric oxide formation during human sperm capacitation. Free Radic Biol Med 2009; 46:1420–1427.

7. de Lamirande E, Lamothe G. Reactive oxygen-induced reactive oxygen formation during human sperm capacitation. Free Radic Biol Med 2009;46:502–510.

8. van der Vusse GJ. Albumin as fatty acid transporter. Drug Metab Pharmacokinet 2009; 24:300–307.

9. Jessup W, Gelissen IC, Gaus K, Kritharides L. Roles of ATP binding cassette transporters A1 and G1, scavenger receptor BI and membrane lipid domains in cholesterol export from macrophages. Curr Opin Lipidol 2006; 17:247–257.

10. Aitken RJ, Baker MA. Oxidative stress, sperm survival and fertility control. Mol Cell Endocrinol 2006; 250:66–69.

11. Blake D, Svalander P, Jin M, Silversand C, Hamberger L. Protein supplementation of human IVF culture media. J Assist Reprod Genet2002; 19:137–143.

12. Zitranski N, Borth H, Ackermann F, Meyer D, Viewig L, Breit A, Gudermann T, Boekhoff I. The "acrosomal synapse": subcellular organization by lipid rafts and scaffolding proteins exhibits high similarities in neurons and mammalian spermatozoa. Commun Integr Biol 2010; 3:513–521.

13. Thaler CD, Thomas M, Ramalie JR. Reorganization of mouse sperm lipid rafts by capacitation. Mol Reprod Dev 2006; 73:1541–1549.

14. Gadella BM, Tsai PS, Boerke A, Brewis IA. Sperm head membrane reorganisation during capacitation. Int J Dev Biol 2008; 52:473–480.

15. Nixon B, Aitken RJ. The biological significance of detergent-resistant membranes in spermatozoa. J Reprod Immunol 2009; 83:8–13.

16. van Gestel RA, Brewis IA, Ashton PR, Brouwers JF, Gadella BM. Multiple proteins present in purified porcine sperm apical plasma membranes interact with the zona pellucida of the oocyte. Mol Hum Reprod 2007; 13:445–454.

17. Tsai P, De Vries KJ, De Boer-Brouwer M, Garcia-Gil N, Van Gestel RA, Colenbrander B, Gadella BM, Van Haeften T. Syntaxin and VAMP association with lipid rafts depends on cholesterol depletion in capacitating sperm cells. Mol Membr Biol 2007; 24:313–324.

18. Tsai PS, Garcia-Gil N, van Haeften T, Gadella BM. How pig sperm prepares to fertilize: stable acrosome docking to the plasma membrane. PLoS One 2010; 5:e11204.

19. Tsai PS, Gadella BM. Molecular kinetics of proteins at the surface of porcine sperm before and during fertilization. Soc Reprod Fertil Suppl 2009; 66:23–36.

20. Aitken RJ, Clarkson JS, Fishel S. Generation of reactive oxygen species, lipid peroxidation, and human sperm function. Biol Reprod 1989; 41:183–197.

21. Suchanek M, Hynynen R, Wohlfahrt G, Lehto M, Johansson M, Saarinen H, Radzikowska A, Thiele C, Olkkonen VM. The mammalian oxysterol- binding protein-related proteins (ORPs) bind 25-hydroxycholesterol in an evolutionarily conserved pocket. Biochem J 2007; 405:473–480.

22. Wilson CM. Staining of proteins on gels: comparisons of dyes and procedures. Methods Enzymol 1983; 91:236–247.

23. Gergel D, Misik V, Ondrias K, Cederbaum AI. Increased cytotoxicity of 3- morpholinosydnonimine to HepG2 cells in the presence of superoxide dismutase. Role of hydrogen peroxide and iron. J Biol Chem 1995; 270: 20922–20929.

24. Broekhuijse ML, Sostaric E, Feitsma H, Gadella BM. Additional value of computer assisted semen analysis (CASA) compared to conventional motility assessments in pig artificial insemination. Theriogenology 2011; 76:1473–1486.

25. Schoevers EJ, Kidson A, Verheijden JH, Bevers MM. Effect of follicle- stimulating hormone on nuclear and cytoplasmic maturation of sow oocytes in vitro. Theriogenology 2003; 59:2017–2028.

26. Harrison RA. Capacitation mechanisms, and the role of capacitation as seen in eutherian mammals. Reprod Fertil Dev 1996; 8:581–594.

27. Bajpai M, Asin S, Doncel GF. Effect of tyrosine kinase inhibitors on tyrosine phosphorylation and motility parameters in human sperm. Arch Androl 2003; 49:229–246.

28. van Gestel RA, Helms JB, Brouwers JF, Gadella BM. Effects of methyl-b- cyclodextrin-mediated cholesterol depletion in porcine sperm compared to somatic cells. Mol Reprod Dev 2005; 72:386–395.

29. Shadan S, James PS, Howes EA, Jones R. Cholesterol efflux alters lipid raft stability and distribution during capacitation of boar spermatozoa. Biol Reprod 2004; 71:253–265.

30. Choi YH, Toyoda Y. Cyclodextrin removes cholesterol from mouse sperm and induces capacitation in a protein-free medium. Biol Reprod 1998; 59: 1328–1333.

31. Aitken RJ. The capacitation-apoptosis highway: oxysterols and mamma- lian sperm function. Biol Reprod 2011; 85:9–12.

32. Osheroff JE, Visconti PE, Valenzuela JP, Travis AJ, Alvarez J, Kopf GS. Regulation of human sperm capacitation by a cholesterol efflux-stimulated signal transduction pathway leading to protein kinase A-mediated up-regulation of protein tyrosine phosphorylation. Mol Hum Reprod 1999; 5: 1017–1026.

33. Yan D, Olkkonen VM. Characteristics of oxysterol binding proteins. Int Rev Cytol 2008; 65:253–285.

34. Marques A, Santos P, Antunes G, Chaviero P, Moriero da Silva F. Effect of a-tocopherol on bovine in vitro fertilization. Reprod Dom Anim 2010; 45:81–85.

35. Dalvit GC, Cetica PD, Beconi MT. Effect of a-tocopherol and ascorbic acid on bovine in vitro fertilization. Theriogenology 1998; 49:619–627.

36. Rahman MB, Vandaele L, Rijsselaere T, Zandi M, Maes D, Shamsuddin M, van Soom A. Oocyte quality determines bovine embryo development after fertilization with hydrogen peroxide-stressed spermatozoa. Reprod Fert Dev 2012; 24:608–618.

37. Vihervaara T, Jansen M, Uronen RL, Ohsaki Y, Ikonen E, Olkkonen VM. Cytoplasmic oxysterol-binding proteins: sterol sensors or transporters? Chem Phys Lipids 2011; 164:443–450.

38. Xia J, Ren D. The BSA-induced $Ca(2^{+})$ influx during sperm capacitation is CATSPER channel-dependent. Reprod Biol Endocrinol 2009; 7:119.

39. Takeo T, Hoshii T, Kondo Y, Toyodome H, Arima H, Yamamura K, Irie T, Nakagata N. Methyl-beta-cyclodextrin improves fertilizing ability of C57BL/6 mouse sperm after freezing and thawing by facilitating cholesterol efflux from the cells. Biol Reprod 2008; 78:546–551.

40. Kato Y, Shoei S, Nagao Y. Capacitation status of activated bovine sperm cultured in media containing methyl-beta-cyclodextrin affects the acrosome reaction and fertility. Zygote 2011; 19:21–30.

41. Visconti PE, Galantino-Homer H, Ning X, Moore GD, Valenzuela JP, Jorgez CJ, Alvarez JG, Kopf GS. Cholesterol efflux-mediated signal transduction in mammalian sperm. beta-cyclodextrins initiate transmem- brane signaling leading to an increase in protein tyrosine phosphorylation and capacitation.J Biol Chem 1999; 274:3235–3242.

42. Martin C, Chevrot M, Poirier H, Passilly-Degrace P, Niot I, Besnard P. CD36 as a lipid sensor. Physiol Behav 2011; 105:36–42.

43. Feugang JM, Rodriguez-Osorio N, Kaya A, Wang H, Page G, Ostermeier GC, Topper EK, Memili E. Transcriptome analysis of bull spermatozoa: implications for male fertility. Reprod Biomed Online 2010; 21:312–324.

44. Nieland TJ, Chroni A, Fitzgerald ML, Maliga Z, Zannis VI, Kirchhausen T, Krieger M. Cross-inhibition of SR-BI- and ABCA1-mediated cholesterol transport by the small molecules BLT-4 and glyburide. J Lipid Res 2004; 45:1256–1265.

45. Morales CR, Marat AL, Ni X, Yu Y, Oko R, Smith BT, Argraves WS. ATP-binding cassette transporters ABCA1, ABCA7, and ABCG1 in mouse spermatozoa. Biochem Biophys Res Commun 2008; 376:472–477.

46. Ban N, Sasaki M, Sakai H, Ueda K, Inagaki N. Cloning of ABCA17, a novel rodent sperm-specific ABC (ATP-binding cassette) transporter that regulates intracellular lipid metabolism. Biochem J 2005; 389:577–585.

4

Removal of GPI-anchored membrane proteins cause clustering of lipid microdomains in the apical head area of porcine sperm

Arjan Boerke[1,2]
Joost van der Lit[1]
J. Bernd Helms[1]
Bart M. Gadella[1,2]

[1]Department of Biochemistry and Cell Biology, Faculty of Veterinary Medicine, Utrecht University, Yalelaan 2, 3584 CM Utrecht, The Netherlands

[2]Department of Farm Animal Health Faculty of Veterinary Medicine, Utrecht University, Yalelaan 104, 3584 CM Utrecht, The Netherlands

Submitted

ABSTRACT

Part of the sperm capacitation process is the release of extracellular proteins, which allows a sperm surface reorganization enabling the sperm to functionally interact with the cumulus oocyte complex and to fertilize. These released components are called decapacitation factors as a preliminary release causes surface destabilization and premature capacitation. The involvement of glycosylphosphatidylinositol (GPI) anchored proteins in sperm capacitation is studied and we showed that glycosylphosphatidylinositol anchored proteins such as CD52 and CD55 are released during sperm capacitation. When sperm was treated with phosphatidyl inositol specific phospholipase C this resulted in the cleavage of CD55 under non-capacitation conditions. Moreover, the phospholipase treatment caused a bicarbonate and albumin independent surface reorganization including the decoating of the ganglioside GM1 and the aggregation of flotillin. Phospholipase treatment under these -not fully capacitation supporting- conditions caused activation of sperm hypermotility, protein tyrosine phosphorylation and a swelling of the apical acrosome region, all signs of sperm capacitation. Under these conditions no sperm deterioration was noted while the phospholipase treatment was detrimental to sperm incubated under full capacitation conditions. The possible involvement of GPI anchor cleaving enzymes in sperm capacitation is discussed.

Keywords: sperm capacitation, membrane raft, PI phospholipase C, GPI anchored protein release

INTRODUCTION

The sperm cell surface is coated with extracellular glycoproteins that form a protective layer and stabilize the sperm cell during its transit through the male and female genital tracts [1]. A number of extracellular coating proteins become attached to the sperm surface during its transit through the epididymal duct while other factors become surface associated during ejaculation when sperm cells are mixed with secretory fluids from diverse accessory sex-glands (seminal plasma) [2]). Some of the extracellular proteins associate with the sperm surface via electrostatic interactions while others are covalently linked to lipids by GPI anchors or interact with hydrophobic moieties towards the lipid bilayer (this phenomenon can be facilitated by post translational acylation). In sperm physiology it has become clear that the extracellular coating is not only protecting the integrity of the sperm membrane but also that it inhibits premature sperm capacitation (the process where sperm cells become competent to initiate fertilization of the oocyte, for review see [1,3]. The released components are, therefore, also termed decapacitation factors. Decapacitation factors, when attached to the sperm surface, are believed to mask underlying proteins involved in (i) sperm zona binding and (ii) docking of the acrosome required for the initiation of the acrosome reaction. Processes that are inhibited until the decapacitation factors are released [4,5]).

The removal of the decapacitation factors from the sperm surface allows the reorientation of membrane lipids and surface proteins [5]. During this process an albumin dependent efflux of non-lipid raft sterols is induced [6]. Probably the removal of decapacitation factors causes beyond this sterol efflux also an aggregation of lipid-ordered micro-domains to the apical ridge area of the sperm head. This allows the generation of functional protein complexes involved in zona binding and in the acrosome reaction at the sperm surface [7-10].

Isolated detergent-resistant resistant sperm membranes (DRM, representing the lipid raft fraction of sperm cells) are enriched in cholesterol, desmosterol and glycolipids such as the ganglioside GM 1 and a sulphated glycolipid specific for sperm (seminolipid) [4,11-13]. The DRMs are also enriched in GPI anchored proteins (GPI-APs) that are indeed considered to be markers for membrane rafts (an example is the protein CD55 [14]. During epididymal maturation a number of proteins become GPI anchored to the sperm surface via a yet not well-understood mechanism [15]. A number of these GPI-APs block the recognition of the sperm surface by phagocytes and also have an anti-coagulant function (CD52, CD55). Interestingly, CD52 also interacts with the peripheral sperm surface decapacitation factor seminogelin [16]. When a GPI-AP cleaving enzyme would cleave CD52 this could thus result in the concomitant removal of associating decapacitating factors from the sperm surface. Another GPI-AP the enzyme carbonyl reductase (or P34h) is reported to be involved in sperm-zona binding and originates from the epididymis [9,17]. Thus at least specific GPI-APs need to be removed from the capacitating sperm surface while others remain or even become associated for instance at the area where sperm-zona binding will take place. Interestingly, capacitation induces the release of GPI-APs [18]. A testis specific Angiotensin converting enzyme (AcE) with GPIase activity was shown to be responsible for this release [19]. Once active this enzyme releases

the entire protein part of a GPI-AP by cutting within the glycosidic GPI moiety. The AcE mediated removal of GPI-APs appears to be important for capacitation as knock out mice for AcE were infertile [19]. An alternative way to cleave the GPI anchors is to use phospholipase C or D; both enzymes can cleave the diacylglycerol or phosphatidic acid moiety from the GPI-AP, respectively. Effectively this also results in the release of the entire protein domain of the GPI-AP albeit that the released protein also contains the sugars from the GPI anchor (and in case of phosphatidylinositol specific phospholipase C (PIPLC) also the phosphate group).
In this study we have incubated sperm cells with *in vitro* capacitation media in the presence or absence of PIPLC in order to compare spontaneous and PIPLC induced removal of GPI anchored proteins and to unravel the role of these processes of cell signalling in lateral surface reorganization characteristic for sperm capacitation.

MATERIALS AND METHODS

Sperm incubations

Ejaculates were collected from boars with proven fertility at Varkens KI Nederland (Deventer, the Netherlands), a commercial enterprise producing insemination doses for pig artificial insemination for sow herds. Freshly ejaculated sperm was filtered through gauze to remove gelatinous material and subsequently diluted and washed in Hepes buffered saline (137 mM NaCl, 2.5 mM KCl, 20 mM Hepes, pH 7.4; HBS). Next, sperm was washed through a discontinuous Percoll® (GE, Healthcare, Diegem, Belgium) gradient of 70% (v/v) and 35% (v/v) as described [9]. All solutions were made iso-osmotic (290-310 mOsm/kg) with HBS at 23ºC. Percoll® layers were discarded and sperm pellets were resuspended at a final concentration of 100 million sperm cells/mL in Hepes buffered Tyrodes media (HBT; 120 mM NaCl, 21.7 mM lactate, 20 mM Hepes, 5 mM glucose, 3.1 mM KCl, 2.0 mM $CaCl_2$, 1.0 mM pyruvate, 0.4 mM $MgSO_4$, 0.3 mM NaH_2PO_4; 300 mOsm/kg, pH 7.4; HBT condition further referred to as –Bic/-BSA) or supplemented with 15 mM $NaHCO_3$, equilibrated with 5% CO_2 in humidified atmosphere (further referred to as +Bic/-BSA). Similarly sperm were incubated media supplemented with 0.3 % w/v bovine serum albumin (defatted fraction V, Boehringer Mannheim, Almere, the Netherlands; BSA) in absence (-Bic/+BSA) or presence (+Bic/+BSA) of bicarbonate. The +Bic/+BSA medium is fully supportive for sperm capacitation and can be used for pig in vitro fertilization. All bicarbonate-enriched conditions were incubated with open vials in 5% CO_2 atmosphere for 2 hours at 38.5 ºC. All bicarbonate-depleted conditions were incubated in airtight vials for 2 hours at 38.5 ºC in a water bath. Sperm was incubated in the presence of the enzyme the enzyme PIPLC (Sigma-Aldrich, Mannheim, Germany) with a final concentration of 0.1 units/mL

FACS

Incubated sperm were washed in HBT and subsequently incubated for 5 minutes in 1 µg/mL fluorescein conjugated peanut-agglutinin (PNA-FITC) in order to discriminate acrosome intact cells

from acrosome reacted cells. Next, 25 nM of the membrane impermeable vital stain propidium iodide (PI) was added to discriminate vital sperm from deteriorated sperm. Sperm suspensions were then analyzed on a FACScalibur flow cytometer equipped with a 100 mW argon laser (Becton Dickinson, San Jose, CA, USA). Excitation of both fluorescent probes was efficient at the wavelength of 488 nm. The resulting FITC and PI –emission intensity was detected in logarithmic mode of FL-1 (530/30 nm band pass filter) and FL-3 (620 nm long pass filter). Respectively, the forward and sideway scatter signal were detected in linear mode and sperm specific events were gated for further analysis [20]. The resulting 2 dimensional dot plots represented 10,000-gated events and were made with FL-1 data expressed on the x-axis and FL-3 data on the y-axis. The amount of cells positively stained with one or both fluorescent dyes were scored using quadrant analysis in Win MDI software (Version 2.8 J. Trotter, freeware)

Lipid Extraction and High Performance Thin Layer Chromatography (HPTLC)

Total lipid fractions from equal amount of sperm cells (100 million cells) under different incubation conditions were extracted [21]. The resulting organic layer containing the extracted lipids was collected and dried under a steady nitrogen flow and subsequently used for further analysis with thin layer chromatography. Silica Gel 60 HPTLC (10x10 cm; Merck, Darmstadt, Germany; the plates were activated at 180 ºC for 1 hour and brought to room temperature before use. Lipids were spotted on the activated HPTLC plates and the plates were developed with ethanol : chloroform : triethylamine : water (40:35:35:9 v/v/v/v) as eluent. Lipids were visualized by spraying the plates with a phosphate stain solution, 16g of ammonium molybdate in 120 mL water (solution (a)). 10 mL of mercury was added to a 40 mL concentrated HCl solution and 80 ml of solution (a). The resulting solution was shaken for 30 minutes and filtered (solution b). The final spray reagent was the remainder of solution (a) added to 200 ml of concentrated H_2SO_4 and all of solution (b). This was then cooled and subsequently diluted to a total volume of 1 L with water. With this final solution the HPTLC plates were sprayed and phospholipids appeared as blue bands on a white background [22].

Hyper motility assessment of incubated sperm

After sperm incubations in HBT media, sperm motility was measured using the Spermvision™ computer assisted sperm analysis (CASA; Minitube GmbH, Tiefenbach, Germany) system for 2 hours. Sperm motility measurements were performed in this system by using 20 µm deep Leja-4 chambers (Leja Products B.V.; Nieuw Vennep, the Netherlands). Standard instrument settings of SpermVision Version 3.0 were used for the analysis of motility, as used by the artificial insemination center (Varkens KI, Deventer) [23].

Western blot

After incubation, sperm cells were solubilised in Laemmli Buffer with Dithiotreitol (DTT) and boiled at 90 °C for 5 minutes [24]. Solubilized proteins were loaded in a 12% polyacrylamide SDS-PAGE

gels and separated and transferred to a nitrocellulose membrane (Protran BA85, Whatmann, Dassel, Germany). After blocking in 5 % (w/v) BSA and 0.05 % (v/v) Tween-20 in Tris Buffered Saline (TBS; Tris 25 mM, 150 mM NaCl, and adjusted with HCl, to pH 7.4) overnight at 4°C, the blots were incubated with primary antibodies (either rabbit-anti-goat polyclonal CD52 or monoclonal anti-mouse-CD55 both from Santa Cruz Biotechnology, Inc.; Heidelberg, Germany), diluted 1:1,000 in blocking buffer, for 1 hour at room temperature. After washing in TBS with 0.05% v/v Tween-20, blots were subsequently incubated with secondary antibodies for 30 minutes at room temperature. Subsequently, after extensive washing the nitrocellulose membrane with TBS containing 0.05% (v/v) Tween-20, protein bands indirectly immunolabelled with horseradish peroxidase were visualized by chemiluminescence for 5 minutes using an enhanced chemiluminescence (ECL)-detection kit; (Supersignal West Pico Pierce, Rockford, IL, USA) and captured on a Molecular Imager Chemidoc XRS Biorad laboratories (Hercules, CA, USA).

Dot Blot

To investigate the release of glycoproteins CD52, CD55 and Ganglioside M1 (GM1) a dot blot was performed. ~5 µg of total protein from incubated sperm was spotted on nitrocellulose (Protran BA 85) by means of the Easy-Titer™ ELIFA dot blot system (Pierce, Rockford, IL, USA). Spots were dried using a vacuum system (flow rate 100 µL/ 1.5 minute/well). Subsequently, the blots were blocked overnight in 5% w/v Protifar (Nutricia, Zoetermeer, The Netherlands) in TBS-Tween20 (0.05%). For detection of GM1, Choleratoxin-B conjugated to Horse Radish Peroxidase (CTX-HRP, Sigma-Aldrich) was dissolved in a ratio of 1:10,000 in 1% Protifar in TBST-0.05% and the nitrocellulose membrane was incubated for 3 hours at room temperature. After several washing steps in TBST-0.05% (3x) and 1x TBS, CTX-HRP staining was visualized by means of enhanced chemiluminescence (ECL-detection kit; Supersignal West Pico, Pierce). Quantitative analysis of dot blot labeling was performed by scanning the blots with a GS-700 densitometer (Bio-Rad Laboratories, Hercules, CA, USA) using Quantity One acquisition software (version 4.3, Biorad) and subsequently analyzed by computer software ImageJ [25].

Western-blot immunodetection of tyrosine phosphorylation

After incubation sperm cells were washed and a total of 2 million sperm cells were re-suspended in 25 µL of lithium dodecyl sulfate loading buffer (NuPAGE®, Invitrogen, Carlsbad, CA, USA) in the presence of 0.1 M dithiothreitol and heated for 10 minutes at 95 °C. The solubilized proteins were loaded and separated on a 12% polyacrylamide gel and run at 40 mA for 45 minutes. The electrophorized proteins were blotted onto nitrocellulose paper at 60V for 1.5 hours. The nitrocellulose papers with blotted proteins were first incubated in blocking buffer (Tris 25 mM, 150 mM NaCl, pH7.4, with 0.5% Tween, (TBS-Tween 0.5%)) for 10 minutes at room temperature in order to prevent non-specific antibody binding. Subsequently, the nitrocellulose paper with the blotted and blocked proteins was incubated with 1% BSA TBS-Tween 0.05% for 1 hour at room temperature. After this step the nitrocellulose paper, with the blotted proteins, was incubated in 0.1% BSA TBS-Tween 0.05%

supplemented with a mouse monoclonal antibody raised against phosphotyrosine residues (PY20; Becton Dickinson Transduction laboratories, Franklin Lakes, NJ, USA) at a final concentration of 1 µg/mL overnight at 4 °C. The resulting nitrocellulose paper with blotted proteins was washed six times with 10 minutes per washing step in TBS. After this washing the nitrocellulose was placed into TBS-Tween 0.05% containing 0.5 µg/mL monoclonal goat-anti mouse antibody conjugated with horse radish peroxidase (Nordic Immunology, Tilburg, the Netherlands) for 90 minutes at 4 °C. The resulting nitrocellulose paper with blotted and immunolabeled proteins were washed as described before for removal of unbound PY20 above. Protein bands indirectly immunolabeled with horse radish peroxidase were visualized by chemiluminescence for 5 minutes (ECL detection kit) and captured on a Molecular Imager Chemidoc XRS from Biorad Laboratories.

Immunofluorescence

After incubation in different conditions sperm cells were fixed in 2% paraformaldehyde in TBS and smeared on glass slides. After drying the glass slides sperm cells were blocked in 1% BSA TBS for 1 hour. Subsequently, the smears were incubated with mouse monoclonal anti-CD55 (Santa Cruz Biotechnology Inc.) in a 1:50 ratio in 0.1% BSA TBS-Tween 0.05% for 1-hour at 37 °C in a humid environment. After rinsing with 0.1% BSA TBS-Tween 0.05% the smears were thoroughly washed with 0.1% BSA-TBS-Tween 0.05% and after washing incubated with a 1:100 dilution of secondary antibody goat-anti-mouse-Alexa488 (Invitrogen, Carlsbad, CA, USA) for 1 hour at 37 °C. Smears were washed with TBS and subsequently imaged under identical conditions with a Nikon Eclipse Ti microscope (Nikon Cooperation, Tokyo, Japan) equipped with a CCD camera (Jenoptik, Jena, Germany) and a mercury arc lamp excitation system. In case of immunodetection of flotillin-1, prior to the blocking step with 1% BSA-TBS Tween 0.05%, the smears were soaked with -20 °C methanol for 2 minutes in order to permeabilize the sperm cells. For the fluorescence detection of GM1, CTX-FITC (Sigma-Aldrich, Mannheim, Germany) was used and the same method was used as described for the CD55 immunolabeling.

Atomic Force Microscopy

Sperm cells were fixed in 4% gluteraldehyde (w/v) in phosphate buffered saline (PBS) for 10 minutes and subsequently washed in PBS and transferred on superfrost glass slides. Next, sperm cells were centrifuged at 100 x *g* for 2 minutes. This was done in order to prevent de-attachment of the tail and head under imaging conditions in buffer. All images were recorded on a Nanowizard II (JPK Instruments, Berlin, Germany) in intermittent contact mode in liquid (PBS). Cantilevers used were from Mikromash (Tallinn, Estonia) CSC38no Al. Cantilevers spring constants were calibrated within the JPK software. The resolution was a minimum of 512x512 pixels and the line rate was around 1.0 Hz. In order to compare height differences in the apical area the following formula was used: ½ width multiplied by the height. This was compared between for the different sperm incubations used in this study.

RESULTS

Bicarbonate dependent release of CD52 in capacitating sperm

When sperm cells incubated for 2 hours in a fully capacitation supporting medium (+Bic/+BSA) a spontaneous release of CD52 was detected (Fig. 1). Interestingly, this effect was more pronounced when sperm was incubated with bicarbonate alone where as in the presence of only BSA there was no release noted of CD52. This indicates that the release of CD52 from the sperm surface is a bicarbonate dependent phenomenon occurring during sperm capacitation.

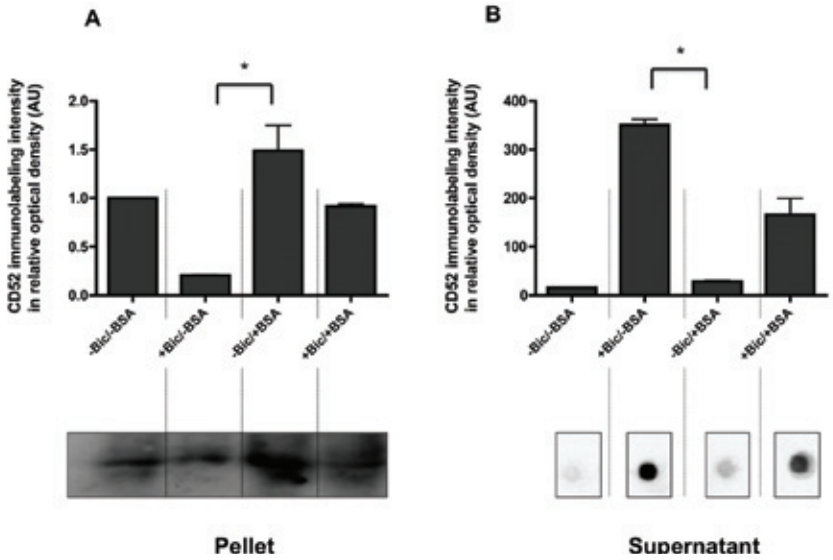

Figure 1. The release of CD52 from in vitro capacitating sperm.

Panel A) Western blot detection of CD52 indicates the bicarbonate dependent release of CD52. –Bic/+BSA alone did not result in release of CD52. A significant difference (*) was observed between the condition with only bicarbonate and the condition with –Bic/+BSA. (n=2, Bonferroni's multiple comparison test; $P < 0.05$). Panel B) In the supernatant the release of CD52 was detected by the method of Dot-Blot and was significantly higher compared to control conditions and the condition with only BSA. (n=2, Bonferroni's multiple comparison test; $P<0.05$).

Bicarbonate dependent release of CD55 in capacitating sperm

Control sperm cells contained CD55 at the post-equatorial region as well as in the mid-piece (Fig. 2). Cells incubated for 2 hours in fully supporting medium (+Bic/+BSA) showed a reduction 80% of the CD55 labelling. The decrease in CD55, similar to CD52 was higher in sperm with +Bic/-BSA than in the other conditions. Thus also the removal of CD55 is a bicarbonate dependent step occurring during sperm capacitation. Incubation in presence of PIPLC nearly completely reduced CD55 labelling under all sperm incubation conditions (Fig. 2).

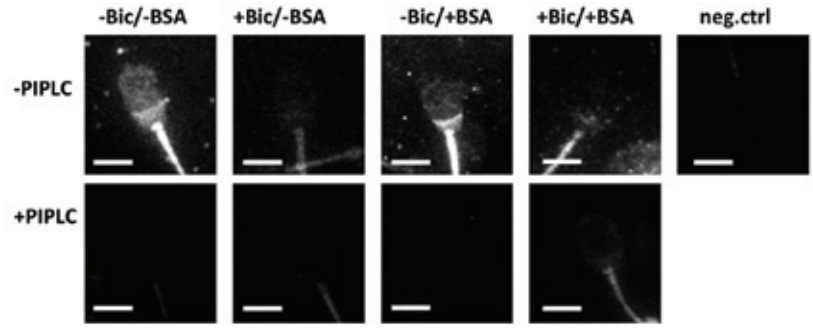

Figure 2. Sperm cells submitted to different IVF media containing either Bic, BSA or both showed a decrease in immunofluorescence staining of CD55 under bicarbonate conditions and bicarbonate together with BSA. PIPLC treatments lead to a reduced CD55 detection in all incubations (scale bar = 5 µm, n=3, representative images are shown).

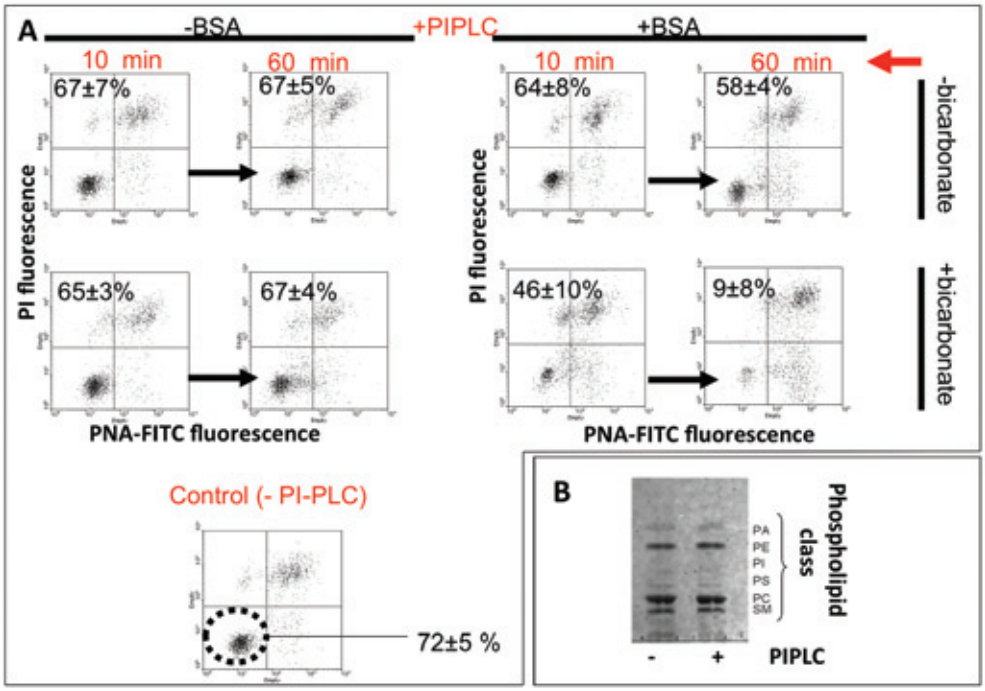

Figure 3. Viability and membrane integrity of PIPLC treated sperm.

Panel A) FACS analysis revealed that sperm viability is only affected by PIPLC treatment under full capacitating conditions after 1 hour. A drop was observed from 46% till 10% of viable sperm of sperm incubated with +Bic/+BSA and PIPLC from 10 till 60 minutes. In the remaining conditions (with or without Bic or BSA and PIPLC) sperm remained viable around 60%. Panel B) Lipid membrane species were separated by means of HPTLC. There were no differences detected in the amount of lipid species present. PhosphatidylInositol (PI) was looked at with special interest to investigate if the enzyme PIPLC did not disrupt the amount of PI present.

Sperm membrane integrity after incubation with PIPLC

Since capacitation induced the release of CD52 and CD55 we investigated whether sperm cells incubated with GPI-AP release by PIPLC treatment resulted also in sperm capacitation and whether or not sperm can survive a PIPLC treatment. The cells remained intact under the 1-hour incubation condition with PIPLC under control conditions or under conditions where only one of the capacitation factors (either +Bic/-BSA or –Bic/+BSA) was added (Fig. 3). However, under full capacitation supporting media (+Bic/+BSA) the PIPLC treatment led to cell disruption. Since PIPLC is a lipase we checked whether or not the lipid composition and total amount of the five major phospholipid classes was altered by PIPLC incubations. As depicted in Fig. 3B PIPLC treatment did not alter the composition or the amount of the phospholipids and PI (probably cleaved by PIPLC if residing in the outer lipid leaflet of the sperm plasma membrane) is only a minor phospholipid class (Fig. 3B).

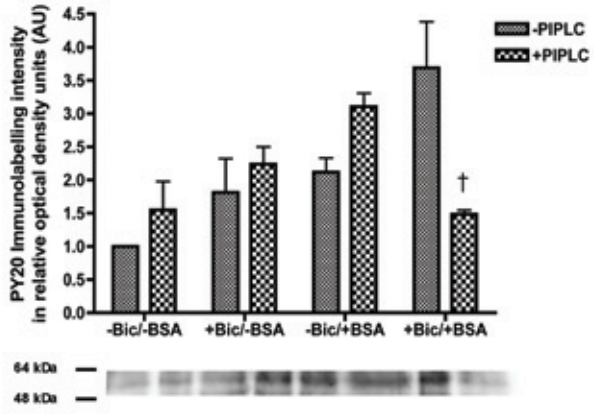

Figure 4. Tyrosine phosphorylation of sperm proteins.

Western blot show that PIPLC has a mild stimulating (yet not significant) effect on the amount of tyrosine phosphorylation of proteins in sperm submitted to different stimuli. The only drop in tyrosine phosphorylation was observed in full capacitating (+Bic/+BSA) media with PIPLC. This was also the fraction were sperm was no longer viable (n=2, bar represents mean±SD).

Effects of PIPLC on protein tyrosine phosphorylation

Since the release of GPI anchored proteins is also reported to occur during sperm capacitation we tested whether PIPLC treatment induced protein tyrosine phosphorylation in sperm incubated in media that do not fully support sperm capacitation. Protein tyrosine phosphorylation is considered to be a hallmark of sperm capacitation [26]. In our hands PIPLC did not induce protein tyrosine phosphorylation in control treated cells (-Bic/-BSA; Fig. 4). An increase in protein tyrosine phosphorylation was noted for the +Bic/-BSA and for -Bic/ +BSA compared to -Bic/-BSA. Introducing PIPLC caused protein tyrosine phosphorylation in both cases (Fig. 4). The synergistic activation of

protein tyrosine phosphorylation under +BSA/+Bic (Fig. 4.) was severely reduced by co-incubation with PIPLC. Likely this is caused by sperm deterioration (see Fig. 3A). Taken together PIPLC mediated GPI anchored protein removal does not have a large impact on the induction of protein tyrosine phosphorylation.

Effects of PIPLC treatments on activation of sperm motility

Another sign of sperm capacitation is the induction of hyperactivated sperm motility required for zona drilling [10]. Therefore, we investigated the effect of PIPLC treatment on sperm motility. Hyperactivated motility of sperm was measured by computer assisted semen analysis (CASA) as previously described [23] whereby the progressive cells average path of velocity needed to be higher then 25 µm/s and the progressive cells straightness was cut off to 30%. As is depicted in Fig. 5, PIPLC did not affect motility in control (-Bic/-BSA) incubated cells. In all other treatments it reduced the hyper activated motility (Fig. 5). Again the full supporting capacitation (+Bic/+BSA) condition in presence of PIPLC caused cell death and this is probably reflected in the low hypermotility percentage measured (Fig. 3A). Thus PIPLC mediated GPI-AP removal had no inhibiting effects on induction of hyper activated sperm motility.

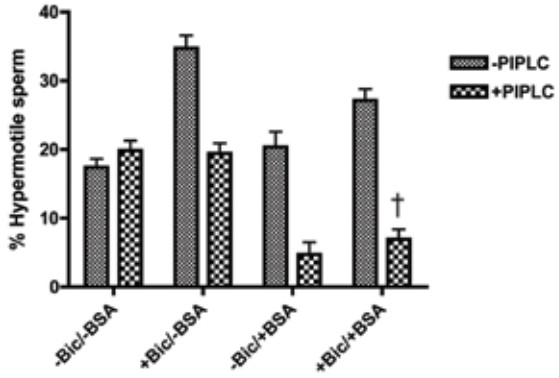

Figure 5. Induction of hyperactivated motility in incubated sperm.

Sperm incubated in the indicated media with or without PIPLC were scored for hyperactivated motility. In the condition -Bic/-BSA PIPLC did not have an effect on hypermotility observed. However, in all the other conditions there was a significant drop in hypermotility of sperm after 2 hours. (n=15, bar represents mean±SD).

Exposure of flotillin 1 after sperm treatment with PIPLC

Another result of capacitation is the decoating and reorientation of raft markers towards the apical ridge area [1,9]. We studied whether this phenomenon could be induced by PIPLC treatment. To this end sperm was incubated in presence or absence of PIPLC either i) in control (-Bic/-BSA), ii) in only partly capacitation supporting media (+Bic/-BSA or -Bic/+BSA) or iii) in full capacitation

supporting media (+Bic/+BSA). After fixation and permeabilization the immunolabeling of flotillin-1 was compared in the apical area of the sperm head for these conditions. In sperm cells incubated in -Bic/-BSA without PIPLC no exposure of flotillin-1 in the apical area was detected (Fig. 6A), whereas, +Bic/+BSA without PIPLC more then 60 percent of the sperm cells were stained at the apical ridge area. In -Bic/-BSA some 45 % of the sperm cells showed the same apical ridge labelling as a result of PIPLC treatment (Fig. 6). Only a small population of sperm was apically labelled for flotillin-1 after a +Bic/-BSA or -Bic/+BSA treatment irrespective of PIPLC treatment. In +Bic/+BSA the PIPLC treatment had a detrimental effect on sperm resulting in damage at the flotillin exposing area (Fig. 6). Thus the concerted +Bic/+BSA effect on spontaneous exposure of flotillin 1 in the apical ridge area can be induced in control cells (-Bic/-BSA) by PIPLC treatment.

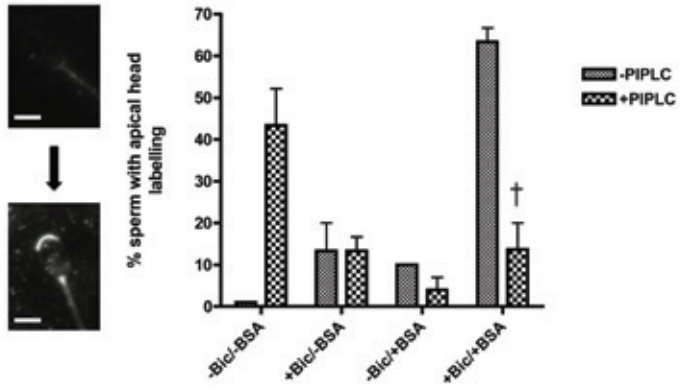

Figure 6. Immunolabeling of flotillin-1 exposure in PIPLC treated sperm.

The amount of sperm showing apical flotillin-1 labelling was counted. Interestingly, sperm incubated with PIPLC only showed apical area staining in the –Bic/-BSA condition (43±8%). The other conditions led to only <15±5% of sperm positively stained for flotillin-1 at the apical area (scale bar = 5 µm, n=3, bar represents mean±SD).

Another lipid raft marker is the ganglioside GM1, which in control cells (-Bic/-BSA), was not exposed at the sperm surface (Fig. 7A). When sperm cells were in treated in –Bic/-BSA with PIPLC no GM1 labelling was observed. Interestingly, sperm cells incubated by +Bic/-BSA or -Bic/+BSA showed GM-1 staining at the post equatorial sperm head area and in the mid-piece region. Addition of PIPLC in both treatments caused additional exposure of GM-1 in the apical ridge area of the sperm head (Fig. 7A). This apical ridge exposure of GM-1 was spontaneously evoked under full capacitation supporting incubations (+Bic/+BSA; Fig. 7A). Addition of PIPLC to this condition caused diminished apical ridge labelling of GM-1 and acrosome deterioration (Fig. 7A). Despite the varying amounts and patterns of GM-1 exposure (measured with fluorescein conjugated cholera toxin B; CTX-FITC) the amount of GM-1 in the incubated sperm was similar under all incubations tested (Fig. 7B). Thus the observed GM-1 staining in the apical ridge area of capacitating sperm is likely due to the

spontaneous or PIPLC–mediated removal of GPI anchored proteins that initially were coating these gangliosides.

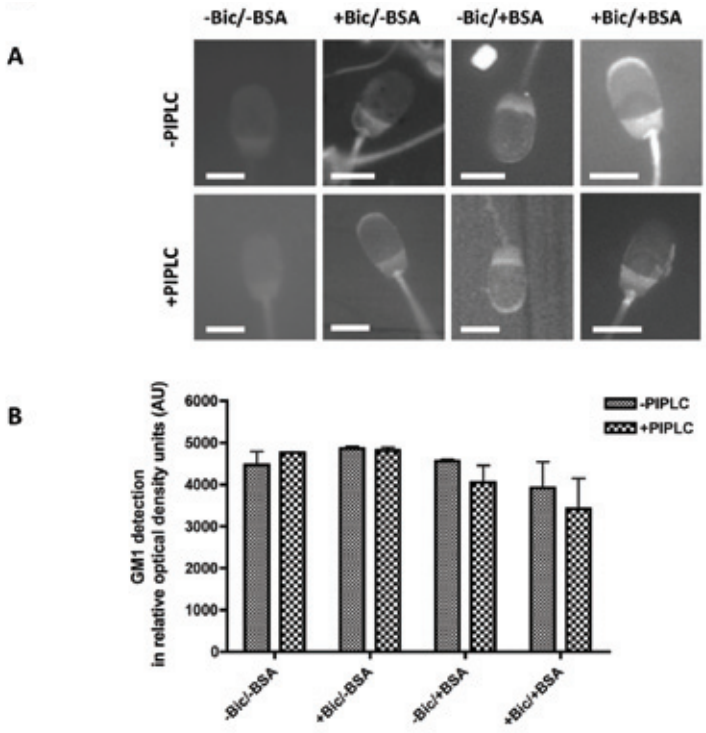

Figure 7. Choleratoxin labeling of GM-1 in PIPLC treated sperm.

A) CTX-FITC staining of sperm under different conditions with or without PIPLC. PIPLC induced detection of GM1 in the conditions with +Bic/-BSA or –Bic/+BSA. However, due to cell death there was no longer sperm positively stained in the apical area in the condition with +Bic/+BSA and +PIPLC (scale bar= 5 µm, representative images are shown). B) Intensity of CTX-HRP labeling of dot blots containing equal amounts of sperm material. Under all treatments the amount of GM-1 did not change significantly. This indicates that the total amount of GM1 does not change but the exposure of GM1 is in some conditions (+Bic/-BSA/+PIPLC;-Bic/+BSA/+PIPLC) dependent on PIPLC. (n=2, bars represent mean±SD)

Effect PIPLC treatment on acrosome swelling

Sperm capacitation induces the swelling of the apical area of the acrosome [27]. Our data thus far showed that GPI anchored proteins and membrane raft markers are subsequently exposed or released by PIPLC. It is possible that the removal of GPI-AP is sufficient for the observed swelling and thus we tested whether PI-PLC treatment could induce swelling of the acrosome in control incubated sperm. The volume of the apical ridge area was monitored by atomic force microscopy: The boar sperm cell has a relative flat and rigid surface which makes it an ideal candidate to study by Atomic Force Microscopy where the surface height can be scanned at nanometer scale physically

with a cantilever tip. Compared to control (-Bic/-BSA) acrosomal swelling was seen both in +Bic/-BSA and –Bic/+BSA and a synergistic effect as seen in complete capacitation supporting media (+Bic/+BSA; Fig. 8). PIPLC had variable effect on sperm, it induced acrosomal swelling in –Bic/-BSA sperm, it reduced acrosome swelling in +Bic/-BSA treated cells and had minor effects on –Bic/+BSA and +Bic/+BSA treated cells (Fig. 8). The effect of PIPLC in +Bic/+BSA is difficult to interpret as acrosome damage was also monitored (Fig 3A and Fig 7).

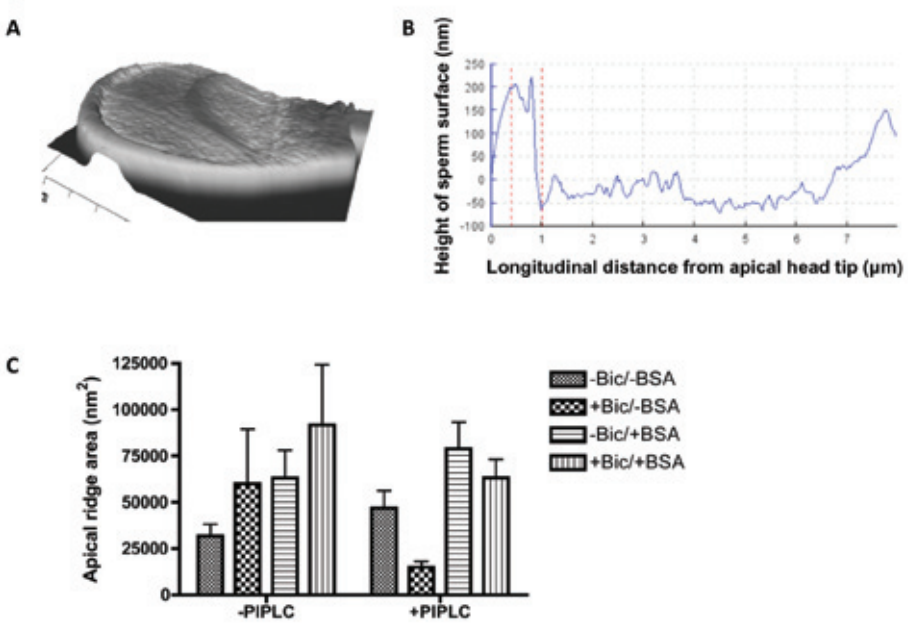

Figure 8. Capacitation dependent swelling of the apical sperm head area as measured by AFM.

Under full capacitation (+Bic/+BSA, without PIPLC) conditions the apical area has the largest volume as measured by AFM. PIPLC has a negative effect on apical area height in sperm incubated in +Bic/-BSA or +Bic/+BSA. +Bic/-BSA/+PIPLC led to the largest decrease of the apical area. Sperm incubated with -Bic/+BSA with or without PIPLC showed similar swelling of the apical ridge (n=8, bar represents mean±SD).

In vitro fertilization in the presence of PIPLC

We also determined if PIPLC treated sperm was able to fertilize the oocyte. In none of the conditions fertilization took place (results not shown). This may imply that enzymatic release of GPI anchored proteins is also depleting GPI anchored proteins required for zona binding and other processes involved in fertilization.

DISCUSSION

Capacitation induces the los of GPI anchored proteins

During capacitation we observed a spontaneous release of the sperm surface GPI anchored proteins CD55 and CD52. CD55 and CD52 are members of a group of proteins involved in evading the immune system [28]. It seems that sperm that encounter higher concentrations of bicarbonate *in vitro* (this mimics the higher bicarbonate levels of the fluids sperm encounter *in vivo* in the oviduct) induces shedding of proteins involved in evading the immune system (the so called complement mediated proteins) [33]. The loss of these proteins may be required to allow the formation of a proper ZP binding complex, for review see [5]. In fact in mouse sperm, the loss of GPI anchored proteins was observed during sperm capacitation [18].

Recently, an angiotensin converting enzyme (AcE) has been reported to cause the release of GPI anchored proteins [19]. Interestingly, without AcE and its enzymatic release of GPI anchored proteins sperm is not able to bind properly to the ZP [19]. In order to examine the effects of the release of GPI anchored proteins on sperm physiology and morphology, we designed experiments in which sperm is incubated with the enzyme PIPLC to enzymatically induce the release of the protein moiety of GPI-APs from the sperm surface. It has been reported that the action of PIPLC mimics that of endogenous AcE, which is activated upon capacitation *in vitro* [19]. Sperm treated with PIPLC indeed caused removal of GPI anchored proteins CD55 and CD52. We observed that PIPLC treatment exerted, under control or only partly capacitation supporting conditions, only slightly affected the induction of hyperactivated sperm motility and protein tyrosine phosphorylation. While on the other hand, PIPLC treatment under full capacitation supporting conditions was detrimental to sperm. PIPLC treatment caused under partly capacitation supporting conditions the exposure of GM-1 in the apical ridge are of the sperm head as well as the aggregation of flotillin-1 at the same area. This phenomenon only occurred spontaneously when sperm were incubated under full capacitation supporting conditions. Therefore, the removal of GPI anchored proteins seems to be important for the exposure and lateral reordering of lipid raft markers, which is reported to occur during sperm capacitation [7,13].

Part of the GPI-APs may serve in sperm-zona binding and penetration. One candidate who is hypothesized to be important for zona pellucida recognition and GPI anchored is PH20 [29]. PH20 is known to hyaluronidase activity that enables sperm to penetrate the ZP (van Gestel et al. 2007). Another GPI-AP involved in sperm-zona binding is carbonyl reductase (or P34h), which originates from the epididymis where it is secreted and covalently linked to the sperm surface [9, 17]. Removal of such GPI-APs spontaneously or by PIPLC treatment would render sperm infertile. In fact this phenomenon is shown in the present study under IVF conditions for PIPLC treated cells whereby GPI removal induces cell death. This shows that only a selection of GPI-APs is spontaneously removed during sperm capacitation. On the other hand the raft aggregation at the apical ridge area is an important step in sperm capacitation enabling the assembly of protein complexes involved in

sperm-zona binding [9] the docking of the acrosome with the plasma membrane as preparative step for the zona-induced acrosome reaction [8]. The fact that PIPLC treatment under not fully capacitation supporting incubations caused a similar apical ridge organizational change may indicate that the raft aggregation forming steps requires the removal of local GPI-APs. Membrane raft markers are known to reside in signalling complexes [1,7,9,13] and it remains unclear whether PIPLC treatment is rendering membrane changes with the same potential in evoking signalling processes as in fully supporting capacitation incubations where this is a spontaneous process. PIPLC may, by cleaving phosphatidylinositides, induce artificial signalling pathways causing artefacts (such as cell deterioration under full sperm capacitation incubations).

Conclusion

The results discussed in this paper support the hypothesis that during sperm cell capacitation there is loss of extracellular proteins which includes the partial spontaneous removal of a GPI-APs (described here for CD52 and CD55) [18]. This phenomenon can enzymatically be induced by PIPLC. PIPLC induced the induction of lateral aggregation of lipid rafts at the apical ridge of sperm in partial sperm capacitation supporting media in a similar fashion as to that of sperm that showed spontaneous lateral aggregation of lipid rafts in full capacitation media at the apical ridge (in the absence of PIPLC). The PIPLC treatment had no effect on protein tyrosine phosphorylation induction nor on the induction of hypermotility of sperm cells. However, the involvement of GPI –AP release by endogenous enzymes, such as reported for AcE, should be investigated to further detail. Beyond the partial removal of GPI-APs, sperm cells migrating through the uterus and oviduct will interact with other surface modifying extracellular compounds such as the metalloproteinases [30-32]. Therefore, future research should also focus on other endogenous extracellular matrix modifying enzymes on the sperm surface and the female genital tract playing a role in sperm activation for proper zona pellucida binding and penetration and subsequent oocyte fertilization. Probably the PIPLC treatment removes these GPI anchored proteins and thus results in sperm stripped for GPI-APs involved in fertilization. This could explain why PIPLC treatment does not result in fertilization *in vitro*. This might aid in elucidating the key surface modifying processes required for sperm to become fully capacitated and as a result aid in solving sperm infertility problems.

ACKNOWLEDGEMENTS

Dr. B.M. Gadella is a recipient of the High Potential award from Utrecht University, from which this research project and the atomic force microscope was financed.

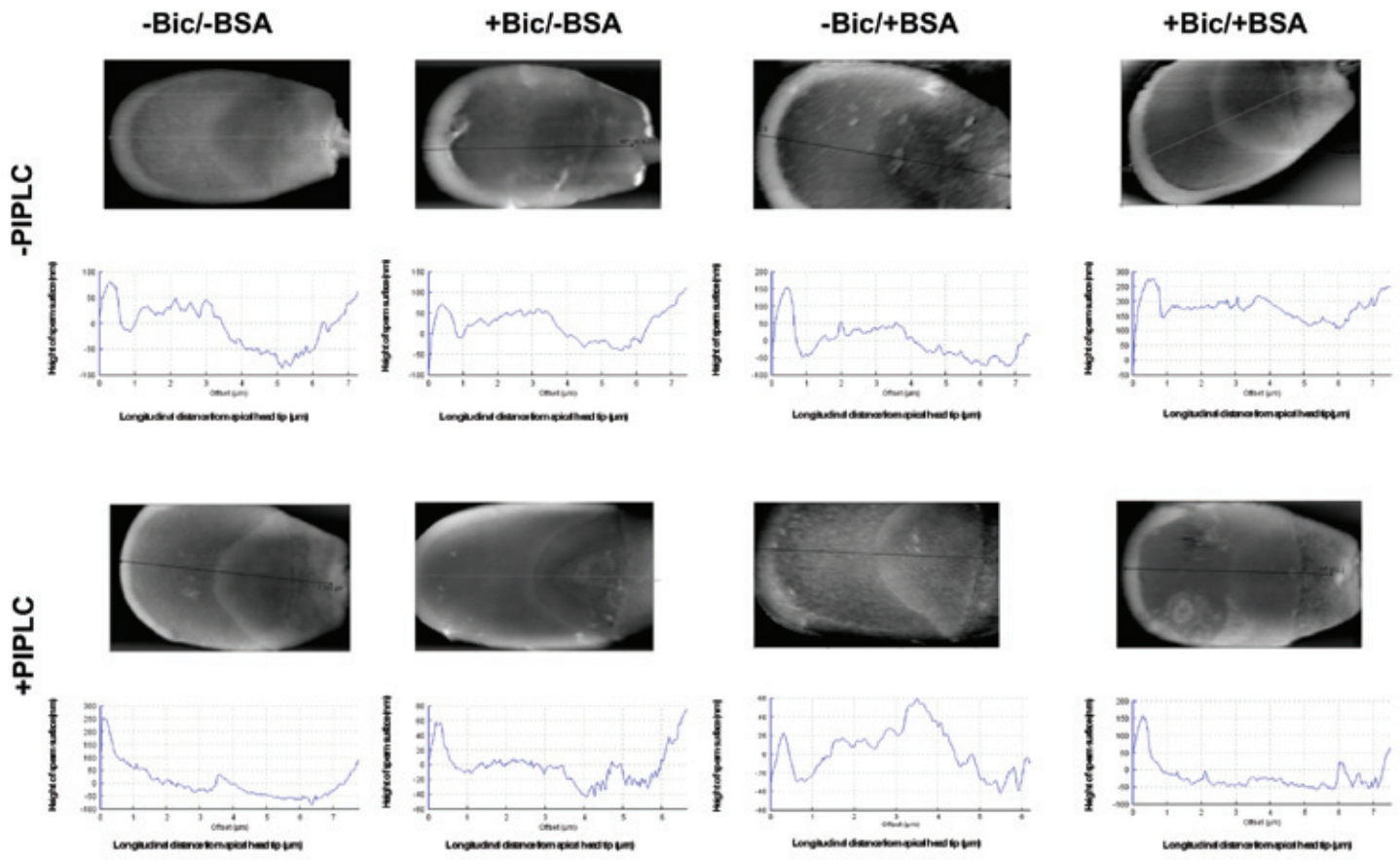

Supplemenatry information S1. Representative height surface profiles of the sperm head, as measured by AFM, are shown of sperm incubated in the presence or absence of PIPLC incubated in different conditions (either with/or without Bic (-Bic/+Bic) or with/or without BSA (-BSA/+BSA).

REFERENCES

1. Boerke A, Tsai PS, Garcia-Gil N, Brewis IA, Gadella BM. 2008. Capacitation-dependent reorganization of microdomains in the apical sperm head plasma membrane: Functional relationship with zona binding and the zona-induced acrosome reaction. Theriogenology 70:1188-1196.

2. Tsai PS, Gadella BM. 2009. Molecular kinetics of proteins at the surface of porcine sperm before and during fertilization. Soc Reprod Fertil Suppl 66:23-36.

3. Gadella BM, Tsai PS, Boerke A, Brewis IA. 2008. Sperm head membrane reorganisation during capacitation. Int J Dev Biol 52:473-480.

4. Yoshida M, Kawano N, Yoshida K. 2008. Control of sperm motility and fertility: diverse factors and common mechanisms. Cell Mol Life Sci 65:3446-3457.

5. Leahy T, Gadella BM. 2011. Sperm surface changes and physiological consequences induced by sperm handling and storage. Reproduction 142:759-778.

6. Brouwers JF, Boerke A, Silva PF, Garcia-Gil N, van Gestel RA, Helms JB, van de Lest CH, Gadella BM. 2011. Mass Spectrometric Detection of Cholesterol Oxidation in Bovine Sperm. Biol Reprod .

7. van Gestel RA, Brewis IA, Ashton PR, Helms JB, Brouwers JF, Gadella BM. 2005. Capacitation-dependent concentration of lipid rafts in the apical ridge head area of porcine sperm cells. Mol Hum Reprod 11:583-590.

8. Tsai PS, Garcia-Gil N, van Haeften T, Gadella BM. 2010. How pig sperm prepares to fertilize: stable acrosome docking to the plasma membrane. PLoS One 5:e11204.

9. van Gestel RA, Brewis IA, Ashton PR, Brouwers JF, Gadella BM. 2007. Multiple proteins present in purified porcine sperm apical plasma membranes interact with the zona pellucida of the oocyte. Mol Hum Reprod 13:445-454.

10. Tsai PS, Brewis IA, van Maaren J, Gadella BM. 2012. Involvement of complexin 2 in docking, locking and unlocking of different SNARE complexes during sperm capacitation and induced acrosomal exocytosis. PLoS One 7:e32603.

11. Sion B, Grizard G, Boucher D. Quantitative analysis of desmosterol, cholesterol and cholesterol sulfate in semen by high-performance liquid chromatography. Journal of Chromatography A 935:259-265.

12. Jones R, Howes E, Dunne PD, James P, Bruckbauer A, Klenerman D. 2010. Tracking diffusion of GM1 gangliosides and zona pellucida binding molecules in sperm plasma membranes following cholesterol efflux. Dev Biol 339:398-406.

13. Selvaraj V, Buttke DE, Asano A, McElwee JL, Wolff CA, Nelson JL, Klaus AV, Hunnicutt GR, Travis AJ. 2007. GM1 dynamics as a marker for membrane changes associated with the process of capacitation in murine and bovine spermatozoa. J Androl 28:588-599.

14. van Beek J, van Meurs M, 't Hart BA, Brok HP, Neal JW, Chatagner A, Harris CL, Omidvar N, Morgan BP, Laman JD, Gasque P. 2005. Decay-accelerating factor (CD55) is expressed by neurons in response to chronic but not acute autoimmune central nervous system inflammation associated with complement activation. J Immunol 174:2353-2365.

15. Girouard J, Frenette G, Sullivan R. 2009. Compartmentalization of proteins in epididymosomes coordinates the association of epididymal proteins with the different functional structures of bovine spermatozoa. Biol Reprod 80:965-972.

16. Koyama K, Hasegawa A, Komori S. 2009. Functional aspects of CD52 in reproduction. J Reprod Immunol 83:56-59.

17. Legare C, Gaudreault C, St-Jacques S, Sullivan R. 1999. P34H sperm protein is preferentially expressed by the human corpus epididymidis. Endocrinology 140:3318-3327.

18. Watanabe H, Kondoh G. 2011. Mouse sperm undergo GPI-anchored protein release associated with lipid raft reorganization and acrosome reaction to acquire fertility. J Cell Sci 124:2573-2581.

19. Kondoh G, Tojo H, Nakatani Y, Komazawa N, Murata C, Yamagata K, Maeda Y, Kinoshita T, Okabe M, Taguchi R, Takeda J. 2005. Angiotensin-converting enzyme is a GPI-anchored protein releasing factor crucial for fertilization. Nat Med 11:160-166.

20. Tsai P, De Vries KJ, De Boer-Brouwer M, Garcia-Gil N, Van Gestel RA, Colenbrander B, Gadella BM, Van Haeften T. Syntaxin and VAMP association with lipid rafts depends on cholesterol depletion in capacitating sperm cells. Mol Membr Biol 2007; 24:313-324.

21 Bligh EG, Dyer WJ. 1959. A rapid method of total lipid extraction and purification. Can J Biochem Physiol 37:911-917.

22. Vaskovsky VE, Kostetsky EY. 1968. Modified spray for the detection of phospholipids on thin-layer chromatograms. J Lipid Res 9:396.

23. Broekhuijse ML, Sostaric E, Feitsma H, Gadella BM. 2011. Additional value of computer assisted semen analysis (CASA) compared to conventional motility assessments in pig artificial insemination. Theriogenology 76:1473-86.e1.

24. Laemmli UK. 1970. Cleavage of structural proteins during the assembly of the head of bacteriophage T4. Nature 227:680-685.

25. Abramoff MD, Magelhaes PJ, Ram SJ. 2004. Image Processing with ImageJ. Biophotonics International 11:36.

26. Bajpai M, Asin S, Doncel GF. 2003. Effect of tyrosine kinase inhibitors on tyrosine phosphorylation and motility parameters in human sperm. Arch Androl 49:229-246.

27. Esteves SC, Sharma RK, Thomas AJ,Jr, Agarwal A. Effect of swim-up sperm washing and subsequent capacitation on acrosome status and functional membrane integrity of normal sperm. Int J Fertil Womens Med 2000; 45:335-341.

28. Mizuno M, Donev RM, Harris CL, Morgan BP. 2007. CD55 in rat male reproductive tissue: Differential expression in testis and expression of a unique truncated isoform on spermatozoa. Mol Immunol 44:1613-1622.

29. Cherr GN, Yudin AI, Overstreet JW. 2001. The dual functions of GPI-anchored PH-20: hyaluronidase and intracellular signaling. Matrix Biol 20:515-525.

30. Ferraro GB, Morrison CJ, Overall CM, Strittmatter SM, Fournier AE. 2011. Membrane-type matrix metalloproteinase-3 regulates neuronal responsiveness to myelin through Nogo-66 receptor 1 cleavage. J Biol Chem 286:31418-31424.

31. Saengsoi W, Shia WY, Shyu CL, Wu JT, Warinrak C, Lee WM, Cheng FP. 2011. Detection of matrix metalloproteinase (MMP)-2 and MMP-9 in canine seminal plasma. Anim Reprod Sci 127:114-119.

32. Tentes I, Asimakopoulos B, Mourvati E, Diedrich K, Al-Hasani S, Nikolettos N. 2007. Matrix metalloproteinase (MMP)-2 and MMP-9 in seminal plasma. J Assist Reprod Genet 24:278-281.

33. Holt WV, Fazeli A. 2010. The oviduct as a complex mediator of mammalian sperm function and selection. Mol Reprod Dev 77:934-943.

ABBREVIATIONS

AcE = angiotensin converting enzyme
Bic = bicarbonate
BSA = bovine serum albumin
CASA = computer assisted sperm analysis
CTX-FITC = fluorescein conjugated cholera toxin B
CTX-HRP = horse radish peroxidase conjugated cholera toxin B
DRM = detergent-resistant resistant sperm membranes
GPI = glycosylphosphatidylinositol
GPI-AP = GPI- anchored protein
HBS = Hepes buffered saline
HBT = Hepes buffered Tyrodes media
HPTLC = high performance thin layer chromatography
PI = propidium iodide
PIPLC = phosphatidylinositol specific phospholipase C
PNA-FITC = fluorescein conjugated peanut-agglutinin
SD = standard deviation
TBS = Tris buffered saline
TBS-T = TBS-Tween20

5

Atomic force microscopy of wet mounted boar sperm reveals unique surface changes in the anterior part of the equatorial segment during capacitation and the acrosome reaction

Arjan Boerke[1]
Joost van der Lit[1]
Christian Löbbe[4]
Ian A. Brewis[2]
Bernd Helms[1]
E. Verheyen[3]
C.F. van Nostrum[3]
Bart M. Gadella[1]

[1]Department of Biochemistry, Faculty of Veterinary Medicine, Utrecht University, Utrecht, The Netherlands.

[2]Cardiff University School of Medicine, Cardiff, United Kingdom.

[3]Department of Pharmaceutics, Utrecht Institute for Pharmaceutical Sciences, Utrecht University, the Netherlands.

[4]Scitech P/L, 4/72-74 Chifley Drive, 3072 Preston, Australia.

In preparation

SUMMARY

Capacitation of sperm is essential for sperm to be able to fertilize an oocyte. Part of this process involves the removal of extracellular matrix (ECM) components from the sperm surface. This ECM decoating the sperm head serves to functionally expose proteins at the surface that are required for proper interactions with the oocyte and thus to enable fertilization. The most recent innovations in atomic force microscopy (AFM) with scanning cantilever tips in physiological buffers allowed us to study for the first time the surface of Super-frost adhered live porcine sperm cells. The rigid and flattened sperm head surface enabled detection of sperm surface molecular rearrangements at a nanometer scale. Compared to control sperm a 2 hour capacitation incubation induced an ECM decoating that was specific for the anterior part of the equatorial segment (aEqS). High resolution AFM revealed the exposure of a highly ordered hexagonal arrangement of particles with a particle distance of 17 nm in this aEqS. After induction of the acrosome reaction, this aEqS underwent a specific fusion with the underlying acrosome membrane leaving fingershaped structures that were sprouting from the distal and non-fusogenic area of the equatorial segment. The parallel orientation of these membrane fenestrations to the sperm surface is likely the result of a calcium dependent reconfiguration of the hexagonads in the aEqS. The membrane fenestrations were highly enriched in ganglioside GM1, a lipid that was not exposed at this area prior to the acrosome reaction. The membrane fenestrations represent a unique feature for the sperm surface as, at this fertilization fusion specific structure, extensive exposure and mixing of membrane components originating from the acrosome membrane takes place. Interestingly, an antibody raised against the trimerization domain of haemagglutinin recognized an epitope at the membrane fenestrations of the aEqS of acrosome reacted cells. Sperm incubated with this antibody showed normal zona binding, reduced zona penetration and an almost complete block to fertilize porcine oocytes. Therefore, we hypothesize that the formation of the membrane fenestrations and the exposure of acrosomal membrane proteins in the aEqS are required for the sperm-oocyte fertilization fusion.

Keywords: Atomic Force Microscopy, microdomains, GM1, acrosomal reaction, hexagonal arrangement, equatorial segment, membrane villi, zona pellucida, fertilization

INTRODUCTION

Ejaculated sperm are coated with factors originating from accessary sex glands that serve to stabilize sperm cells. In the female genital tract (especially in the oviduct) and during sperm processing for *in vitro* fertilization different stimuli cause the activation of sperm and render it capable to fertilize the oocyte (sperm capacitation). Part of this process is the removal of so-called decapacitation factors from the sperm surface [1]. A result of sperm capacitation is that the activated sperm cell shows hyperactivated motility due to increased glycolysis in the sperm tail [2] and in the increased affinity for the zona pellucida and the subsequent zona-induced acrosome reaction, which combine together to enable proper zona drilling [3].

The acrosome reaction is a very specialized secretion event of the acrosome at the apical part of the sperm head. Interestingly, sperm capacitation coincides with the multiple docking of the plasma membrane with the underlying outer acrosomal membrane by formation of complexin stabilized trans trimeric SNARE complexes [4]. When such capacitated sperm bind to the zona pellucida the subsequent entry of extracellular Ca^{2+} [5] causes removal of complexin to the trans SNARE complexes as well as the trans to cis conformational change of trimeric SNARE complexes [4]. Thus, the entire docked surface area (20-40 μm^2) induces multiple membrane fusions resulting in mixed vesicles containing plasma membrane and outer acrosomal membrane material. Once these mixed vesicles are formed they are shed from the sperm surface and the resulting vesicular debris is called an acrosomal shroud; [6]. The now exposed inner acrosomal membrane is continuous with the distal plasma membrane leaving the sperm cell membrane intact. The inner acrosomal membrane is still covered with a matrix of acrosomal proteins that enable sperm to penetrate the zona pellucida. The consensus is that the equatorial area of the sperm surface is not involved in acrosome fusions but form a hairpin shaped structure (the equatorial segment) where the covering plasma membrane is continuous with the underlying non-fused outer acrosomal membrane which in turn was already continuous with the inner acrosomal membrane covering the sperm nucleus. Interestingly, this so called equatorial segment, which is formed after the acrosome reaction, is the specific sperm surface structure involved in sperm binding to the oocyte plasma membrane and is also the specific site of sperm that is used to initiate the fertilization fusion [7].

The scope of the present study was to examine the surface rearrangements of the equatorial region of porcine sperm during induced capacitation and after induction of the acrosome reaction. To this end we have used novel atomic force microscopy (AFM) technologies in which fixed sperm was adhered to Super-frost glass in buffer. The surface properties of adhered cells were scanned by a cantilever tip that was brought into the mounting buffer (wet mount). The technique allowed us to monitor dramatic surface rearrangements at nanometer resolution in the equatorial segment of sperm cells both during capacitation and after the induction of the acrosome reaction. The relevance of these surface rearrangements for this area of the sperm specifically involved in the fertilization fusion is discussed.

MATERIALS/METHOD

Chemicals

All chemicals used were obtained from Merck (Darmstad, Germany) unless stated otherwise. Choleratoxin B-FITC, which specifically detects the ganglioside GM1 was obtained from Sigma-Aldrich (St. Louis, MO, USA) [8]. All buffers used were iso-osmotic (295-310 mOsm) and at room temperature unless stated otherwise.

Semen preparation and incubation

Sperm was collected at a commercial pig artificial insemination centre (Varkens KI centrum Deventer) from proven highly fertile boars, which are also used for artificial insemination. The collected sperm was filtered for gelatinous material, approximately 10 x diluted in Beltsville Thawing Solution [9] and transported by courier at 17 ^{0}C as is the standard operating procedure for pig artificial insemination. For experimentation, spermatozoa were isolated by centrifugation through a two-step discontinuous gradient of 35% and 70% isotonic Percoll® as previously described [10]. After removal of the supernatant layers, the resultant loose pellet was resuspended at a final concentration of about 6×10^8 cells/mL in the basal Hepes-buffered bicarbonate-free Tyrode medium (HBT-Bic) for control sperm or its bicarbonate-supplemented form (HBT+Bic) for capacitating sperm [11]. For the present experiments, unless otherwise indicated, both were supplemented with 3 mg/mL BSA and with 2 mM $CaCl_2$. Incubations were initiated by the addition of aliquots of washed spermatozoa to the prewarmed media (final concentration 10^7 cells/mL). The sperm suspensions in HBT-Bic were incubated at 38°C for 2 hr in air-tight closed tubes under normal humidified atmosphere, whereas sperm in HBT+Bic were incubated for 2 hr at 38°C under humidified 5% CO_2 in air. The acrosome reaction was induced by addition of 5 µM Ca^{2+} ionophore A21387 (Sigma) to the medium and additional incubation for 1 hr at 38°C [10].

Atomic Force Microscopy

All images were recorded on a JPK Instruments Nanowizard II in intermittent contact mode in liquid. Cantilevers used were CSC38noAl from Mikromasch (Wetzlar, Germany). Cantilevers were calibrated within the JPK software (version 3.3.32). The resolution was a minimum of 512x512 pixels and the line rate was around 1.0 Hz. Sperm cells were fixed in 4% (w/v) gluteraldehyde in phosphate buffered saline (137 mM NaCl, 2.7 mM KCl, 8 mM Na_2HPO_4, 1.5 mM KH_2PO_4, pH 7.4; PBS) for 30 minutes and deposited on Superfrost™ glass slides and the glass slides were centrifuged at 100*g* for 2 minutes to enable solid attachment of sperm. This was sufficient for the prevention of sperm detachment of the tail and head under cantilever tip scanning conditions in PBS.

AFM functionalized cantilever preparation

In order to measure specific interactions between the cantilever tip and GM1 subunits on the surface of boar sperm, we immobilized rabbit anti-GM1 antibody (Abcam, Cambridge, United Kingdom) onto AFM cantilever tips. Mikromasch gold coated cantilevers (CSC38/Au) were labelled in the same manner as previously described [12]. Briefly, prior to immobilization, AFM cantilever probes were washed in distilled organic solvents (3 times 2 minutes in methanol and subsequently 3 times 2 minutes in chloroform) to remove oils and gross contaminants. The washed cantilever tips were dried and exposed for 20 min to UV light, in order to further remove organic and other oxidizable surface contaminants. The antibody immobilization procedure was based on the use of an 8 nm sized flexible cross-linker pyridyldithio-polyethyleneglycol-succinimidyl-propionate (PDP-PEG-NHS, Polypure, Oslo, Norway): The cleaned cantilever tip was immediately immersed in a PDP-PEG-NHS/chloroform solution for 1 hr. (linker concentration: 2 mg/mL) followed by two rinsing steps in chloroform and one in PBS. The modified cantilever tip was functionalized by immersed it in a drop of PBS containing antibody (1 mg/mL) for 30 min. Once functionalized, cantilevers were washed thoroughly three times in PBS solution and then immediately used for experiments or sometimes stored at 2–8 C under sterile conditions for a maximum of two days. Cantilever tip was calibrated by using the JPK Imaging software cantilever calibration tool (3.3.23).

Western blotting

Sperm proteins were Western blotted as described before [13]) Briefly, after incubation, sperm cells were solubilised in Laemmli buffer with DTT and boiled at 90 °C for 5 minutes. Subsequently solubilized proteins were loaded in a 12% polyacrylamide SDS-PAGE gels and separated. Proteins were then transferred to a nitrocellulose membrane. After blocking in 5% (w/v) BSA and 0.05% (v/v) Tween-20 in Tris buffered saline (TBS (overnight at 4°C), blots were incubated with immunized sera against sH5(3) diluted in blocking buffer (1:1000), for 1 hr at room temperature. After washing in TBS with 0.05% v/v Tween-20, blots were subsequently incubated with secondary antibodies (rabbit anti-chicken HRP) (Invitrogen, Carlsbad, CA) for 30 minutes at room temperature. After washing in TBS with 0.05% (v/v) Tween-20, The horseradish peroxidase signal was visualized by using chemiluminescence (ECL-detection kit; Supersignal West Pico, Pierce).

Immunofluoresence

After incubation in different conditions sperm cells were smeared on glass slides and subsequently fixed in 4% glutaraldehyde (w/v) in PBS for 10 min. After removal of fixative and multiple washing steps with 0.05% (v/v) Tween in PBS, sperm cells were subsequently incubated in blocking buffer for 1 hr (PBS-0.05% (v/v) Tween 1% (w/v) BSA). In the case of the detection with GM1, after extensive washing, sperm was incubated with Choleratoxin B conjugated to FITC (1:100 dilution) in (PBS-0.05% (v/v) Tween containing 0.1% (w/v) BSA) (Sigma-Aldrich, Mannheim, Germany). After 1 hour at 37 °C in a humidified chamber, smears were washed three times with PBS-0.05% (v/v) Tween and

three times with PBS. Smears were subsequently imaged with a Nikon Eclipse Ti microscope (Nikon Cooperation, Tokyo, Japan) equipped with a CCD camera (Jenoptik, Jena, Germany) and a mercury arc lamp excitation system.

For the detection of the sH5(3) motif , sperm cells were incubated in IVF media at 38 °C with 5% CO_2 for 1 hour. After 1 hour Ca-ionophore was added and sperm was left for another hour at 38 °C with 5% CO_2. After this cells were fixed in 4% (v/v) paraformaldehyde. Subsequently sperm cells were smeared on glass slides and then blocked with 3% (w/v) BSA in PBS for 1 hr. After 1hr. anti-sH5(3) chicken sera was used in a concentration of 1:50 dilution in 0.1% (w/v) BSA with PBS-0.05% (v/v) Tween (Kind gift from de R. de Vries [14]). After 1hr slides were rinsed gently with PBS and then incubated with Rabbit-anti Chicken-FITC (Invtrogen, Carlsbad, CA) for 1 at 38°C with 5% CO_2 hr. Subsequently slides were gently washed three times with PBS and covered with a glass slide. Chicken sera without sH5(3) motif challenge was used as a negative control. Subsequently sperm cells were imaged with a Nikon Ti Eclipse microscope (Nikon Instruments, Tokyo, Japan) with a super high-pressure mercury lamp with appropriate filters. Pictures were taken with a Jenoptik Progres® MFcool DCC camera (Jena, Germany).

Sperm cells were also imaged by AFM and the fixed cells were directly placed in the Biocell® chamber (JPK, Berlin, Germany). Choleratoxin-FITC (1:100 in PBS) was added into the Biocell® chamber and labelling was performed for 2 hrs at 37 °C. The Biocell® was washed twice with 1.5 mL PBS and the signal of previously AFM imaged sperm cells was compared with its immunofluorescence signal and its morphology.

In vitro fertilization in the presence of either anti-sH5(3) serum or control serum.

In vitro fertilization and maturation of the oocytes was performed as described previously [15]. Briefly, after maturation of the oocytes, they were pre-incubated for 1 hr in the presence of anti-sH5(3) chicken sera or non-challenged sera in a 1:100 in IVF medium. This sera was a kind gift of de Vries [14]. As negative controls sperm were not brought in dilutions of chicken sera but remained in the IVF medium. Fresh extended semen from two randomly selected boars was equally pooled, washed and spermatozoa concentration determined. The different groups contained 30–50 denuded oocytes and were co-incubated with spermatozoa at a ratio of 1000 spermatozoa per oocyte for 24 h. Twenty-four hours after the onset of fertilization, adherent sperm cells were removed from the oocytes by repeated pipetting. Thereafter, oocytes were fixed with 4% (v/v) formaldehyde in PBS, washed with PBS, stained for 5 minutes with 0.1 µg/mL 4,6-diamino-2-phenylindole (DAPI; Invitrogen, Carlsbad, CA), and mounted on slides to allow the assessment of the nuclear chromatin organization in the stained oocytes by fluorescence microscopy on a bright field view on a Leica TCS SP2 confocal system (Leica Microsystems, GmbH, Wetzlar, Germany) equipped with a 488 nm laser using the laser power and acquisition settings at a submaximal pixel value. Oocytes with two pronuclei (without additional sperm heads) or with one pronucleus together with one decondensing sperm head, or cleaved embryos with two to four normal blastomeres were considered monospermic fertilized while oocytes with 3 or more pronuclei or additional sperm

heads were considered to be polyspermic fertilized. Oocytes with signs of degeneration or that remained in metaphase II arrest were considered unfertilized.

Gel-based protein identification

Gel plugs (1.5 mm diameter) were manually excised, placed in a 96-well plate and peptides recovered following trypsin digestion using a slightly modified version of the Shevchenko et al. (1996) method. Sequencing grade modified trypsin (Promega, UK Ltd) was used at 6.25 ng/mL in 25mM NH_4HCO_3 and incubated at 37°C for 3 hours. Finally the dried peptides were resuspended in 50% (v/v) acetonitrile in 0.1% (v/v) trifluoroacetic acid (TFA; 5 µL) for mass spectrometry (MS) analysis and an aliquot corresponding to 10% of the material (0.5 µL) was spotted onto a 384 well MS plate. The samples were allowed to dry and then overlaid with α-cyano-4-hydroxycinnamic acid (CHCA, Sigma, Dorset, UK; 0.5 µL prepared by mixing 5mg matrix with 1ml of 50% (v/v) acetonitrile in 0.1% (v/v) TFA).

Mass spectrometry was performed using a MALDI TOF/TOF mass spectrometer (Applied Biosystems 4800 MALDI TOF/TOF Analyzer; Foster City, CA, USA) with a 200 Hz solid state laser operating at a wavelength of 355nm [16-18]. MALDI mass spectra and subsequent MS/MS spectra of the 8 most abundant MALDI peaks were obtained following routine calibration. Common trypsin autolysis peaks and matrix ion signals and precursors within 300 resolutions of each other were excluded from the selection and the peaks were analyzed with the strongest peak first. For positive-ion reflector mode spectra 800 laser shots were averaged (mass range 700-4000 Da; focus mass 2000). In MS/MS positive ion mode 4000 spectra were averaged with 1 kV collision energy (collision gas was air at a pressure of 1.6×10^{-6} Torr) and default calibration.

Combined PMF and MS/MS queries were performed using the MASCOT Database search engine v2.1 (Matrix Science Ltd, London, UK) [19] embedded into Global Proteome Server (GPS) Explorer software v3.6 (Applied Biosystems) on the Swiss-Prot database (download date 31st March 2011). Searches were restricted to the taxonomy with trypsin specificity (one missed cleavage allowed), the tolerances set for peptide identification searches at 50 ppm for MS and 0.3 Da for MS/MS. Cysteine modification by iodoacetamide was employed as a fixed modification with methionine oxidation as a variable modification. Search results were evaluated by manual inspection and conclusive identification confirmed if there was high quality tandem MS (good y-ion) data for ≥2 peptides (e value (probability of a match happening as a random event) < 0.05 for each peptide; overall e < 0.0025) or one peptide (only if the e value was < 0.0001).

RESULTS

In vitro capacitation induces strong flattening and exposure of hexagonal arranged surface particles in the aEqS.

Control sperm that were treated with buffer in the absence of bicarbonate (HBT-Bic) for 2 hrs showed surface characteristics of acrosome intact sperm with a pronounced apical ridge area and a smooth

flattened surface area until the anterior ring structure of the connecting piece at the distal area of the sperm head (Fig. 1A). Interestingly, a 2 hrs capacitation incubation of sperm in the presence of bicarbonate (HBT+Bic) induced a pronounced more flattened aEqS region (Fig. 1B) while the Equatorial Sub Segment (EqSS) surface was more prominent compared to control sperm. Further zooming in of the AFM into the flattened aEqS of HBT+Bic treated cells revealed a characteristic hexagonal arrangement of surface particles over the entire flattened area with a particle distance of around 18 nm and with particle angles of 60 degrees. (Fig. 2A-E). When the aEqS of control sperm (Fig. 3A) was compared to that of capacitated cells (Fig. 3B) it became evident that besides the lack of flattening of the control aEqS it also lacks the hexagonal arrangement of surface particles.

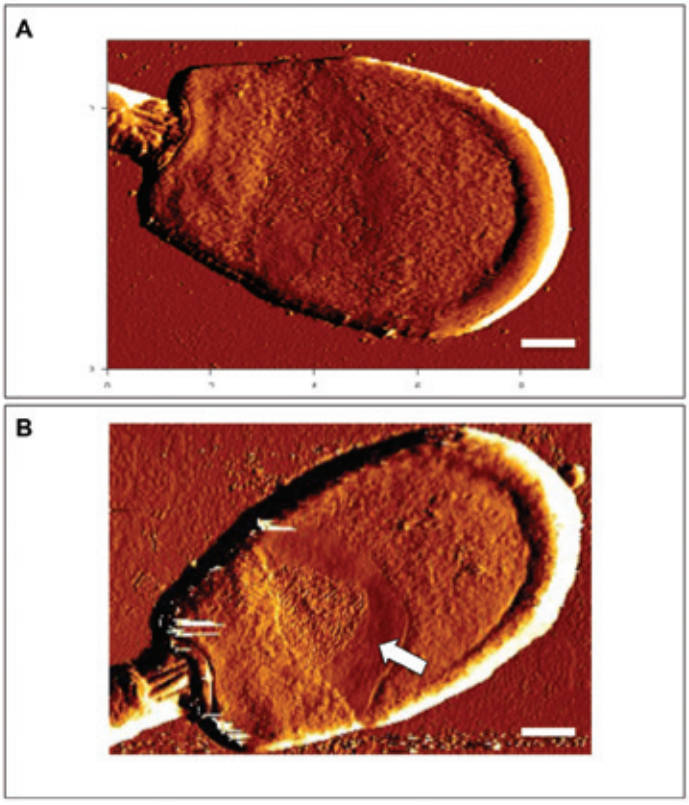

Figure 1. Representative AFM images of wet mounted boar sperm.

Prior to fixation and immobilization on Superfrost coverslips sperm were treated with (A) HBT-Bic (non capacitated sperm) or (B) with HBT+Bic (capacitated sperm). Both sperm heads had intact acrosomes as can be distinguished by their characteristic apical ridges (indicated by a * in the pictures). Note the more defined and flattened structure at the aEqS of the capacitated sperm indicated with an arrow (B). The distance bar reflects 1 µm.

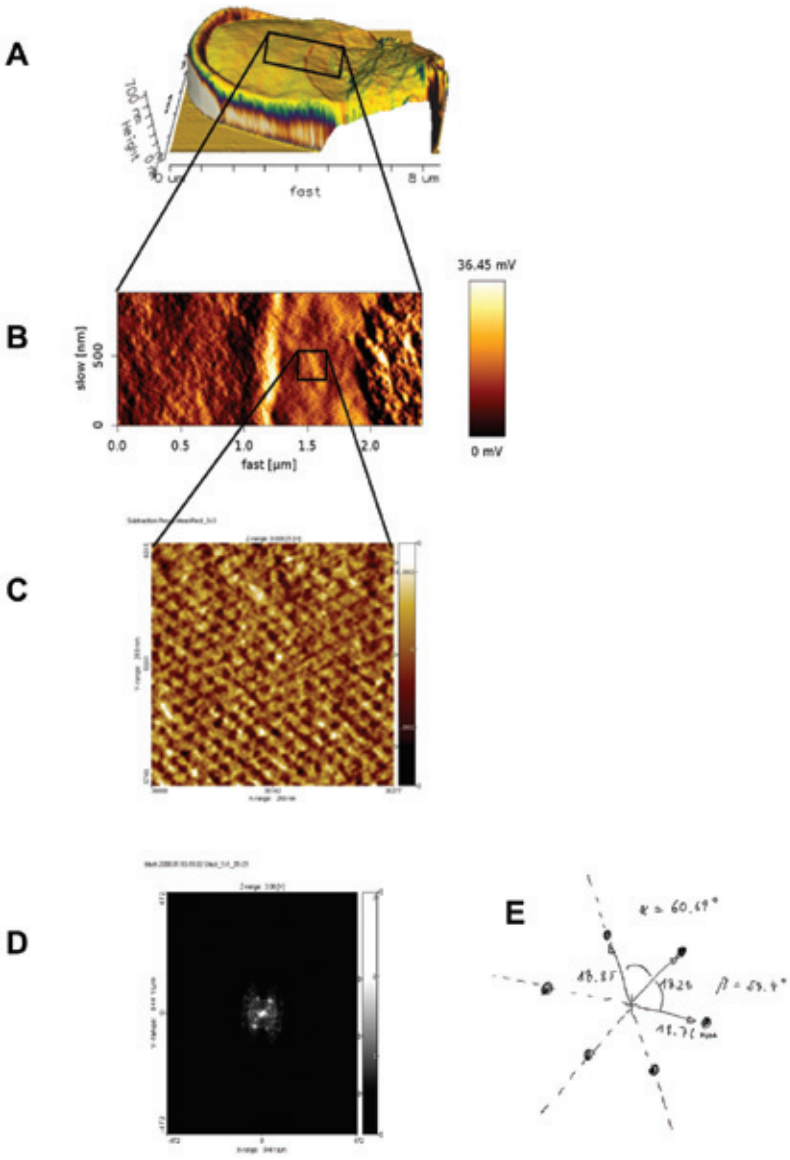

Figure 2. AFM images of wet mounted capacitated boar sperm.

With increasing resolution (from A-C) of the same region (indicated as squares) show a 17 nm hexagonal surface pattern which is present in the entire aEqS. Distance bars indicate 1 µm (panel A), 0,5 µm (panel B) and 50 nm (panels C and D). Panel D shows the observed average of the hexagonal pattern as was measured in the Fourier transfer imaging mode. Panel E provides a description of actual distance of particles to a central particle and angles between two particles and the central particle as was measured by Fourier transfer.

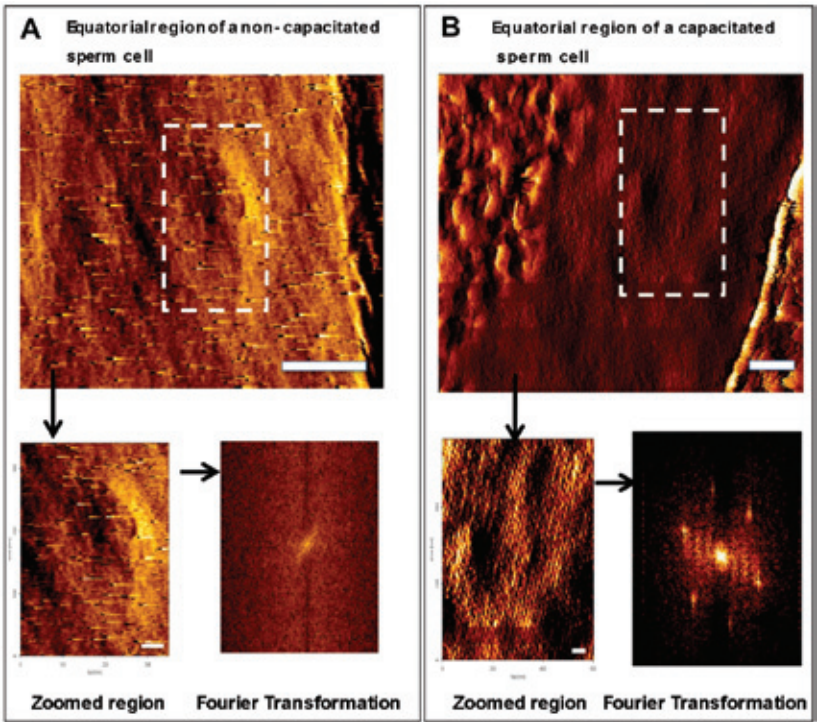

Figure 3. Representative wet mount AFM images of non-capacitated (HBT-Bic) sperm (A) and capacitated (HBT+Bic) boar sperm (B).

At the aEqS the control sperm (A) showed no hexagonal pattern of particles (see zoom and Fourier transformation data of the aEqS) while the hexagonal pattern was clearly detectable in the capacitated aEqS (B). Scale bar indicates 200nm (upper panels) and 50nm (lower panels).

Induction of the acrosome reaction results in the villi shaped mixed membrane structures at the aEqS of sperm surface

Sperm cells that were capacitated were further incubated with HBT+Bic and Ca^{2+}-ionophore in order to induce the acrosome reaction. As expected AFM imaging clearly shows the removal of the acrosome in the apical area and of the apical ridge (Fig. 4A). Unexpectedly, the AFM image also revealed that the entire area of the aEqS showed finger shaped protrusions (fenestrated structures of approximately 50 nm in diameter and 1 µm in length) of membranes that were continuous with the EqSS (Fig 4A). An ultrathin section of sperm under Transmission Electron Microscopy (TEM) shows that these fenestrations are in fact 50 nm tubules in which plasma membrane and outer acrosomal membrane components become mixed but continuous to the sperm surface (Fig 4B). At the pre-equatorial area mixed vesicles are released from the sperm surface (Fig 4B). These mixed vesicles were released as an acrosomal shroud and not present on the pre-equatorial surface of the AFM image (Fig. 4A).

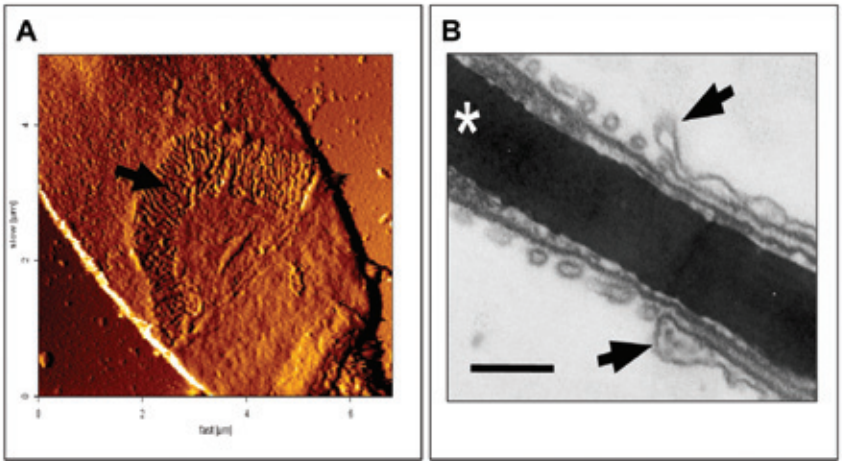

Figure 4. Representative images of the aEqS of boar sperm after induction of the acrosome reaction with Ca^{2+} ionophore.

(A) Wet mount surface AFM view of the sperm shows that at the apical side the acrosome overlying surface is removed while at the aEqS fenestrations are visible over the entire area where exposure of hexagonal surface proteins became apparent during sperm capacitation (compare with Fig. 1A). The fenestrations are approximately 50 nm in diameter and 1 µm long. (B) An ultrathin section of a boar sperm cell with TEM [4] shows that at the apical edge of the equatorial segment (representing the tip of the fenestrations as indicated with arrows in A and B) is contacting the plasma membrane with the outer acrosomal membrane (scale bar = 200 nm). This distance is also 50 nm thus predicting that the fenestrations depicted in (A) are membrane tubules connected to the EqSS plasma membrane and outer acrosome membrane, respectively.

The aEqS specific protrusions expose outer acrosomal membrane components

We observed an acrosome reaction dependent emergence of GM-1 in the aEqS (Fig. 5A). Light microscopy does not have the resolution to determine whether GM-1 is present or not in the fenestrated structures (Fig. 5A). However, with functional anti GM-1 antibody activated cantilever tips we were able to map interactions of GM-1 on the fenestrated structures and between these structures (for topologies see Fig. 5B). Clearly, the fenestrations showed a high interaction of above 100 pN while in between the interaction was comparable to background interaction (below 50 pN). The appearance of fenestrations apparently allowed GM-1 exposure at the aEqS. Possibly this GM-1 is from an outer acrosomal origin and becomes exposed after the merging of this membrane with the plasma membrane that is specific for the aEqS.

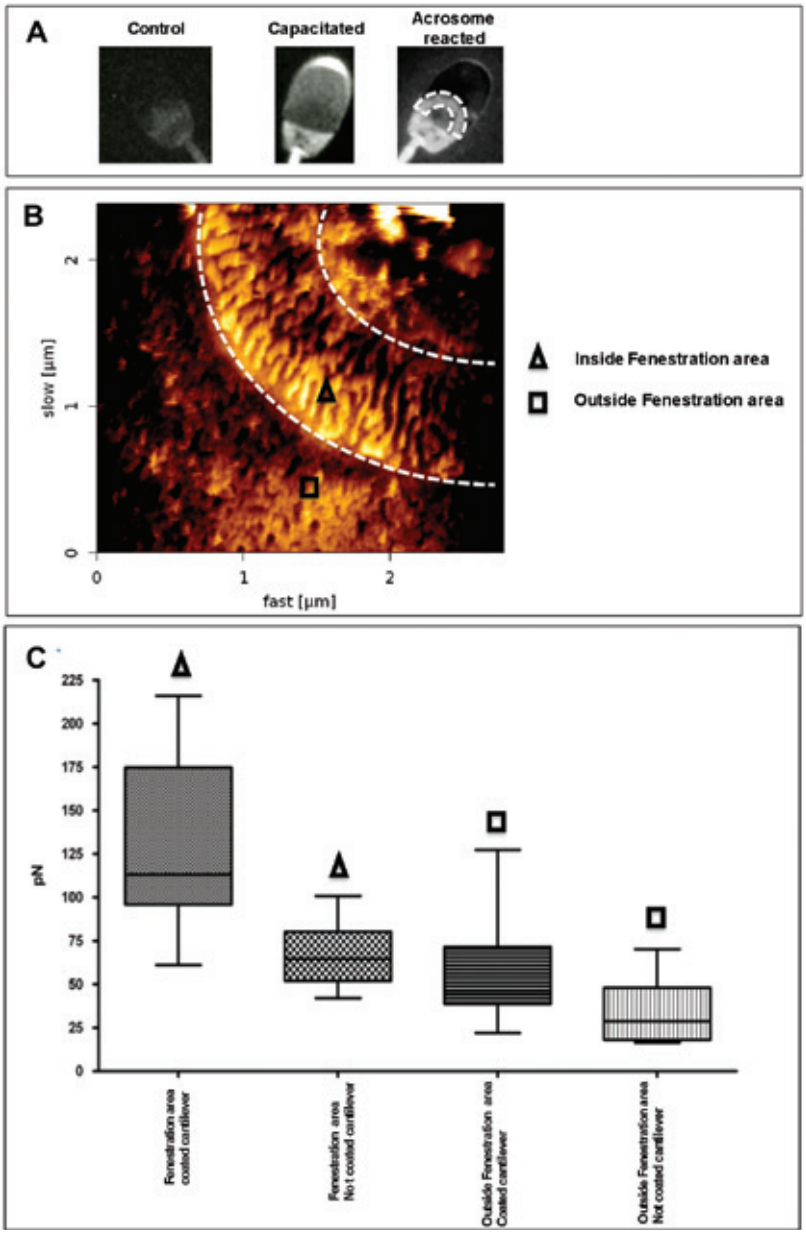

Figure 5. Specific exposure of GM-1 at the membrane fenestrations of the aEqS.

Cantilever tips were functionally activated with an anti GM-1 antibody to detect the presence of GM-1 by nanometer sized force mapping. (A) GM-1 signal was only present in the aEqS after the induced acrosome reaction (cholera toxin B-FITC staining). (B) Imaging of the aEqs of a boar sperm cell after the induction of the acrosome reaction showing the membrane fenestrations. (C) Dedicated force mapping of cantilever associated anti GM-1 antibodies and the sperm surface at membrane fenestrations (triangles) and outside the fenestrated area (squares) are provided in pN. (n=15, Bonferonni Multiple Comparison test $P<0.01$).

Involvement of a trimerization domain in proteins in the aEqS and in vitro fertilization

During the acrosome reaction another macromolecule which is a protein becomes exposed in the sperm head at the aEqS, namely a protein with an epitope shared with a chicken specific virus protein (haemagglutinin sH5(3) [14]. The epitope is in fact the trimerization domain of haemagglutinin and we used this antibody as we thought the hexagonal pattern of the aEqS in capacitated sperm might be due to similar protein to protein interactions. Clearly, the sperm protein lysates contain proteins that are recognized by the positive serum (Fig. 6A) while the control chicken serum did not show any reactivity (data not shown). Interestingly, acrosome reacted sperm showed anti-sH5(3) antibody binding as determined by fluorescence microscopy (Fig. 6B). When *in vitro* fertilization was performed in the presence of (control) negative chicken serum approximately 85% of the metaphase 2 arrested mature oocytes were fertilized while only 15 % were not fertilized (Fig. 6C). In contrast, *in vitro* fertilization in the presence of α-sH5-epitope specific almost entirely blocked fertilization (approximately 15 % fertilization and 85 % remained unfertilized; Fig. 6C). The amount of sperm that remained bound to the zona pellucida after IVF (an indication of acrosome reaction) was not different between control IVF (on average 32 sperm cells) and IVF in the presence of control α-sH5-epitope specific chicken serum (on average 30 sperm) but was significantly lower in chicken serum (on average 14 sperm).

Mass spectrometry analysis of protein bands reacting to HA-1 anti-sera.

To identify sperm proteins that are recognized by α-sH5-epitope specific antibody, proteins were separated by SDS-PAGE and analysed by western blotting using the sH5 epitope antibody. The corresponding positive sH5trimer band was excised from the SDS-PAGE gel and the proteins in this excised material were further processed for mass spectrometry. The mass spectrometry analysis revealed the presence of acrosin binding protein-1, collagen-1 alpha chain and a zona pellucida binding protein (Table 1). It is of interest that collagen at its neck region trimerizes and it is possible that this region has similarities with the binding epitope of the antibody directed against sH5(3) as well as the protein present at the aEqS.

Table 1. Protein identification from the region of an SDS-PAGE gel corresponding to the sH5(trimer) band achieved by Western blotting. The data depicted here combined PMF and MS/MS queries using the MASCOT Database search engine for protein identification. Proteins detected multiple times in different SDS-PAGE lanes were acrosin-binding protein and Collagen alpha-1(I) chain. Zona pellucida-binding protein was also identified once.

Accession number	Name	Mascot score	Total number of peptides	Pep 1	e value	Pep 2	e value
CO1A1_BOVIN	Collagen alpha-1(I) chain	120	1	**SGDRGETGPAGPAGPIGPVGAR**	1.50E-09		
ACRBP_PIG	Acrosin-binding protein (Fragment)	96	1	**FYGLDLYGGLR**	1.20E-07		
CO1A1_BOVIN	Acrosin-binding protein (Fragment)	87	1	**SGDRGETGPAGPAGPIGPVGAR**	2.50E-06		
ACRBP_PIG	Acrosin-binding protein (Fragment)	73	1	**FYGLDLYGGLR**	2.20E-05		
ZPBP1_PIG	Acrosin-binding protein (Fragment)	74	1	**FFNQQVEVLGR**	7.00E-05		
CO1A1_BOVIN	Acrosin-binding protein (Fragment)	147	1	**GETGPAGPAGPIGPVGAR**	3.30E-05		
ACRBP_PIG	Acrosin-binding protein (Fragment)	215	2	**FYGLDLYGGLR**	9.90E-07	**LEQCHSETNLQR**	2.30E-06
ACRBP_PIG	Acrosin-binding protein (Fragment)	172	2	**LEQCHSETNLQR**	7.90E-06	**FYGLDLYGGLR**	6.70E-05
ACRBP_PIG	Acrosin-binding protein (Fragment)	116	1	**FYGLDLYGGLR**	2.00E-06		
ACRBP_PIG	Acrosin-binding protein (Fragment)	144	2	**FYGLDLYGGLR**	2.60E-05	**LEQCHSETNLQR**	0.00039
ACRBP_PIG	Acrosin-binding protein (Fragment)	115	1	**FYGLDLYGGLR**	1.60E-07		

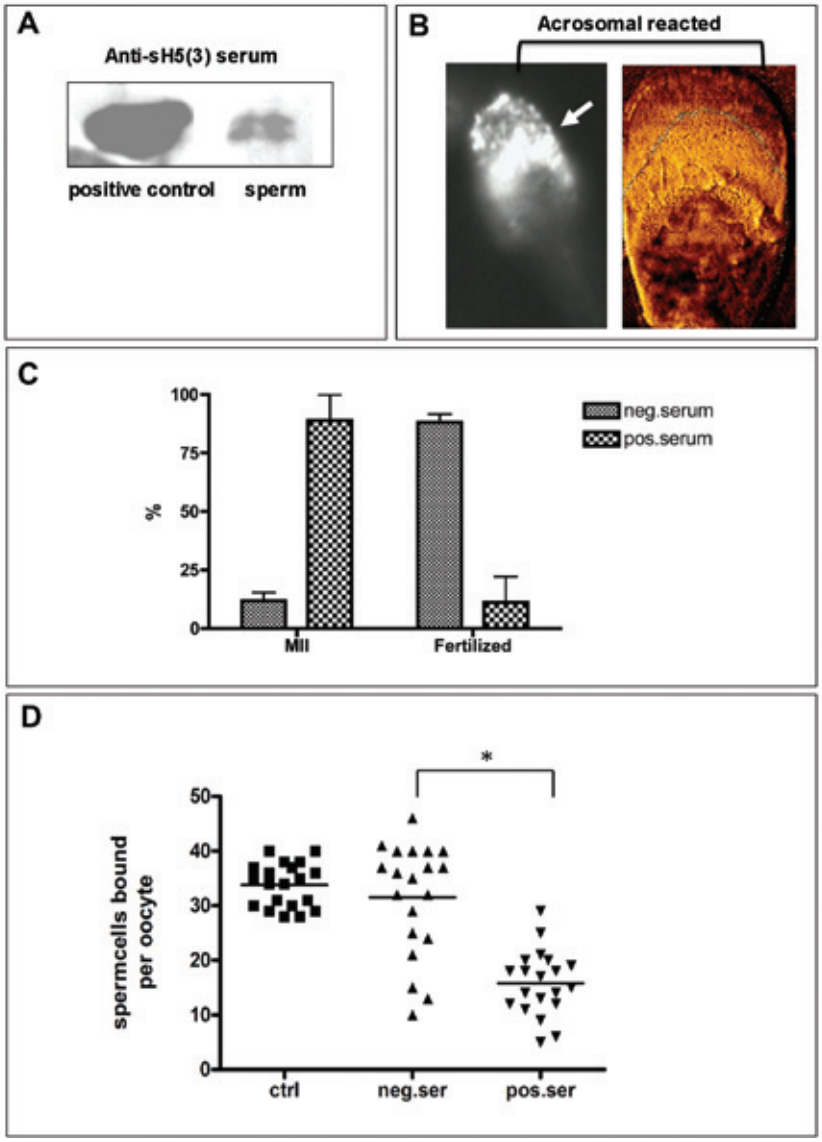

Figure 6. A serum containing sH5(3) antibodies recognizes an epitope on the membrane fenestrations of boar sperm that were induced for the acrosome reaction.

(A) Western blot detection of the epitope on sperm protein lysates. (B) Indirect immunofluorescent detection (left panel) of surface labelling of the epitope on the membrane fenestration region (right panel; AFM image) of an acrosome reacted boar sperm cell. (C) *In vitro* fertilization results with sperm incubated in IVF medium with 100 diluted chicken serum (negative control) versus anti-sH5(3) positive serum clearly depicting that the positive serum essentially blocked *in vitro* fertilization while negative serum did not inhibit *in vitro* fertilization MII refers to mature unfertilized metaphase 2 arrested oocytes. Fertilized oocytes showed at least two pronuclei or signs of normal cleavage. (D) Effects of negative control and positive serum IVF conditions on sperm penetration in the zona pellucida. The positive serum inhibited the zona penetration by 50% (n=20, asterisk indicates P <0.05).

DISCUSSION

In this manuscript we reveal two typical surface events that occur at the fertilization specific surface of the sperm cell namely at the apical area of the equatorial segment (aEqS). These surface phenomena cannot be observed with light microscopy where resolution is limited by the diffraction properties of light. Even super resolution light microscopy does not allow structural detection <50 nm accurately [20]. However, by using wet mount AFM we found:

1. The aEqS strongly flattens after capacitation and at the entire aEqS a 17 nm dispersed perfectly hexagonal arrangement of surface particles became apparent. In contrast to control cells where the aEqS was less flattened and the hexagonal pattern was absent. Hexagonal arrangements of plasma membrane of the equatorial segment of guinea pig and rat sperm [21] and in cyprinid fishes [22] were observed in the past by freeze fracture. The freeze fractures were made on specimens of fresh washed sperm that was not capacitated. In combination with the current AFM study on boar sperm we extrapolate these findings and show that (a) the 17 nm dispersed hexagonal arrangement of particles refers to similar transmembrane particles observed in the equatorial segment of guinea pig sperm and (b) that the hexagonal arrangement of these proteins was probably present before sperm capacitation. A new insight, which comes from our study, is that the hexagonal arranged transmembrane proteins were not exposed directly to the cantilever tip in control sperm but became exposed after capacitation. Taken together we postulate that a 17 nm hexagonal arranged transmembrane protein network is present in the aEqS and decoating of extracellular matrix materials makes this structure accessible for the cantilever tip (for a model see Figure 7).

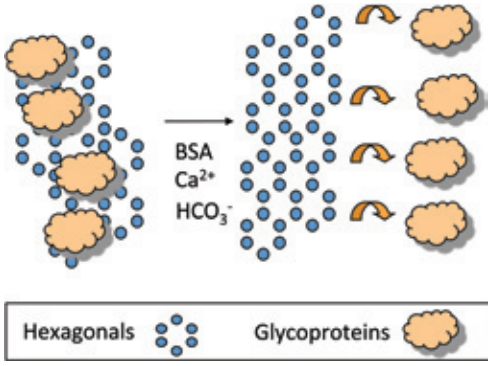

Figure 7. Model explaining how pre-existing hexagonal arranged transmembrane proteins become exposed for the wet mount AFM cantilever tip.

Extracellular matrix components present on the sperm surface of control sperm are released by the indicated capacitation factors present in IVF media or in HBT+Bic treatment. The cantilever tip does not sense the underlying hexagonal structure before but does recognize these characteristic structures after capacitation-specific removal of glycoproteins.

Scanning electron microscopy of the sperm surface as well as light microscopy cannot reveal these structures on the sperm surface due to limitations in surface resolution. Of further note is that our wet mount approach to image the sperm surface gives unparalleled ultrastructural information when compared to conventional AFM of dried sperm specimen (as described by Saeki et al. and Ellis et al. [23, 24]). Flattened features of the aEqS were also shown on dried specimens of ram, bull, boar and goat sperm [24].

2. After induction of the acrosome reaction fingerlike fenestrated membrane structures sprout from the EqSS over the entire aEqS. These tubules were oriented in parallel to the sperm head axis and were 50 nm in diameter and 1 µm in length. In contrast to transmission electron microscopy (where ultrathin sections of cells can be made for ultrastructural organization) AFM provides a surface view of the sperm. On the other hand TEM showed at the aEqS that the plasma membrane and outer acrosomal membrane positions of these fenestrations were at a distance of again 50 nm suggesting strongly that the fenestrations are tubular shaped. The tips of these tubules are where they end towards the pre-equatorial surface. However, the basis of the tubules is at the EqSS as can be seen at the surface with AFM (this study) and has been captured in the past by freeze fracture on the outer acrosomal membrane [25]. This relatively large surface area (the entire aEqS) is generated where surface molecules of the plasma membrane are mixed with membrane molecules of the outer acrosomal membrane. The relevance of exposing and mixing molecules of the acrosome at the sperm surface has been acknowledged with respect to exposure of acrosome specific tetraspanins [26] and to fusogenic properties with artificial membrane vesicles [27]. Both may relate to the fertilization competence of sperm and it is of interest that the equatorial segment is the specific surface area of the sperm involved in binding and fusing with the oolemma (for review see Gadella and Evans 2011 [28]).

3. During the induced acrosome reaction the fenestrations in the aEqS contained GM-1, which is most likely originating from the outer acrosomal membrane. It is known that GM-1 is absent on the surface of intact sperm [29] as detected with cholera toxin b –FITC staining while acrosome disrupted cells become positive for this stain. Lipid extracts from the cavitated plasma membrane fraction does not contain GM-1 while the whole sperm lipid extracts do contain GM-1 [29]. GM-1 is a lipid that prefers lipid ordered membrane substructures [30] and thus it is therefore possible that an outer acrosomal raft structure is involved in the fenestration phenomenon of the aEqS during the acrosome reaction.

4. An antibody raised against the trimerization domain of haemaglutinin recognized an epitope at the fenestration structures at the aEqS and blocked *in vitro* fertilization without affecting primary sperm zona binding and reducing secondary sperm-zona binding (which occurs after the acrosome reaction). Mass spectrometry identification of the protein band recognized by the antibody revealed

the presence of several proteins. The most prominent one was the acrosin binding protein also termed sp32 [31, 32] which has been reported to be involved in zona binding [33]. Interestingly, an anti-acrosin monoclonal antibody AcrC5F10 was reported to inhibit proacrosin activation, proacrosin-human zona pellucida glycoprotein binding, and inhibit the zona pellucida (ZP)-induced acrosome reaction of the ZP-bound spermatozoa but was reported to have no significant effect on sperm-ZP binding [34]. Another identified protein was the collagen alpha chain, which is of interest as collagens are notoriously stringent in trimeric organization and a common epitope between haemagglutinin and collagen alpha may explain why this cross-reacted with the α-sH5-epitope specific antigen. The third protein recognized was zona pellucida-binding protein 1 may also be involved in zona binding and although, like acrosin-binding protein, their identification may not relate to epitope binding of the antibody used, the antibody may cap these proteins indirectly by binding to another primary target and thus shield them for proper secondary zona binding. This could explain the reduction of 50% in penetration rates of acrosome reacted sperm (that is, those that remained attached after IVF). This preliminary data has revealed possible candidates but not necessarily all candidate proteins. Future experiments should focus on fully elucidating the identity of proteins that regulate the specific features of the aEqS with special emphasis on the role of the hexagonal network of transmembrane proteins, and the exact role in the fertilization fusion. Sperm decoating revealed the hexagonal structures as well as the formation of fenestrated mixed membrane tubules, which was made possible by recent advances in wet mount AFM. The significance of proteins that are exposed in the fenestrated membrane tubules at the aEqS (that is at the sperm surface specifically involved in the fertilization fusion) remains to be determined. We suppose that the hexagonal organized transmembrane proteins will undergo conformational changes that play a role in the formation of membrane fenestrations but this also needs to be confirmed with future experiments.

ACKNOWLEDGMENTS

This work and the atomic force microscopy equipment were financed with the High Potential award provided by Utrecht University to Rene van Nostrum and Bart Gadella. We thank Eric Schoevers and Jason Tsai for fruitful discussions and for their contribution to the IVF experiments. We are grateful to Cardiff University CBS Proteomics Facility (http://medicine.cf.ac.uk/cbs) for the protein identification work achieved on their tandem mass spectrometry platform. We thank Robbert de Vries for providing the anti- sH5(3) chicken sera from the Virology Division, Department of Infectious Diseases & Immunology, Faculty of Veterinary Medicine, Utrecht University, Utrecht, The Netherlands.

REFERENCES

1. Leahy T, Gadella BM. Sperm surface changes and physiological consequences induced by sperm handling and storage. Reproduction 2011; 142:759-778.

2. Goodson SG, Qiu Y, Sutton KA, Xie G, Jia W, O'Brien DA. Metabolic substrates exhibit differential effects on functional parameters of mouse sperm capacitation. Biol Reprod 2012; 87:75.

3. Boerke A, Tsai PS, Garcia-Gil N, Brewis IA, Gadella BM. Capacitation-dependent reorganization of microdomains in the apical sperm head plasma membrane: Functional relationship with zona binding and the zona-induced acrosome reaction. Theriogenology 2008; 70:1188-1196.

4. Tsai PS, Brewis IA, van Maaren J, Gadella BM. Involvement of complexin 2 in docking, locking and unlocking of different SNARE complexes during sperm capacitation and induced acrosomal exocytosis. PLoS One 2012; 7:e32603.

5. Fukami K, Nakao K, Inoue T, Kataoka Y, Kurokawa M, Fissore RA, Nakamura K, Katsuki M, Mikoshiba K, Yoshida N, Takenawa T. Requirement of phospholipase Cdelta4 for the zona pellucida-induced acrosome reaction. Science 2001; 292:920-923.

6. Sutovsky P, Manandhar G, McCauley TC, Caamano JN, Sutovsky M, Thompson WE, Day BN. Proteasomal interference prevents zona pellucida penetration and fertilization in mammals. Biol Reprod 2004; 71:1625-1637.

7. Yanagimachi R. Mammalian fertilization. In: Knobil E and Neill JD (eds.), The physiology of reproduction, 2nd ed. New York, USA: Raven Press; 1994: 189.

8. Masco D, Flott B, Seifert W. Astrocytes in cell culture incorporate GM1 ganglioside. Glia 1989; 2:231-240.

9. Gadella BM, Miller NG, Colenbrander B, van Golde LM, Harrison RA. Flow cytometric detection of transbilayer movement of fluorescent phospholipid analogues across the boar sperm plasma membrane: elimination of labeling artifacts. Mol Reprod Dev 1999; 53:108-125.

10. Tsai P, De Vries KJ, De Boer-Brouwer M, Garcia-Gil N, Van Gestel RA, Colenbrander B, Gadella BM, Van Haeften T. Syntaxin and VAMP association with lipid rafts depends on cholesterol depletion in capacitating sperm cells. Mol Membr Biol 2007; 24:313-324.

11. Gadella BM, Harrison RA. The capacitating agent bicarbonate induces protein kinase A-dependent changes in phospholipid transbilayer behavior in the sperm plasma membrane. Development 2000; 127:2407-2420.

12. Caneva Soumetz F, Saenz JF, Pastorino L, Ruggiero C, Nosi D, Raiteri R. Investigation of integrin expression on the surface of osteoblast-like cells by atomic force microscopy. Ultramicroscopy 2010; 110:330-338.

13. Boerke A, Brouwers JF, Olkkonen VM, van de Lest CH, Sostaric E, Schoevers EJ, Helms JB, Gadella BM. Involvement of bicarbonate-induced radical signaling in oxysterol formation and sterol depletion of capacitating mammalian sperm during in vitro fertilization. Biol Reprod 2013; 88:21.

14. Cornelissen LA, de Vries RP, de Boer-Luijtze EA, Rigter A, Rottier PJ, de Haan CA. A single immunization with soluble recombinant trimeric hemagglutinin protects chickens against highly pathogenic avian influenza virus H5N1. PLoS One 2010; 5:e10645.

15. Schoevers EJ, Kidson A, Verheijden JHM, Bevers MM. Effect of follicle-stimulating hormone on nuclear and cytoplasmic maturation of sow oocytes in vitro. Theriogenology 2003; 59:2017-2028.

16. Medzihradszky KF, Campbell JM, Baldwin MA, Falick AM, Juhasz P, Vestal ML, Burlingame AL. The characteristics of peptide collision-induced dissociation using a high-performance MALDI-TOF/TOF tandem mass spectrometer. Anal Chem 2000; 72:552-558.

17. Bienvenut WV, Deon C, Pasquarello C, Campbell JM, Sanchez JC, Vestal ML, Hochstrasser DF. Matrix-assisted laser desorption/ionization-tandem mass spectrometry with high resolution and sensitivity for identification and characterization of proteins. Proteomics 2002; 2:868-876.

18. Gluckmann M, Fella K, Waidelich D, Merkel D, Kruft V, Kramer PJ, Walter Y, Hellmann J, Karas M, Kroger M. Prevalidation of potential protein biomarkers in toxicology using iTRAQ reagent technology. Proteomics 2007; 7:1564-1574.

19. Perkins DN, Pappin DJ, Creasy DM, Cottrell JS. Probability-based protein identification by searching sequence databases using mass spectrometry data. Electrophoresis 1999; 20:3551-3567.

20. Buss J, Coltharp C, Xiao J. Super-resolution Imaging of the Bacterial Division Machinery. J Vis Exp 2013; (71). pii: 50048. doi:10.3791/50048.

21. Friend DS, Fawcett DW. Membrane differentiations in freeze-fractured mammalian sperm. J Cell Biol 1974; 63:641-664.

22. Ohta T, Matsuda M. Sperm morphology and IMP distribution in membranes of spermatozoa of cyprinid fishes II. Cell Struct Funct 1995; 20:293-300.

23. Saeki K, Sumitomo N, Nagata Y, Kato N, Hosoi Y, Matsumoto K, Iritani A. Fine Surface Structure of Bovine Acrosome-Intact and Reacted Spermatozoa Observed by Atomic Force Microscopy. J Reprod Dev 2004;

24. Ellis DJ, Shadan S, James PS, Henderson RM, Michael E, Hutchings A, Jones R. Post-testicular development of a novel membrane substructure within the equatorial segment of ram, bull, boar, and goat spermatozoa as viewed by atomic force microscopy. J Struct Biol 2002; 138:187-98.

25. Jones R, James PS, Oxley D, Coadwell J, Suzuki-Toyota F, Howes EA. The equatorial subsegment in mammalian spermatozoa is enriched in tyrosine phosphorylated proteins. Biol Reprod 2008; 79:421-431.

26. Ito C, Yamatoya K, Yoshida K, Maekawa M, Miyado K, Toshimori K. Tetraspanin family protein CD9 in the mouse sperm: unique localization, appearance, behavior and fate during fertilization. Cell Tissue Res 2010; 340:583-594.

27. Arts EG, Wijchman JG, Jager S, Hoekstra D. Protein involvement in the fusion between the equatorial segment of acrosome-reacted human spermatozoa and liposomes. Biochem J 1997; 325 (Pt 1):191-198.

28. Gadella BM, Evans JP. Membrane fusions during mammalian fertilization. Adv Exp Med Biol 2011; 713:65-80.

29. van Gestel RA, Brewis IA, Ashton PR, Helms JB, Brouwers JF, Gadella BM. Capacitation-dependent concentration of lipid rafts in the apical ridge head area of porcine sperm cells. Mol Hum Reprod 2005; 11:583-590.

30. Moreno-Altamirano MMB, Aguilar-Carmona I, Sánchez-García FJ. Expression of GM1, a marker of lipid rafts, defines two subsets of human monocytes with differential endocytic capacity and lipopolysaccharide responsiveness. Immunology 2007; 120:536-543.

31. Nagdas SK, Hamilton SL, Raychoudhury S. Identification of acrosomal matrix-specific hydrolases binding proteins of bovine cauda epididymal spermatozoa. J Androl 2010; 31:177-187.

32. Ono T, Kurashige T, Harada N, Noguchi Y, Saika T, Niikawa N, Aoe M, Nakamura S, Higashi T, Hiraki A, Wada H, Kumon H, Old LJ, Nakayama E. Identification of proacrosin binding protein sp32 precursor as a human cancer/testis antigen. Proc Natl Acad Sci U S A 2001; 98:3282-3287.

33. van Gestel RA, Brewis IA, Ashton PR, Brouwers JF, Gadella BM. Multiple proteins present in purified porcine sperm apical plasma membranes interact with the zona pellucida of the oocyte. Mol Hum Reprod 2007; 13:445-454.

34. Veaute C, Liu de Y, Furlong LI, Biancotti JC, Baker HW, Vazquez-Levin MH. Anti-human proacrosin antibody inhibits the zona pellucida (ZP)-induced acrosome reaction of ZP-bound spermatozoa. Fertil Steril 2010; 93:2456-2459.

6

Summarizing discussion

The fusion of 2 gametes to form new life is a highly regulated event. The activation -also termed capacitation- of the sperm cell is one of the key preparative steps required for this process. The sperm cell has to become motile and has to make a journey through the female uterus and oviduct before it can approach the oocyte. At the same moment the oocyte has to become prepared for fertilization. The mature oocyte has specific strategies to facilitate monospermic fertilization and to block polyspermic fertilization. This thesis is focused on sperm cells and in particular on sperm cell surface dynamics prior to fertilization. Interestingly, freshly ejaculated sperm cells are not able to fertilize the oocyte despite the fact that key players involved in sperm cell–zona binding are already attracted to the sperm cell surface during epididymal maturation. During the capacitation process in the female genital tract the formation of competent lipid-protein domains on the sperm head provides the sperm cell with the ability to bind to the oocyte. The binding of the sperm cell to the oocyte is the onset for a cascade reaction ultimately resulting in oocyte-sperm cell fusion. Many different lipids and proteins are involved in this process. In recent years *in vitro* fertilization (IVF) has been become a widely used tool to achieve successful fertilization in both the veterinary field and human medicine. Although IVF procedures are very successful, scientific knowledge is still far from complete. Knowledge is fragmented concerning the identity of molecular players and processes during preparative stages and the actual fertilization fusion of 2 gametes eventually resulting in a new living organism. In this thesis the current understanding of the process of capacitation and the sperm cell surface changes is reviewed in **chapter 1**. The scope of thesis and the attempt to fill some gaps of knowledge in sperm cell surface physiology that have been investigated in **chapters 2-5** were also described in **chapter 1**.

PART 1: CHOLESTEROL EFFLUX FROM CAPACITATING SPERM CELLS

The role of cholesterol (and of desmosterol) in sperm cells is one of the hallmarks of capacitation. During this process, cholesterol is released to a cholesterol acceptor such as albumin [1]. Without this cholesterol extraction sperm cells cannot become fully competent in fertilizing the oocyte. Probably the removal of sperm cell surface cholesterol is required for lateral rearrangements of surface components and especially for the migration of proteins to the apical ridge area. This is the sperm surface region where membrane raft aggregation was noted, where membrane protein complexes required for zona binding reside, and where docking proteins required for the initiation of the acrosome reaction were observed (see **chapter 1** for an overview). The mechanism how lipoproteins can remove cholesterol from the sperm cell surface of bicarbonate-activated sperm cells is not understood.

In recent literature [2-4] it has become evident that cholesterol is a substrate for auto-oxidation by intrinsically formed ROS. Alternatively, specific enzymes can oxidize cholesterol. Oxysterol formation may alter the sperm cell surface properties and may be related to sterol efflux in capacitating sperm cells. Thus, not only the amount of sterols but also the oxidation of sterols and partition of molecular

sterol species into the incubation media was measured under various capacitation incubation conditions (**chapters 2 and 3**).

Chapter 2 describes HPLC and mass spectrometry-based techniques that were applied and optimized to enable a highly sensitive detection range (fmole-mmole) of sterol species. This allowed both identification and quantification of various oxidation products formed from cholesterol and desmosterol. Cryopreservation of bovine sperm cells resulted in increased levels of oxysterols and we hypothesize that this can lead to lipotoxicity or to membrane destabilization. Prevention of oxysterol formation during cryopreservation may result in higher sperm cell survival rates after thawing. A more pronounced increase in oxysterols was observed when bovine sperm cells were incubated under capacitating conditions. Remarkably, only capacitation resulted in the depleted sperm cell sterols while the sterol levels remained unchanged after cryopreservation. This discrepancy may illustrate that oxysterol formation *per se* is not sufficient to allow sperm cell surface depletion of sterols and that other cellular responses not elicited during cryopreservation of sperm are required. In chapter 2 the differences in molecular composition of oxysterols formed after pro-oxidant treatments of reconstituted sperm membrane vesicles or of intact sperm were studied and compared to *in vitro* capacitation conditions. More detailed analyses of the differences in the formation of molecular species of oxysterols may elucidate auto-oxidative and enzymatic steps involved in oxysterol formation [12-14] and identify the pro-oxidation as well as anti-oxidation pathways that are switched on or inhibited during the process of sperm cell activation. This knowledge may be useful to minimize adverse effects of oxysterol formation in sperm cell processing prior to cryopreservation.

Chapter 3 focuses on the relation between oxysterol formation and its role in the depletion of cholesterol in capacitating boar and mouse sperm cells. Indeed, in both mammalian species capacitation led to the formation of oxysterols and to the depletion of free sterols. The formation of oxysterols was bicarbonate-dependent and could also be induced by pro-oxidants in absence of bicarbonate, or blocked by hydrophobic anti-oxidants in presence of bicarbonate. The capacitation conditions that resulted in oxysterol formation also resulted in depletion of cholesterol and desmosterol in both species. However, addition of pro-oxidants did not have these effects showing that the relationship between oxysterol formation and sterol depletion is more complex. This is in line with observations made in **chapter 2**, showing that oxysterol formation in cryopreserved sperm was not succeeded by sterol removal from the sperm surface. Capacitation-dependent sterol depletion is one of the steps required for downstream sperm activation processes including increased protein tyrosine phosphorylation in the sperm tail and the induction of hyperactivated motility. Cholesterol loss also induces lateral rearrangements of membrane components in the sperm head and increases membrane fluidity. Such preparative steps are required for optimal binding of capacitated sperm cells to the zona pellucida to allow rapid induction of the acrosome reaction in sperm cells. Failure of proper capacitation also blocks fertilization. In **chapter 3** it was observed that indeed capacitation was required not only for oxysterol formation and sterol depletion but also for

the generation of protein tyrosine phosphorylation, hyperactivated motility and rearrangements of molecules at the sperm head surface. Under *in vitro* fertilization conditions these changes were required for the induction of the acrosome reaction after zona binding and were required for fertilization. When *in vitro* fertilization was carried out in the presence of hydrophobic anti-oxidants, this not only blocked oxysterol formation but also fertilization of the oocyte. The amount of sperm cells bound to the zona pellucida was, however, not significantly affected. Moreover, the polyspermic fertilization rates of fertilized oocytes in control versus anti-oxidant conditions were identical. Both observations indicate that the anti-oxidant inhibition effect was specific for sperm cells and that the developmental competence of the oocyte was unaffected.

Sperm incubated with oxysterol binding proteins (OBPs) also showed -in part- signs of sperm capacitation **(chapter 3)**. The OBPs induced sperm protein tyrosine phosphorylation, hyperactivated motility, lateral rearrangements of molecules at the sperm head, and affinity for the zona pellucida. In fact, OBP interaction with the sperm surface scavenged oxysterol formation by >50% and induced premature acrosome reactions in sperm cells in capacitation media. However, OBPs did not support *in vitro* fertilization or the efflux of free sterols from the sperm surface (see figure 1 depicting a scheme summarizing the results of **chapter 2 and 3**).

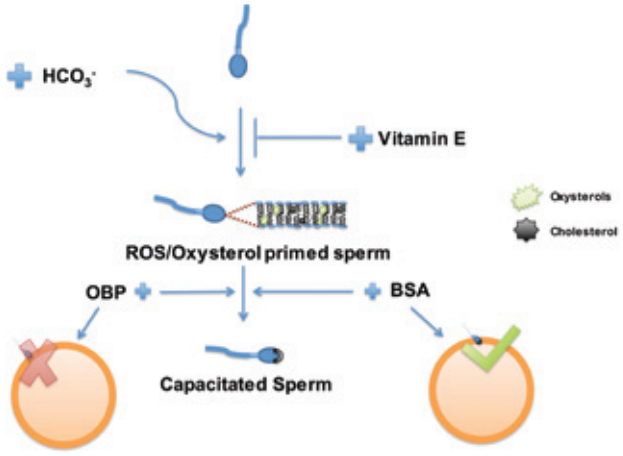

Figure 1. Model depicting the influence of oxysterols on sterol efflux during sperm capacitation and fertilization of the oocyte.

Bicarbonate induces ROS/oxysterol primed sperm. Vitamin E inhibits this process. Incubation with OBP leads to hypermotility and movement of proteins to the apical ridge but does not result in sperm capable of fertilizing the oocyte. Using albumin as a sterol acceptor in IVF procedures does lead to sperm competent in fertilizing the oocyte.

An alternative way to deplete the sperm surface from (oxy)sterols is treatment with cyclodextrin. In **chapter 3** a successful depletion of cholesterol and desmosterol from sperm cells was observed with methylbetacyclodextrin (MBCD). As a result protein tyrosine phosphorylation, hyperactivated

motility and moderate *in vitro* fertilization rates (about 30 % instead of the usual 60 %) were found with sperm incubated with 2 mM MBCD. Lower levels of MBCD did not result in these effects and higher levels were detrimental to sperm (see also van Gestel 2005 [5]) as well as to oocytes. Oocyte deterioration was manifest in 30% of the oocytes showing that IVF in the presence of MBCD is not recommended.

It is of special interest to sperm physiology that oxysterol formation may enable altered lateral and bilayer properties as oxysterols can rigidify or make membranes more fluid [2]. The effect of a more fluid membrane could be detrimental for instance for cryopreserved sperm as altered membrane fluidity could result in membrane damage. Possibly the presence of oxysterols can be used for diagnostics in assessing the cryopreservability of semen donors. Another possibility is that oxysterols promote sterol depletion. Sterols are flat hydrocarbon steroid structures with one polar hydroxyl group in the polar head group region of phospholipid monolayers and the steroid ring structure in parallel oriented with the fatty acids esterified to phospholipids. However, oxysterols by virtue of additional polar hydroxyl groups will be oriented in a more surface exposed orientation (i.e. in parallel with the polar headgroups; see figure 2). This phenomenon may not only lead to changes in the fluidity of the membrane, but may also tilt free sterols into a more accessible topology for sterol accepting proteins [3]. If this is the case in sperm cells the oxysterol formation could be a preparative step for sterol depletion.

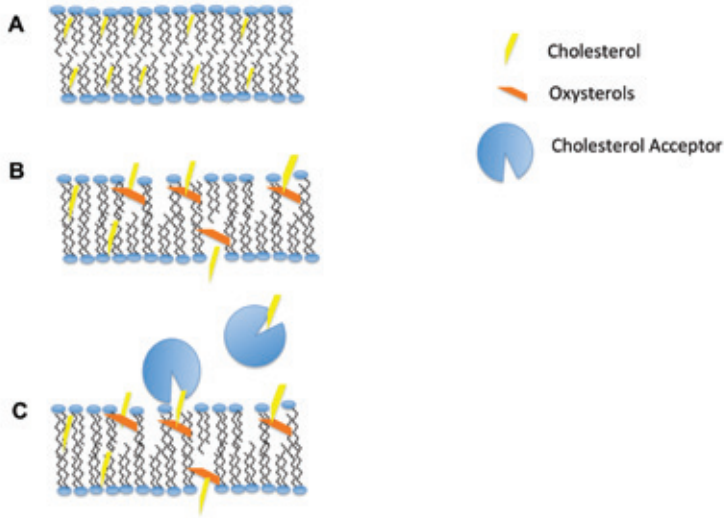

Figure 2. Proposed model of cholesterol efflux mediated by oxysterol-induced changes in the membrane.

A. Model depicting a rigid membrane with cholesterol **B.** When oxysterols are formed they may push the cholesterol partially out of the outer lipid monolayer of the plasma membrane. This mechanism is explained by the parallel position of oxysterols relative to the polar headgroups of phospholipids in the lipid monolayer. **C.** In the presence of oxysterols cholesterol is now accessible to cholesterol acceptors (for IVF this would be albumin). Active cholesterol may also be preferentially transported by sterol transporter proteins such as the ATP-binding cassette transporters ABCA-1, 7, 17 and ABCG-1 [6, 7]. Image is adapted from [41]

Chapter 2 and 3 explore the formation of oxysterols and its relation to cholesterol depletion from sperm cells membrane during capacitation. Sterol depletion during IVF procedures is routinely and commercially performed by albumin. However, it is not clear how cholesterol is provided for specific acceptance by albumin and likely specialized proteins involved in reverse sterol transport are required to achieve this. These proteins could hypothetically also facilitate the reverse transport of cholesterol in sperm. One group of sterol transporters that has been identified in mouse sperm is the ATP-binding cassette transporters ABCA-1, 7, 17 and ABCG-1 [6, 7]. Interestingly, knock-out mice for the ATP-binding cassette transporters have been shown to be infertile [8-10], showing their importance in fertilization processes. Another protein that is involved in reverse cholesterol transport is SRB-1 [11] but its presence on sperm has not been established yet. Interestingly, knock-out mice for SRB-1 are also infertile [12], at least suggesting an important role for these proteins in mammalian fertilization.

Future experiments should focus on identifying other sterol transport proteins as mentioned in the paragraphs above. Using antibodies against the aforementioned sterol transporters could be a tool to identify these proteins in sperm cells. Another option that could be explored is to replace albumin by means of expressing sterol-depleting proteins, such as OBP, and to study their effect on sterol efflux on sperm with the aim of elucidating the mechanism of sterol extraction during capacitation. For instance, molecular biological tools can be used to modify proteins of interest in order to manipulate the efficiency of sterol depletion. One advantage of replacing albumin with *in vitro* produced proteins is that more standardized protein material (from pathogen free cultures such as yeast or bacteria) can be used for IVF with minimal risk of contamination with bio-hazardous materials. As component extracted from blood, albumin is not chemically defined and could bear microbes such as viruses. In addition, each new batch of albumin is a cause for inter-experimental variation and has intrinsic variations in efficiency on sperm activation and IVF.

PART 2: THE REMOVAL OF GPI-ANCHORED PROTEINS AND THEIR ROLE IN FERTILIZATION

In **chapter 4** the involvement of GPI-anchored proteins in sperm capacitation and *in vitro* fertilization was investigated. GPI-anchored proteins are inserted in the membrane via a conserved glycolipid anchor (Figure 3). As a consequence a GPI-anchored protein is covalently attached to the outer lipid monolayer of the sperm cell plasma membrane (Figure 3). This class of membrane proteins is described to have a preference for residing in cholesterol-rich domains [15]. Cholesterol-rich domains are also termed membrane rafts and possess low lateral fluidity of lipids when compared to non-raft membranes [16, 17]. It is thought that the membrane fluidity changes in the sperm cell membrane and that cholesterol extraction is necessary for proper microdomain formation (see **chapter 3**). The formed microdomain in turn is hypothesized to result in a functional ZP binding complex (see **chapter 1,** [18]).

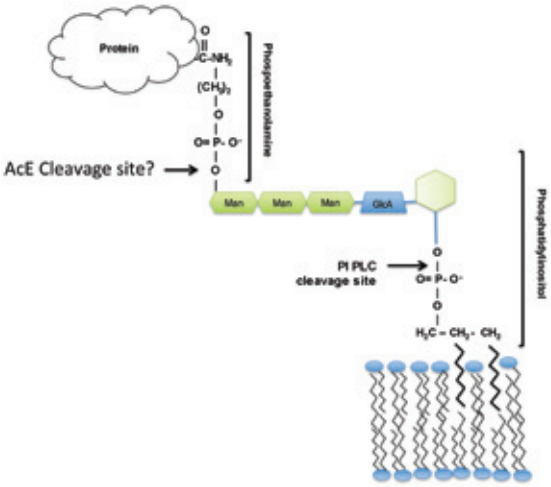

Figure 3. Schematic overview of a GPI-anchored protein and the cleavage site of PI-PLC. The cleavage site of the AcE is still not exactly known but it is expected to cleave somewhere close to the mannose residues near the GPI anchor [25].

The exact role of GPI-anchored proteins in the above-described processes is still elusive, despite the fact that these proteins are highly enriched in the ZP binding area of capacitated sperm (**chapters 1 and 3**). It is known that GPI-anchored proteins are involved in the protection of sperm in the genital tract [19-23]. However, recent reports showed that sperm GPI-anchored proteins also play a role in the recognition of the ZP [5]. For example, PH-20 is known to have hyaluronidase activity, which enables sperm cells to penetrate the ZP [24, 25]. Interestingly, there are reports in literature describing a role of a testis specific angiotensin-converting enzyme (AcE), which is capable of cleaving of GPI-anchored proteins from sperm cells. Kondoh et al. reported that knock-out mice lacking this protein were infertile [25]. This suggests that shedding of GPI-anchored proteins is an important step for sperm cell in order to gain fertilizing competence [25]. **Chapter 4** revealed that there is also spontaneous release of GPI-anchored proteins CD55 and CD52 under the influence of bicarbonate. Both are members of a family of proteins involved in protecting cells from being attacked by the immune system [21, 26]. These results might imply that *in vivo* sperm release these proteins progressively while migrating through the female genital tract, with increasing concentrations of bicarbonate higher up the tract. In turn the membrane is rearranged in such a way that the surface of sperm has a fully competent apical ridge which is the specific surface site for ZP recognition and penetration (see also **chapters 1 and 3**).

An alternative way for *in vitro* release of GPI-anchored proteins from the sperm surface is to treat sperm cell suspensions with PI-PLC (**chapter 4)**. PI-PLC treatment caused an aggregation of flotillin-1 in the apical ridge area of the sperm head in absence of bicarbonate. This suggests that PI-PLC mediated loss of GPI-anchored proteins induces a similar lateral aggregation of lipid

rafts to the apical ridge area as was induced by bicarbonate and that both treatments elicit this by GPI-anchored protein removal. Full capacitation in presence of PI-PLC probably leads to excessive removal of GPI-anchored proteins, which turned out to be destructive for sperm. However, in absence of albumin, bicarbonate or both, PI-PLC induced several other capacitation-like responses in sperm cells such as increased protein tyrosine phosphorylation and increased hyperactivated motility. This shows that regulated removal of GPI-anchored proteins may be required in order to prepare sperm cells for proper interactions with the cumulus oocyte complexes at the site of fertilization. Beyond the aforementioned endogenous enzyme AcE, which has been reported to cleave GPI-anchored proteins on sperm cells, it is possible that *in vivo* sperm cells migrating through the uterus and oviduct will interact with other surface modifying extracellular compounds such as metalloproteinases [27-29]. Therefore, it is of great importance for future studies to investigate whether other extracellular modifying enzymes are present on the sperm surface and/or are present in the female genital tract. Subsequent studies could investigate the role of these enzymes in sperm cell activation and the subsequent binding of sperm to the ZP.

PART 3: ULTRASTRUCTURAL ANALYSIS OF THE SPERM CELL SURFACE DURING CAPACITATION AND AFTER THE INDUCTION OF THE ACROSOME REACTION

In **chapter 5** surface phenomena on sperm were visualized in high detail by wet mount detection of Superfrost glass immobilized fixed sperm with AFM. When compared to control treated sperm a partial stripping of the glycocalyx (probably in part due to processes described in **chapter 4)** was noted during capacitation. In responsive cells a deep and flattened subdomain of the equatorial region (aEqS) was noted and the entire aEqS was filled with surface particles that were hexagonally arranged with an inter-particle distance of 17 nm. A hexagonal structure was observed in the aEqS before in the mid 1970s by freeze fracture in sperm of different mammals [30][31] indicating that the particles are intrinsic transmembrane proteins. These studies also revealed that the hexagonal arrangement was already detected at the trans membrane level in boar sperm cells prior to capacitation induction. The wet mount AFM allowed us to observe at which stage these hexagonal organized transmembrane proteins were exposed to the sperm surface. Our results indicated that interacting extrinsic membrane proteins were covering the hexagonal arranged membrane proteins and that therefore the structure was hidden for cantilever detection in control sperm cell. Sperm cell capacitation resulted in the removal of these extracellular proteins and thus in the exposure of the hexagonal structures allowing cantilever tip detection.

When capacitated sperm were subsequently induced to undergo the acrosome reaction with a Ca^{2+} ionophore, the entire hexagonal arranged surface of the aEqS fused in a specific manner with the underlying outer acrosomal membrane. Fingerlike mixed membrane tubules with a diameter of 50 nm and a length of approximately 1 µm appeared in the entire aEqS. The tip of these membrane

fenestrations was at the edge of the aEqS and the pre-equatorial surface area. The bases of the fenestrations were attached to the still unfused plasma membrane and outer acrosomal membrane of the EqSS. At the pre-equatorial surface area the plasma membrane and the outer acrosomal membrane fused to form mixed vesicles that are shed off the sperm cell. It is interesting to note that the membrane fenestrations are an active site of mixing membrane components of both the sperm plasma membrane and the outer acrosomal membrane. This leads to a highly efficient exposure of outer acrosomal membrane components at the aEqS, which is the specific part of the sperm cell surface involved in the fertilization fusion with the egg's plasma membrane. For instance, the exposure of GM-1 may be involved in membrane fusion related processes [32-34]. The fusion machinery leading to the fertilization of the oocyte is largely unknown but it has been hypothesized that it may resemble the machinery involved in entry of membrane enveloped viruses into the cytosol of target cells (**chapter 1**, [35]). An antibody raised against soluble sH5(3) domain of haemagglutinin protein trimerization) was able to block virus entry into host cells [36]. In **chapter 5** the binding of this antibody to the aEqS of acrosome reacted cells was demonstrated. The antibody essentially blocked *in vitro* fertilization while control sera did not inhibit *in vitro* fertilization. The antibody also reduced secondary zona binding of acrosome reacted sperm cells but did not influence capacitation, inducibility of acrosome reactions, or the recognition of the zona pellucida. The proteins recognized by the antibody were excised from SDS-PAGE gels and were subjected to proteomic analysis. A zona binding protein as well as an intra-acrosomal membrane protein known to be important for fertilization were identified. In addition a collagen alpha chain was identified. Collagen is a very stringently organized trimeric protein [37] and it is tempting to speculate that the trimerization domain of collagen has alignment similarities with the trimerization domain involved in the hexagonal particle organization observed in the aEqS.

How this relates to the reorganization of this area by elevated intracellular Ca^{2+} levels during the induced acrosome reaction is unknown. It is plausible that a Ca^{2+}-dependent reorganization of the hexagonal network allows membrane tubular fenestrations as observed in **chapter 5**. Future research should focus on the identity of the hexagonal aEqS protein and its involvement in formation of the fenestrations. Another relevant area of investigation would be to study whether the fenestrations are involved in the fertilization fusion: the tips of these membrane tubules have a high membrane curvature that is considered to be favourable for forming non-bilayer fusion structures and hemi-fusion structures [38].

In addition to the exposure of acrosomal membrane proteins at the aEqS (**chapter 5**) it has recently been described in literature that the fusion process of sperm with the oocytes membrane involves tetraspanin protein CD9. This protein is not present at the surface of sperm cells but resides in the plasma membrane of oocytes. It has been shown that CD9 enhances membrane fusion between muscle cells and promotes viral infection in some cells. Interestingly, it has been reported that oocytes deficient of CD9 in mice no longer were able to properly fuse with sperm [39]. It has been hypothesized that CD9 performs its function in the vicinity of the fusion site of oocyte and sperm

by changing the rearrangement of microvilli and resulting in successful assembly of an active molecular fusion complex [39]. Ito et al [40] reported CD9 in the acrosome of mouse sperm and its surface exposure in the aEqS after the acrosome reaction. However, in agreement with others, our preliminary experiments with antibodies directed against CD9 using Western blot analysis did not reveal the presence of CD9 on boar sperm. It might be that sperm cells contain homologues of CD9, which have not yet been identified but share similar characteristics as tetraspanin CD9. The combined finding that immunized sera against a hemagglutinin trimerization domain block fertilization and the finding that tetraspanins are involved may indicate that comparison of gamete fusion and viral fusion to host cell membrane can lead to identifying new molecular players involved in the fusion of sperm with the oocyte.

In summary, in this thesis the modifications and dynamics of sperm surface components have been investigated. It appears that bicarbonate-induced and ROS-dependent formation of oxysterols allows efficient sterol depletion of responsive sperm cells. These processes are required for fertilization. During such incubations a spontaneous removal of extracellular matrix components is noted. The removal of GPI anchored proteins is required for activation of sperm cell motility and receptivity for recognizing the zona pellucida and subsequent induction of the acrosome reaction. With wet mount AFM, the stripping of extracellular matrix components at the aEqS uncovered a hexagonal arranged transmembrane structure. When the acrosome reaction was induced, this specific area fused with the underlying outer acrosomal membrane to form 1 µm long 50 nm diameter membrane tubules attached to the EqSS. How the capacitation-dependent lipid- and protein- modifications coincide with removal of sperm surface components, with exposure of the hexagonal structure in the aEqS and with membrane fenestrations at the aEqS during the acrosome reaction is subject of future research.

REFERENCES

1. Visconti PE, Ning X, Fornés MW, Alvarez JG, Stein P, Connors SA, Kopf GS. Cholesterol Efflux-Mediated Signal Transduction in Mammalian Sperm: Cholesterol Release Signals an Increase in Protein Tyrosine Phosphorylation during Mouse Sperm Capacitation. Dev Biol 1999; 214:429-443.

2. Olkkonen VM, Hynynen R. Interactions of oxysterols with membranes and proteins. Mol Aspects Med 2009; 30:123-133.

3. Massey JB. Membrane and protein interactions of oxysterols. Curr Opin Lipidol 2006; 17:296-301.

4. Vejux A, Malvitte L, Lizard G. Side effects of oxysterols: cytotoxicity, oxidation, inflammation, and phospholipidosis. Brazilian Journal of Medical and Biological Research 2008; 41:545-556.

5. van Gestel RA, Brewis IA, Ashton PR, Helms JB, Brouwers JF, Gadella BM. Capacitation-dependent concentration of lipid rafts in the apical ridge head area of porcine sperm cells. Mol Hum Reprod 2005; 11:583-590.

6. Morales CR, Marat AL, Ni X, Yu Y, Oko R, Smith BT, Argraves WS. ATP-binding cassette transporters ABCA1, ABCA7, and ABCG1 in mouse spermatozoa. Biochem Biophys Res Commun 2008; 376:472-477.

7. Ban N, Sasaki M, Sakai H, Ueda K, Inagaki N. Cloning of ABCA17, a novel rodent sperm-specific ABC (ATP-binding cassette) transporter that regulates intracellular lipid metabolism. Biochem J 2005; 389:577-585.

8. Aiello RJ, Brees D, Francone OL. ABCA1-deficient mice: insights into the role of monocyte lipid efflux in HDL formation and inflammation. Arterioscler Thromb Vasc Biol 2003; 23:972-980.

9. Tarling EJ, Bojanic DD, Tangirala RK, Wang X, Lovgren-Sandblom A, Lusis AJ, Bjorkhem I, Edwards PA. Impaired development of atherosclerosis in Abcg1-/- Apoe-/- mice: identification of specific oxysterols that both accumulate in Abcg1-/- Apoe-/- tissues and induce apoptosis. Arterioscler Thromb Vasc Biol 2010; 30:1174-1180.

10. Tarling EJ, Edwards PA. Dancing with the sterols: critical roles for ABCG1, ABCA1, miRNAs, and nuclear and cell surface receptors in controlling cellular sterol homeostasis. Biochim Biophys Acta 2012; 1821:386-395.

11. Nieland TJ, Chroni A, Fitzgerald ML, Maliga Z, Zannis VI, Kirchhausen T, Krieger M. Cross-inhibition of SR-BI- and ABCA1-mediated cholesterol transport by the small molecules BLT-4 and glyburide. J Lipid Res 2004; 45:1256-1265.

12. Trigatti B, Rigotti A. Scavenger receptor class B type I (SR-BI) and high-density lipoprotein metabolism: recent lessons from genetically manipulated mice. Int J Tissue React 2000; 22:29-37.

13. Chen H, Cheung MP, Chow PH, Cheung AL, Liu W, O WS. Protection of sperm DNA against oxidative stress in vivo by accessory sex gland secretions in male hamsters. Reproduction 2002; 124:491-499.

14. Bucak MN, Tuncer PB, Sariozkan S, Baspinar N, Taspinar M, Coyan K, Bilgili A, Akalin PP, Buyukleblebici S, Aydos S, Ilgaz S, Sunguroglu A, Oztuna D. Effects of antioxidants on post-thawed bovine sperm and oxidative stress parameters: antioxidants protect DNA integrity against cryodamage. Cryobiology 2010; 61:248-253.

15. Garner AE, Smith DA, Hooper NM. Sphingomyelin chain length influences the distribution of GPI-anchored proteins in rafts in supported lipid bilayers. Mol Membr Biol 2007; 24:233-242.

16. Simons K, Toomre D. Lipid rafts and signal transduction. Nat Rev Mol Cell Biol 2000; 1:31-39.

17. Lingwood D, Simons K. Lipid Rafts As a Membrane-Organizing Principle. Science 2010; 327:46-50.

18. Boerke A, Tsai PS, Garcia-Gil N, Brewis IA, Gadella BM. Capacitation-dependent reorganization of microdomains in the apical sperm head plasma membrane: Functional relationship with zona binding and the zona-induced acrosome reaction. Theriogenology 2008; 70:1188-1196.

19. Koyama K, Hasegawa A, Komori S. Functional aspects of CD52 in reproduction. J Reprod Immunol 2009; 83:56-59.

20. Flori F, Ermini L, La Sala GB, Nicoli A, Capone A, Focarelli R, Rosati F, Giovampaola CD. The GPI-anchored CD52 antigen of the sperm surface interacts with semenogelin and participates in clot formation and liquefaction of human semen. Mol Reprod Dev 2008; 75:326-335.

21. van Beek J, van Meurs M, 't Hart BA, Brok HP, Neal JW, Chatagner A, Harris CL, Omidvar N, Morgan BP, Laman JD, Gasque P. Decay-accelerating factor (CD55) is expressed by neurons in response to chronic but not acute autoimmune central nervous system inflammation associated with complement activation. J Immunol 2005; 174:2353-2365.

22. Donev RM, Sivasankar B, Mizuno M, Morgan BP. The mouse complement regulator CD59b is significantly expressed only in testis and plays roles in sperm acrosome activation and motility. Mol Immunol 2008; 45:534-542.

23. Perez de la Lastra JM, Harris CL, Hinchliffe SJ, Holt DS, Rushmere NK, Morgan BP. Pigs Express Multiple Forms of Decay-Accelerating Factor (CD55), All of Which Contain Only Three Short Consensus Repeats. J Immunol 2000; 165:2563-2573.

24. Cherr GN, Yudin AI, Overstreet JW. The dual functions of GPI-anchored PH-20: hyaluronidase and intracellular signaling. Matrix Biol 2001; 20:515-525.

25. Kondoh G, Tojo H, Nakatani Y, Komazawa N, Murata C, Yamagata K, Maeda Y, Kinoshita T, Okabe M, Taguchi R, Takeda J. Angiotensin-converting enzyme is a GPI-anchored protein releasing factor crucial for fertilization. Nat Med 2005; 11:160-166.

26. Mizuno M, Donev RM, Harris CL, Morgan BP. CD55 in rat male reproductive tissue: Differential expression in testis and expression of a unique truncated isoform on spermatozoa. Mol Immunol 2007; 44:1613-1622.

27. Ferraro GB, Morrison CJ, Overall CM, Strittmatter SM, Fournier AE. Membrane-type matrix metalloproteinase-3 regulates neuronal responsiveness to myelin through Nogo-66 receptor 1 cleavage. J Biol Chem 2011; 286:31418-31424.

28. Saengsoi W, Shia WY, Shyu CL, Wu JT, Warinrak C, Lee WM, Cheng FP. Detection of matrix metalloproteinase (MMP)-2 and MMP-9 in canine seminal plasma. Anim Reprod Sci 2011; 127:114-119.

29. Tentes I, Asimakopoulos B, Mourvati E, Diedrich K, Al-Hasani S, Nikolettos N. Matrix metalloproteinase (MMP)-2 and MMP-9 in seminal plasma. J Assist Reprod Genet 2007; 24:278-281.

30. Friend DS, Fawcett DW. Membrane differentiations in freeze-fractured mammalian sperm. J Cell Biol 1974; 63:641-664.

31. Ohta T, Matsuda M. Sperm morphology and IMP distribution in membranes of spermatozoa of cyprinid fishes II. Cell Struct Funct 1995; 20:293-300.

32. Moreno-Altamirano MMB, Aguilar-Carmona I, Sánchez-García FJ. Expression of GM1, a marker of lipid rafts, defines two subsets of human monocytes with differential endocytic capacity and lipopolysaccharide responsiveness. Immunology 2007; 120:536-543.

33. Chinnapen DJ, Hsieh WT, te Welscher YM, Saslowsky DE, Kaoutzani L, Brandsma E, D'Auria L, Park H, Wagner JS, Drake KR, Kang M, Benjamin T, Ullman MD, Costello CE, Kenworthy AK, Baumgart T, Massol RH, Lencer WI. Lipid sorting by ceramide structure from plasma membrane to ER for the cholera toxin receptor ganglioside GM1. Dev Cell 2012; 23:573-586.

34. Masco D, Flott B, Seifert W. Astrocytes in cell culture incorporate GM1 ganglioside. Glia 1989; 2:231-240.

35. Gadella BM, Evans JP. Membrane fusions during mammalian fertilization. Adv Exp Med Biol 2011; 713:65-80.

36. Cornelissen LA, de Vries RP, de Boer-Luijtze EA, Rigter A, Rottier PJ, de Haan CA. A single immunization with soluble recombinant trimeric hemagglutinin protects chickens against highly pathogenic avian influenza virus H5N1. PLoS One 2010; 5:e10645.

37. Rasmussen M, Jacobsson M, Bjorck L. Genome-based identification and analysis of collagen-related structural motifs in bacterial and viral proteins. J Biol Chem 2003; 278:32313-32316.

38. Zeniou-Meyer M, Zabari N, Ashery U, Chasserot-Golaz S, Haeberle AM, Demais V, Bailly Y, Gottfried I, Nakanishi H, Neiman AM, Du G, Frohman MA, Bader MF, Vitale N. Phospholipase D1 production of phosphatidic acid at the plasma membrane promotes exocytosis of large dense-core granules at a late stage. J Biol Chem 2007; 282:21746-21757.

39. Kaji K, Oda S, Shikano T, Ohnuki T, Uematsu Y, Sakagami J, Tada N, Miyazaki S, Kudo A. The gamete fusion process is defective in eggs of Cd9-deficient mice. Nat Genet 2000; 24:279-282.

40. Ito C, Yamatoya K, Yoshida K, Maekawa M, Miyado K, Toshimori K. Tetraspanin family protein CD9 in the mouse sperm: unique localization, appearance, behavior and fate during fertilization. Cell Tissue Res 2010; 340:583-594.

41. Olsen BN, Schlesinger PH, Ory DS, Baker NA. Side-chain oxysterols: from cells to membranes to molecules. Biochim Biophys Acta 2012; 1818:330-336.

Nederlandse samenvatting

Dankwoord

Curriculum Vitae

List of publications

NEDERLANDSE SAMENVATTING

De bevruchting van de eicel door de spermacel is een proces dat bestaat uit verschillende opeenvolgende stappen. *In vivo* begint dit proces met de reis van de spermacel naar de eicel. De activering van de spermacel vindt plaats gedurende zijn reis door het vrouwelijk geslachtsorgaan. Dit proces wordt de sperma-capacitatie genoemd. Voor het herkennen en penetreren van het omhulsel van de eicel (een extracellulaire matrix, de zogenaamde zona pellucida (ZP)) vormt de spermacel tijdens de capacitatie functionele eiwit- en lipiden complexen aan zijn oppervlak. Nadat de spermacel de ZP heeft herkend, wordt er een kettingreactie in gang gezet die het mogelijk maakt voor de spermacel om de ZP te penetreren (de acrosomale reactie) en zo uiteindelijk te kunnen fuseren met het oppervlak van de eicel. Om dit proces in het laboratorium tot stand te brengen, wordt gebruik gemaakt van *in vitro* fertilisatie (IVF). Deze methode is erg succesvol, maar het is niet exact bekend welke moleculaire processen zich afspelen tijdens de spermacel-activering en -fusie met de eicel. Hierdoor is het moeilijk te achterhalen wat er mis gaat indien IVF niet succesvol is. Dit proefschrift levert een bijdrage aan de kennis over deze moleculaire processen door de spermacel en zijn oppervlakteveranderingen voorafgaand aan de fertilisatie te bestuderen.

In hoofdstuk 1 van dit proefschrift wordt uiteengezet welke moleculaire spelers en processen betrokken zijn bij het proces van fertilisatie. In hoofdstuk 2 en 3 wordt de rol van cholesterol (en desmosterol) bij capacitatie onderzocht. In hoofdstuk 4 wordt de rol van GPI-verankerde eiwitten op gecapaciteerd sperma en de invloed van het verlies van GPI-verankerde eiwitten op het proces van fertilisatie onderzocht. Hoofdstuk 5 bestudeert het oppervlak van de spermacel tijdens capacitatie en de acrosomale reactie op ultrastructureel niveau. Hierbij wordt vooral de equatoriale regio van de spermacel bestudeerd waar de uiteindelijke fusie van de spermacel plaatsvindt met de eicel.

Een van de belangrijkste processen die optreden tijdens de activering van de spermacel is de extractie van cholesterol en desmosterol uit de plasmamembraan van de spermacel. Desmosterol is een precursor van cholesterol en is in hogere concentraties aanwezig in de spermacel dan in andere celtypen, met uitzondering van de hersencellen. Zonder de extractie van cholesterol en desmosterol is de spermacel niet in staat te fuseren met de eicel. Het is echter niet bekend waarom dit zo is en hoe de sterolextractie tot stand komt.

Recent is duidelijk geworden dat sterolen in de membranen van cellen kunnen worden geoxideerd en dat oxysterolen effecten kunnen hebben op de organisatie van de membranen waarin ze aanwezig zijn. Er kunnen via steroloxidatie een aantal verschillende moleculaire species van oxysterolen worden gevormd. Tot dusverre was onduidelijk of oxysterolen in spermacellen worden gevormd en of dit samenhangt met de extractie van sterolen uit het spermaceloppervlak gedurende *in vitro* capacitatie. In hoofdstuk 2 is daarom onderzocht of er zich in stierenspermacellen oxysterolen bevinden en of deze worden gevormd tijdens spermacel-behandelingen, zoals routinematig gedaan wordt bij het invriezen van stierensperma of bij *in vitro* fertilisatie ten behoeve van embryo productie. Daarnaast is bestudeerd of oxysterolen geëxtraheerd kunnen worden uit het oppervlak van de geïncubeerde spermacelsuspensies.

Voor de detectie van oxysterolen is gebruik gemaakt van hoge druk vloeibare chromatografie, ofwel "high pressure liquid chromatography" (HPLC) en massaspectrometrie (MS). Geïncubeerde spermacelsuspensies werden afgedraaid en lipiden werden geëxtraheerd uit de spermacelfractie en uit het incubatiemedium. Zowel cryopreservering van stierenspermacellen als de *in vitro* capacitatie procedure leidde tot de vorming van oxysterolen ten opzichte van vers stierensperma. In gecapaciteerde spermacellen werd een hogere oxysterolvorming waargenomen in vergelijking met stierenspermacellen die waren ingevroren en ontdooid. Interessant is dat er alleen na spermacel capacitatie sterol depletie van het spermaceloppervlak werd waargenomen. Dit geeft aan dat alleen de vorming van oxysterolen aan het spermaceloppervlak niet voldoende is om de steroldepletie op gang te brengen en dat andere factoren bij het proces van spermacelcapacitatie een -mogelijk aanvullende- rol spelen. Een ander verschil is dat spermacelcapacitatie een andere samenstelling van moleculaire species van de oxysterolen induceert dan het invriezen en ontdooien van stierenspermacellen. Deze verschillen kunnen mogelijk gerelateerd zijn aan het wel of niet optreden van steroldepletie aan het oppervlak van stierenspermacellen onder deze twee condities. De resultaten vormen een aanzet voor vervolgonderzoek naar de aanwezigheid van specifieke enzymen die oxysterolvorming tijdens spermacel capacitatie faciliteren of naar specifieke pro-oxidatie en anti-oxidatie processen die in de spermacel aanwezig zijn. Zulke kennis kan worden gebruikt voor zowel het minimaliseren van de negatieve effecten die oxysterol formatie heeft tijdens invriezen van spermacellen als het optimaliseren van oxysterolvorming bij de spermacelcapacitatie. Hoofdstuk 3 onderzoekt het proces van steroldepletie en de relatie met oxysterol vorming bij varkens- en muizenspermacellen. In beide soorten leidde capacitatie tot de vorming van oxysterolen en de vorming van oxysterolen bleek strikt bicarbonaat afhankelijk te zijn. Bicarbonaat is als capacitatiefactor tezamen met albumine belangrijk tijdens IVF. Tijdens de IVF incubatie induceren beide moleculen synergistisch sperma-hypermotiliteit en eiwit tyrosine-fosforylering. Pro-oxidanten bleken op een bicarbonaat-onafhankelijke manier de formatie van oxysterolen te induceren, terwijl hydrofobe antioxidanten de oxysterolformatie blokkeerden. Alleen na *in vitro* capacitatie bleek naast oxysterol vorming ook sterolextractie van het spermaceloppervlak op te treden. De capacitatie-afhankelijke sterolextractie is een van de stappen die nodig is in spermacellen om hypermotiliteit en een verhoogde eiwit tyrosinefosforylering te veroorzaken. De extractie van het cholesterol van het spermaceloppervlak induceert een laterale herverdeling van spermacel plasmamembraan componenten en verhoogt de vloeibaarheid in dit membraan. Deze stappen zijn nodig voor een optimale spermacelbinding aan de ZP. Tijdens IVF experimenten, uitgevoerd in de aanwezigheid van hydrofobe antioxidanten, werd niet alleen de oxysterolformatie geblokkeerd, maar ook de bevruchting. Interessant genoeg bleek dat er ondanks de blokkering van de eicelbevruchting geen remming was van spermacel binding aan de ZP. Hieruit kan mogelijk worden geconcludeerd dat de spermacelcompetentie afhankelijk is van oxysterolformatie om te fuseren met de oolemma, terwijl de spermacel binding aan de zona pellucida dat niet is.

In hoofdstuk 3 werden spermacelsuspensies in aanwezigheid van een oxysterolbindend eiwit (OBP) geïncubeerd (geproduceerd door een bacterie cultuur die getransfecteerd was met een plasmide dat codeert voor OBP). Tijdens deze incubatie bleek dat OBP capacitatie-afhankelijke processen induceerde: een verhoging van eiwit tyrosine-fosforylering, een verhoogde beweeglijkheid en een laterale herverdeling van moleculen op de kop van de spermacel. De interactie van OBP met het oppervlak van de spermacel verminderde het gehalte van oxysterolen in spermacellen met meer dan 50%. OBP induceerde echter ook de premature acrosomale reactie van geïncubeerde spermacellen. Een interessante bevinding is dat de OBP-geïncubeerde spermacellen niet in staat waren de eicel te bevruchten en dat de cholesterolextractie niet plaatsvond. Het lijkt daarom aannemelijk dat OBP zorgt voor de remming van oxysterolvorming in capaciterende spermacellen en verder niet betrokken is bij de extractie van sterolen van het spermaceloppervlak. Fysiologisch zal OBP dan ook niet bij de fertilisatie betrokken zijn, omdat dit eiwit in het cytosol aanwezig is en vanuit daar aan oxysterolen aan de cytosolaire zijde van membranen zal binden. In hoofdstuk 3 is een niet-fysiologische OBP incubatie gebruikt om de specifieke rol van oxysterolen te kunnen bestuderen.
Een alternatief voor de verwijdering van (oxy)sterolen van het spermaceloppervlak is de toevoeging van cyclodextrines aan de incubatie media. Hoofdstuk 3 laat zien dat methyl-beta-cyclodextrine (MBCD) een verhoogde eiwit tyrosine-fosforylering en een verhoging van de hypermotiliteit van de spermacel induceert. Het fertiliserend vermogen van de spermacel daalde echter naar 30% in plaats van de normaal geobserveerde 60% (en dat alleen in de conditie waar 2 mM MBCD was gebruikt). Lagere concentraties van MBCD resulteerden niet in de hierboven beschreven effecten en hogere concentraties die zijn gebruikt waren zowel schadelijk voor de spermacel alsmede de eicellen. 2 mM MBCD leidde eveneens tot 30% eicel degeneratie zodat het gebruik van MBCD in een bevruchtingsdruppel met spermacellen en te bevruchten eicellen in routine IVF procedure moet worden afgeraden.
Een van de fysiologische eigenschappen van oxysterolen is dat zij het gedrag van membraan-componenten kunnen beïnvloeden; zo kunnen bepaalde oxysterolen het membraan 'vloeibaarder' maken. Dit is mogelijk omdat oxysterolen additionele polaire hydroxylgroepen bezitten waardoor deze zich horizontaler in het membraan oriënteren. Deze oriëntatie kan een rol spelen in de sterolextractie doordat de vrije cholesterol (die verticaal is georiënteerd) nu mogelijk naar de buitenste lipide monolaag van het plasmamembraan wordt "geduwd" en hierdoor beschikbaar wordt voor acceptatie door sterolacceptor eiwitten.

In hoofdstuk 4 is de rol van GPI-verankerde eiwitten op gecapaciteerde spermacellen bestudeerd. GPI-verankerde eiwitten zijn eiwitten die aan de buitenkant van het membraan verankerd zijn via een geconserveerd glycolipid motief. Deze GPI-verankerde eiwitten hebben een voorkeur voor cholesterolrijke membraandomeinen. De rol van deze GPI-verankerde eiwitten in de processen die leiden tot de bevruchting van de eicel is niet exact bekend. Wel is bekend dat GPI-verankerde eiwitten

sterk verrijkt zijn in het gebied waar de spermacel bindt aan de ZP. Ook is bekend dat sommige GPI-verankerde eiwitten betrokken zijn bij de bescherming van de spermacel in het vrouwelijk geslachtsorgaan. Andere GPI-verankerde eiwitten (zoals PH-20) zijn betrokken bij het herkennen van de ZP van de eicel. Deze herkenning zal leiden tot de ZP-geïnduceerde acrosoomreactie die een spermacel in staat stelt de ZP te penetreren. Het belang van GPI-verankerde eiwitten aan het spermaceloppervlak blijkt uit het volgende: een endogeen spermacelenzym kan GPI-eiwitten van het oppervlak van de spermacel knippen (angiotensin conversion enzyme, AcE), terwijl knock-out mannelijke muizen voor AcE niet in staat waren nakomelingen te krijgen. Deze bevindingen impliceren dat het verwijderen van een deel van de GPI-verankerde eiwitten nodig is voor succesvolle fertilisatie bij muizen. Hoofdstuk 4 laat zien dat GPI-verankerde eiwitten het oppervlak van de spermacel verlaten onder invloed van bicarbonaat. Hoe bicarbonaat dit effect bewerkstelligt, is onduidelijk. Het is mogelijk dat bicarbonaat endogeen AcE activeert en zodoende GPI-verankerde eiwitten losmaakt. Toekomstig onderzoek zal dit moeten uitwijzen.

Een alternatieve manier om GPI-verankerde eiwitten van het oppervlak van spermacellen te verwijderen, is door toevoeging van het phosphatidyl inositol specifieke enzym phospolipase C (PI-PLC). Onderzocht werd welke invloed het knippen van GPI-verankerde eiwitten heeft op de toestand van de spermacel tijdens de capacitatie. Op ongecapaciteerde spermacellen bleek flotillin-1 onder invloed van PI-PLC naar de rand van de kop te migreren. Het is bekend dat eenzelfde migratie plaatsvindt tijdens capacitatie. Incubatie van gecapaciteerde spermacellen met PI-PLC medium resulteerde in celdood. De combinatie van spontane verwijdering van GPI-verankerde eiwitten in een volledig capacitatiemedium (mogelijk via AcE activering) en de extra werking door toevoeging van PI-PLC resulteert mogelijk in een te sterke verwijdering van de extracellulaire matrix van de spermacel en dus in beschadiging van het spermaceloppervlak. Deze resultaten laten zien dat een nauw gereguleerde verwijdering van GPI-verankerde eiwitten mogelijk vereist is voor een goede fertilisatie van de eicel. Naast de verwijdering van GPI-verankerde eiwitten is het mogelijk dat er *in vivo* andere veranderingen plaatsvinden aan het spermaceloppervlak. Deze studie vormt de basis voor vervolgonderzoek naar de functie en effecten van extracellulaire enzymen die verantwoordelijk zijn voor veranderingen van het spermaoppervlak en het klaarmaken van de spermacel voor de fertilisatie.

Hoofdstuk 5 bestudeert veranderingen van ultrastructurele eigenschappen aan het spermaceloppervlak gedurende capacitatie en na inductie van de acrosomale reactie. Het spermaceloppervlak werd bestudeerd door middel van een techniek genaamd "Atomic Force Microscopy" (AFM). Door middel van deze techniek kan het oppervlakte van de spermacel nauwkeurig worden afgetast en een beeld worden gevormd van het oppervlak met een hoge resolutie (nanometers (nm)). AFM liet zien dat in gecapaciteerde cellen in de equatoriale regio een vlakke regio was ontstaan met een hexagonale structuurordening van membraanpartikels die op een afstand van 17 nm van elkaar zijn geordend. Deze structuren zijn weliswaar al aanwezig in ongecapaciteerde spermacellen, maar worden pas geëxposeerd aan het oppervlak van de spermacellen na de capacitatie-afhankelijke verwijdering van extracellulaire componenten.

Tijdens de inductie van de acrosoomreactie vormde zich in deze regio, waar eerst de hexagonale structuur te zien was, vervolgens een vingerachtige membraanstructuur. Deze membraanvingers bevatten een mix van membraancomponenten van het spermaceloppervlak alsmede van de onderliggende acrosomale membraan. Deze membraanvingers hadden een diameter van 50nm en een lengte van 1 µm. De basis van deze membraanvingers zat vast aan de nog niet gefuseerde plasmamembraan en de buitenste acrosomale membraan. De membraanvingers dragen impliciet bij aan het mengen van spermacel plasmamembraancomponenten en acrosomale membraancomponenten. De ontstane membraanvingers zorgen er ook voor dat acrosomale membraancomponenten in de equatoriale regio (aEqS) naar buiten zijn gericht en nu gelokaliseerd zijn in het specifieke gedeelte van het spermaceloppervlak dat fuseert met de plasmamembraan van de eicel. Deze nieuwe structurele inzichten vormen een extra aanknopingspunt in het onderzoek naar de machinerie die moet leiden tot de fertilisatiefusie met de eicel. Het is mogelijk dat acrosomale membraancomponenten hierin een cruciale rol hebben. Naast eiwitten kunnen ook versuikerde lipiden betrokken zijn bij membraanfusie en een voorbeeld daarvan is het ganglioside GM1. Het totale fusiecomplex dat tijdens fertilisatie leidt tot de fusie van de eicel met de spermacel is nog steeds grotendeels onbekend. Er zijn hypotheses die veronderstellen dat het mechanisme van de fertilisatiefusie overeenkomt met de membraanfusie van virussen met een gastcel. Bij het griepvirus speelt het eiwit Haemagglutinine een rol bij de entree van het virus bij zijn gastcel. Haemagglutinine is een trimeer eiwit en tegen het trimerisatiedomein van dit eiwit is een antilichaam opgewekt. Dit antilichaam bleek de *in vitro* fertilisatie van varkenseicellen te blokkeren en in mindere mate de spermacel/ZP interacties te remmen. Op western blots bleek het antilichaam een spermaceleiwit te herkennen. De corresponderende eiwitband die herkend werd door het antilichaam is door middel van eiwitanalyse verder onderzocht. Er werd een zona-bindend eiwit herkend alsmede een intra-acrosomaal membraan eiwit die beiden belangrijk blijken te zijn voor de fertilisatie van de eicel. Daarnaast werd een collageen-eiwit herkend. Collageen is tevens een trimeer eiwit met een eiwittrimerisatie domein. Mogelijk vertoont dit domein epitoop alignment met het trimerisatiedomein in het heamagglutinine. Het is verleidelijk om te speculeren dat dit eiwit ook betrokken is bij de hexagonale organisatie van het equatoriale segment. Verder onderzoek kan focussen op de rol van deze eiwitten bij de fusie van de spermacel met de eicel.

CONCLUSIE

Het beschreven onderzoek in dit proefschrift heeft laten zien dat bicarbonaat geïnduceerde oxysterolvorming nodig is om sterolextractie uit het spermaceloppervlak mogelijk te maken en dat dit proces nodig is voor succesvolle fertilisatie van de eicel. Daarnaast induceert bicarbonaat de verwijdering van een subgroep van GPI-verankerde eiwitten van het oppervlak, terwijl andere GPI-verankerde eiwitten een belangrijke rol spelen bij de herkenning van de ZP. Met behulp van AFM is geobserveerd dat het oppervlak van de spermacel verandert en dat er een hexagonale eiwitstructuur in de equatoriale regio detecteerbaar wordt in gecapaciteerde spermacellen. Deze hexagonale

eiwitstructuur was niet detecteerbaar in niet-gecapaciteerde spermacellen. Tijdens de acrosomale reactie verandert de equatoriale regio compleet. Er ontstaat een mix van het buitenste acrosomale membraan met de plasmamembraan en er ontstaan tubulaire structuren die 1 µm lang en 5 nm in diameter zijn. Deze vingerachtige structuur is aanwezig in de regio waarin de uiteindelijke fusie van de spermacel met de eicel plaatsvindt. Het beschreven onderzoek biedt aanknopingspunten voor vervolgonderzoek naar verbeteringen van huidige IVF technieken en naar het identificeren van mogelijke oorzaken van infertiliteit.

DANKWOORD

Eindelijk het doel bereikt; mijn boekje wordt gedrukt! Wat onwerkelijk na al die jaren van onderzoek op het lab, koerswijzigingen, mooie en soms onverwachte resultaten en het schrijven en publiceren van artikelen. Eigenlijk geloof ik zelfs nu nog steeds niet dat het is afgelopen. Wellicht dringt het pas na 27 juni tot me door; als ik mijn verdediging achter de rug heb en ik in de avonden of het weekend niets meer aan mijn promotie hoef te doen. Ik kijk hier nu erg naar uit, maar geloof ook dat ik mijn AIO-periode nog zal gaan missen.

Er zijn veel mensen die me hebben geholpen bij dit eindpunt te komen. Ik wil er hier in het dankwoord een aantal in het bijzonder noemen.

Allereerst Bart en Bernd, bedankt voor het vertrouwen dat ik de juiste persoon was voor dit traject. Bart, bedankt dat je, toen het allemaal meer tijd nodig had dan verwacht, me het vertrouwen bent blijven geven dat het ooit allemaal tot een boekje zou leiden. Menig vrijdag hebben we de voortgang besproken, de koers gewijzigd of juist dingen afgetikt. We gaan onze vrijdagen nu met andere zaken vullen, maar laten we nog een keer afspreken om met een kop koffie terug te kijken en ervan te genieten dat het af is! Bernd, bedankt voor het ondersteunen van de belangrijke beslismomenten en op gezette tijden richting geven aan het onderzoek. Zonder de commitment van jullie alle twee was het niet gelukt.

Ben Colenbrander, we hebben elkaar alleen in mijn 1e jaar gesproken; wat jammer dat we vanwege je pensioen niet meer met elkaar hebben kunnen samenwerken.

Voor de collega's van Farmacie, Ellen, Frits, Joris, Rene en Wim; bedankt voor het uitleggen van het principe van 'imprinting' aan een biochemicus. Wat jammer dat de technische hobbels in het traject groter bleken dan gedacht en we onze samenwerking anders hebben moeten invullen. Ellen bedankt voor de gezellige trip naar Münster en later Berlijn.

Vele uren heb ik doorgebracht op de AIO kamer. Jason, Nuria, Nicole en Rachid bedankt voor de gezelligheid en zowel de inhoudelijke als mentale ondersteuning.
Jason, you not only were my colleague, but you have also become my friend. Unfortunally, you are now living in Boston with your whole family, which means we do not speak each other that much anymore. I really appreciate that you will be attending the promotion as my paranymph. I once got a Chinese wisdom sign from you, which translated into 'Confidence'. You were right. It was exactly what I needed!
Nicole, we zijn ongeveer gelijktijdig gestart aan ons promotietraject en ik heb zo dus dichtbij jouw promotie gestaan. Je optimistisme en vrolijke noot gedurende ons traject zal ik niet vergeten! Dank je wel dat ik bij jouw verdediging een van je paranimfen mocht zijn.
Nuria, we had lots of fun and as a true post-doc mentor you gave advice during my PhD. Thanks for this! I'll miss having you there at my promotion.
Jason, Nuria and Nicole lets try to arrange a reunion in the near future!

Jos, Jeroen en Chris bedankt voor het helpen bij de massaspectrometer en het beantwoorden van mijn vragen. Arend, Edita en Eric bedankt voor de gezelligheid als ik weer aan kwam waaien bij het JDV-gebouw, de deskundige uitleg, het helpen bij het testen van beweeglijkheid parameters en het uitvoeren van IVF experimenten.

Alle andere biochemie en celbiologie collega's Mijke, Wangsa, Mokrish, Mehdi, Koen, Johanna, Ruud, Martijn, Marianne, Els, Toine, Francesca en Petra; bedankt voor de gezelligheid in de koffiehoek onder het genot van de vele bakjes koffie en verjaardagstaarten en tijdens andere buiten lab activiteiten.

Ian Brewis, I appreciated your input and advice! I would also like to thank you for bringing samples for MS analysis to Cardiff and critically reading one of my thesis chapters.

Vesa Olkkonen, thank you for giving the plasmids for the oxysterol binding proteins and the expression protocol and for critically reading the manuscript.

Christian Löbbe, you taught me the AFM and were always willing to give advice about it and the setup of the experiments. Thank you for this.

Gerrianne, Renske en Joost, ik heb jullie met veel plezier begeleid. Gerrianne en Renske bedankt voor het meehelpen met de trips naar het slachthuis om eicellen te verkrijgen. Joost, bedankt voor je enthousiasme en het verzetten van veel werk in je vrije tijd achter de AFM. Succes met je eigen AIO-schap!

Jan Jaap, Stijn, Norbert, Geert-Jan, Ferry, Johan, Ingmar, Daan en mijn collega's op het werk; jullie hebben langs de zijlijn mijn promotie gevolgd. Bedankt voor de keren dat je mijn verhaal met interesse en soms medeleven hebt aangehoord en de keren dat je tactisch mijn promotie even niet ter sprake bracht.
Ingmar, we kennen elkaar al sinds de hogeschool en daar is een mooie vriendschap uit voortgekomen. Samen hebben we heel wat rondjes hardgelopen en gezellige avonden gehad. Dank je wel dat je ook de 27e als paranimf achter me wilt staan. Ik heb straks meer tijd over. Laten we dan weer eens hardlopen of onder het genot van een biertje mooie ideeën bedenken!
Aan de vriendinnen van Iris; ook jullie bedankt voor de interesse in mijn promotietraject en dat jullie via Iris meegeleefd hebben.

Degenen die mijn promotietraject het meest intensief hebben mee gevolgd, zijn mijn familieleden. Lieve pa, ma, Janette en Hjalmar; bedankt voor het bieden van een basis om de dingen te doen die ik wilde bereiken en dat jullie er voor me zijn als ik het nodig heb. Wim, Lia en Merel, ook jullie hebben het hele traject intensief meegeleefd, bedankt hiervoor!

Als laatste maar zeker niet de minste, Iris zonder jou had ik het niet kunnen doen. Het meedenken, helpen en achter mij blijven staan om mijn promotie onderzoek tot een goed eind te brengen heeft ons dichter bij elkaar gebracht. Soms moesten er dingen voor wijken en iedere keer toonde je daar

weer begrip voor. Nu hebben we samen onze zoon Maarten waar we allebei heel veel van genieten. Ik kan me geen toekomst indenken zonder jullie! Ik kijk er naar uit om straks weer meer dingen samen te kunnen doen zonder dat ik 'eigenlijk nog iets aan mijn promotie moet doen'. Op naar heerlijk rustige avonden en weekenden vol andere mogelijkheden!

CURRICULUM VITAE

Arjan Boerke werd geboren op 13 maart 1979 te Zuidelijke IJsselmeerpolders (Lelystad). Na zowel de MAVO als de HAVO te hebben afgerond, verliet hij de middelbare school om in 1997 te starten aan de opleiding Hoger Laboratorium Onderwijs in Utrecht met als studierichting Biochemie. Na een half jaar als analist bij Isogen Lifesciences te hebben gewerkt, startte hij in 2002 aan de Universiteit van Utrecht met de Master voor Drug Innovation bij Chemische Wetenschappen. Gedurende deze Master liep hij 9 maanden stage bij de afdeling Farmacologie onder leiding van dr. Antoon van Oosterhout en dr. Sue Mckay waarbij hij de biologische rol van de receptor L-SIGN in astma onderzocht. Ook deed hij 6 maanden onderzoek bij TNO Preventie en Gezondheid bij de afdeling Biomedisch Onderzoek naar de inductie en suppressie van NF-kappaB bij arteriosclerose onder supervisie van dr. Robert Kleemann. Gedurende zijn Master heeft hij Artikel 9 voor Proefdierkunde gehaald en in 2004 rondde hij zijn Master af met een thesis genaamd 'The possible role of NF-kappaB as a drug target for the treatment of cancer' onder begeleiding van dr. C.J. Beukelman van het departement Medicinale Chemie van de faculteit Farmaceutische Wetenschappen. Na een reis van een half jaar door Zuid-Oost Azië met zijn vriendin Iris Ooms ging hij op zoek naar zijn volgende uitdaging in het onderzoek. Deze vond hij aan de Universiteit van Utrecht. In januari 2006 startte hij als Assistent in Opleiding met het promotieonderzoek waarvan de resultaten staan beschreven in dit proefschrift. Dit onderzoek werd uitgevoerd aan de Universiteit van Utrecht bij de faculteit Diergeneeskunde bij de afdeling Biochemie en Celbiologie onder leiding van dr. Bart Gadella, Prof. dr. Bernd Helms en dr. Rene van Nostrum. Naast zijn promotie was hij actief in het AIO bestuur van het Instituut voor Biomembranen voor de bevordering van interfacultaire contacten tussen AIO's met als gemeenschappelijke deler membraanonderzoek. Ook was hij AIO vertegenwoordiger voor de Graduate School of Life Sciences (GSLS). Gedurende zijn promotie heeft hij de volgende opleidingen gevolgd: in 2008 Scientific writing in English van het James Bosswell Institute in Utrecht en Biostatistiek aan de Universiteit van Utrecht en in 2009 JPK Force Spectroscopy Course van JPK Instruments in Berlijn.

LIST OF PUBLICATIONS

Haselberg R, Flesch FM, **Boerke A**, Somsen GW. *Thickness and morphology of polyelectrolyte coatings on silica surfaces before and after protein exposure studied by atomic force microscopy.* Anal Chim Acta 2013; 779:90-95.

Boerke A, Brouwers JF, Olkkonen VM, van de Lest CH, Sostaric E, Schoevers EJ, Helms JB, Gadella BM. *Involvement of bicarbonate-induced radical signaling in oxysterol formation and sterol depletion of capacitating mammalian sperm during in vitro fertilization.* Biol Reprod 2013; 88:21.

Brouwers JF, **Boerke A**, Silva PF, Garcia-Gil N, van Gestel RA, Helms JB, van de Lest CH, Gadella BM. *Mass spectrometric detection of cholesterol oxidation in bovine sperm.* Biol Reprod 2011; 85:128-136.

Boerke A, Tsai PS, Garcia-Gil N, Brewis IA, Gadella BM. *Capacitation-dependent reorganization of microdomains in the apical sperm head plasma membrane: functional relationship with zona binding and the zona-induced acrosome reaction.* Theriogenology 2008; 70:1188-1196.

Gadella BM, Tsai PS, **Boerke A**, Brewis IA. *Sperm head membrane reorganisation during capacitation.* Int J Dev Biol 2008; 52:473-480.

Boerke A, Dieleman SJ, Gadella BM. *A possible role for sperm RNA in early embryo development.* Theriogenology 2007; 68 Suppl 1:S147-55.

Ono N, Van der Heijden I, Scheffer GL, Van de Wetering K, Van Deemter E, De Haas M, **Boerke A**, Gadella BM, De Rooij DG, Neefjes JJ, Groothuis TA, Oomen L, Brocks L, Ishikawa T, Borst P. *Multidrug resistance-associated protein 9 (ABCC12) is present in mouse and boar sperm.* Biochem J 2007; 406:31-40.